

1998

Synthesis and characterization of chiral stationary phases for HPLC

Pik Fong Fu
San Jose State University

Follow this and additional works at: https://scholarworks.sjsu.edu/etd_theses

Recommended Citation

Fu, Pik Fong, "Synthesis and characterization of chiral stationary phases for HPLC" (1998). *Master's Theses*. 1696.
DOI: <https://doi.org/10.31979/etd.8ug4-y5ba>
https://scholarworks.sjsu.edu/etd_theses/1696

This Thesis is brought to you for free and open access by the Master's Theses and Graduate Research at SJSU ScholarWorks. It has been accepted for inclusion in Master's Theses by an authorized administrator of SJSU ScholarWorks. For more information, please contact scholarworks@sjsu.edu.

INFORMATION TO USERS

This manuscript has been reproduced from the microfilm master. UMI films the text directly from the original or copy submitted. Thus, some thesis and dissertation copies are in typewriter face, while others may be from any type of computer printer.

The quality of this reproduction is dependent upon the quality of the copy submitted. Broken or indistinct print, colored or poor quality illustrations and photographs, print bleedthrough, substandard margins, and improper alignment can adversely affect reproduction.

In the unlikely event that the author did not send UMI a complete manuscript and there are missing pages, these will be noted. Also, if unauthorized copyright material had to be removed, a note will indicate the deletion.

Oversize materials (e.g., maps, drawings, charts) are reproduced by sectioning the original, beginning at the upper left-hand corner and continuing from left to right in equal sections with small overlaps. Each original is also photographed in one exposure and is included in reduced form at the back of the book.

Photographs included in the original manuscript have been reproduced xerographically in this copy. Higher quality 6" x 9" black and white photographic prints are available for any photographs or illustrations appearing in this copy for an additional charge. Contact UMI directly to order.

UMI

A Bell & Howell Information Company
300 North Zeeb Road, Ann Arbor MI 48106-1346 USA
313/761-4700 800/521-0600



NOTE TO USERS

**The original manuscript received by UMI contains indistinct, slanted and or light print. All efforts were made to acquire the highest quality manuscript from the author or school.
Microfilmed as received.**

This reproduction is the best copy available

UMI

**SYNTHESIS AND CHARACTERIZATION OF CHIRAL STATIONARY PHASES
FOR HPLC**

A Thesis

Presented to

The faculty of the Department of Chemistry

San Jose State University

In Partial Fulfillment

of the Requirements for the Degree

Master of Science

by

Pik Fong Fu

August 1998

UMI Number: 1391519

UMI Microform 1391519
Copyright 1998, by UMI Company. All rights reserved.

**This microform edition is protected against unauthorized
copying under Title 17, United States Code.**

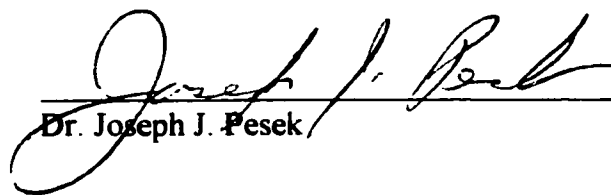
UMI
300 North Zeeb Road
Ann Arbor, MI 48103

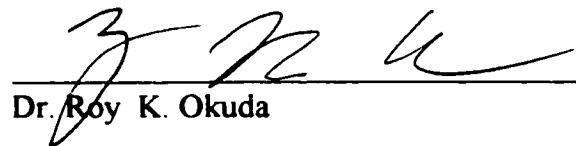
© 1998

Pik Fong Fu

ALL RIGHTS RESERVED

APPROVED FOR THE DEPARTMENT OF CHEMISTRY


Dr. Joseph J. Pesek


Dr. Roy K. Okuda


Dr. Paul S. Wagenknecht

APPROVED FOR THE UNIVERSITY


William Fisher

ABSTRACT

SYNTHESIS AND CHARACTERIZATION OF CHIRAL STATIONARY PHASES FOR HPLC

by Pik Fong Fu

Enantiomeric separation has been considered as one of the most difficult problems in chemistry but it is of great importance in various fields of science. With the development of chiral stationary phases (CSP) and the advanced technology in HPLC, chromatographic separation of enantiomers has become an efficient and rapid technique. In this research, four chiral selectors, namely 2-hydroxy-3-methacryloyloxypropyl- β -cyclodextrin, (R)-(+)-acrolein- β , β -dimethyl- γ -butyrolactone, (8S,9R)-(-)-benzylcinchonidium chloride and (R)-(+)-limonene were chosen to synthesize different chiral stationary phases.

All chiral selectors used in this study contain a terminal olefinic C=C group and they were bonded to the silica surface via TES silanization and hydrosilation. The modified surfaces were then characterized by elemental analysis, CP-MAS NMR spectroscopy and DRIFT spectroscopy. Furthermore, the performance of the new chiral stationary phases was evaluated by using drugs and dansyl-DL-amino acids. It was found that β -cyclodextrin CSP can separate optical isomers of temazepam, oxazepam and dansyl-DL-leucine.

Acknowledgements

I would like to deliver my greatest thanks to my thesis advisor, Dr. Joseph Pesek, and his research scientist, Dr. Maria Matyska, for their continuous guidance and support. Their expertise in separation chemistry and their patience in teaching are very much appreciated. Throughout my research study, they have spent their valuable time to help me solving my research problems and troubleshooting the instruments. In addition I would also like to thank my committee members, Dr. Roy Okuda and Dr. Paul Wagenknecht, for reviewing the manuscript and giving me recommendation on my thesis. Furthermore, I would also like to seize this opportunity to thank for all the colleagues in Dr. Pesek's group for sharing and exchanging ideas with me.

Finally, I wish to thank my family for their love and encouragement throughout my study.

Table of Contents

CHAPTER I - INTRODUCTION

A. Chiral compounds	1
B. Importance of Chiral Separations	4
C. History and Development of Chiral Separations	5
D. Chromatographic chiral separation by HPLC using chiral stationary phases	
1. High Performance Liquid Chromatography	7
2. Chiral Recognition and Chiral Stationary Phases	9
E. Synthesis of Chiral Stationary Phases	
1. The Solid Support - Silica Gel	25
2. Methods for Synthesis of Bonded Phases	28
F. Goal	32

CHAPTER II - EXPERIMENTAL

A. Materials	
1. Chemicals	34
2. Materials for Synthesis of Bonded Synthesis	35
B. Synthesis Procedures	
1. Preparation of Speier's Catalyst	36
2. Preparation of 1.0mM Triethoxysilane	37
3. Preparation of silica hydride	37
a. Vydac Silica hydride	
b. Kromasil silica hydride	
4. Preparation of Chiral bonded phases	
a. Synthesis of β-cyclodextrin bonded chiral stationary phases on Kromasil silica hydride using Speier's catalyst	39
b. Synthesis of β-cyclodextrin bonded chiral stationary phases on Kromasil silica using free tert-butyl peroxide	40
c. Synthesis of β-cyclodextrin bonded chiral stationary phase on Vydac silica hydride using Speier's catalyst	41
d. Synthesis of (R)-(+)- acryloxy-β,β-dimethyl-γ-butyrolactone chiral stationary phase on Kromasil silica hydride	41

e. Synthesis of (8S,9R)-(-)-N-benzylcinchonidium chloride chiral stationary phase on Kromasil silica hydride	42
f. Synthesis of (R)-(+)-Limonene chiral stationary phase on Kromasil silica hydride	43
C. Instrumentation and Operating Procedures	
1. Diffuse Reflectance Infrared Fourier Transform Spectrometry	44
2. Cross-Polarization Magic Angle Spinning Nuclear Magnetic Resonance Spectroscopy	45
3. Elemental Analysis	45
4. Column Packing	46
5. High Performance Liquid Chromatography	47
CHAPTER III - RESULTS AND DISCUSSION	
A. Elemental Analysis Results	49
B. Spectroscopic Analysis for the confirmation of the bonding of the chiral selector on the silica	
1. Success of TES silanization	51
a. CP-MAS Spectra	
b. DRIFT spectra	
2. Hydrosilation of β -cyclodextrin on silica hydride intermediate by Speier's catalyst	
a. Hydrosilation of β -cyclodextrin in 1:1 ethanol/water solvent system on Vydac hydride	58
b. Hydrosilation of β -cyclodextrin in 19:1 ethanol/water solvent system on Vydac silica hydride	61
c. Hydrosilation of β -cyclodextrin in 3:1 methanol/ethanol solvent system on Vydac silica	65
d. Hydrosilation of β -cyclodextrin on Kromasil silica in 3:1 methanol/ethanol solvent system	73
3. Hydrosilation of β -cyclodextrin on Kromasil hydride via free radical initiation	77
4. Hydrosilation of (8S,9R)-(-)-N-benzylcinchonidium chloride (BENZ) on Kromasil silica hydride using Speier's catalyst	84
5. Hydrosilation of (R)-(+)- acryloxy- β , β -dimethyl- γ - butyrolactone on Kromasil silica hydride using Speier's catalyst	87

6. Hydrosilation of (R)-(+)-Limonene on Kromasil hydride by Speier's catalyst	91
C. Spectroscopic studies on stability of β -cyclodextrin modified Kromasil silica chiral stationary phase	94
D. Chromatographic Studies	
1. Structure and Chirality of Samples for chromatographic studies	98
a. Benzodiazepines	
b. Dansyl amino acids	
c. Drugs	
2. Chromatographic conditions	104
3. Chromatographic measurements	104
4. Interpretation of chromatographic data	
a. Chiral separation of optical isomers of Benzodiazepines	105
i. β -cyclodextrin modified silica stationary phase	
ii. On (R)-(+)-acryloxy- β , β -dimethyl- γ -butyrolactone modified silica based chiral stationary phase	
b. Chiral separation of Dansyl-DL- amino acids	128
i. β -cyclodextrin modified silica based chiral stationary phase	
ii. On (R)-(+)-acryloxy- β , β -dimethyl- γ -butyrolactone modified silica based chiral stationary phase	
c. Chiral separation of drugs	144
i. β -cyclodextrin modified silica based chiral stationary phase	
ii. On (R)-(+)-acryloxy- β , β -dimethyl- γ -butyrolactone modified silica based chiral stationary phase	
5. Study of temperature effects on chiral separations	145
 CHAPTER IV - CONCLUSION	 150
 CHAPTER V - REFERENCES	 152

List of Figures

Figure 1a.	Schematic diagram showing a pair of enantiomers.	2
Figure 1b	Stereochemistry of Tetroses.	2
Figure 2a	Molecules that are chiral due to hindered free rotation along a single bond.	3
Figure 2b	Chirality arising from the rigidity of the structure.	3
Figure 3	Chiral ligand exchange stationary phase.	11
Figure 4	Schematic diagram showing how enantioselectivity can be achieved by three point interaction.	12
Figure 5a	Structure of fluoroalcoholic chiral stationary phase.	14
Figure 5b	Schematic diagram showing the three point interaction between DNB amine molecule and fluoroalcoholic CSP.	14
Figure 6	Preparation of cellulose CSP.	16
Figure 7a	Structure of native β -cyclodextrin.	17
Figure 7b	Geometry of β -cyclodextrin.	17
Figure 8	Structure of chiral selectors. (A) 2-hydroxy-3-methacryloyloxy-propyl- β -cyclodextrin (B) (R)-(+)-Acryloxy- β,β -dimethyl- γ -butyrolactone (C) (R)-(+)-Limonene (D) (8S 9R)-(-)-N-benzylcinchonidium chloride	20
Figure 9a	DRIFT Spectrum for 2-hydroxy-3-methacryloyloxy-propyl- β -cyclodextrin.	21
Figure 9b	^{13}C CP-MAS NMR spectrum for 2-hydroxy-3-methacryloyloxy-propyl- β -cyclodextrin.	22
Figure 10	Possible interaction sites of the chiral selectors.	24
Figure 11	Structure of silica.	26

Figure 12a	Esterification of silanol group by alcohol.	29
Figure 12b	Organosilanization.	29
Figure 12c	Modification by chlorination/organometallic reaction.	29
Figure 12d	TES silanization and hydrosilation.	29
Figure 13a	²⁹ Si CP-MAS NMR spectrum for Kromasil silica hydride.	52
Figure 13b	²⁹ Si CP-MAS NMR spectrum for Vydac silica hydride.	53
Figure 14	¹³ C CP-MAS NMR spectrum for Vydac silica hydride.	55
Figure 15a	DRIFT spectrum for Kromasil silica hydride.	56
Figure 15b	DRIFT spectrum for Vydac silica hydride.	57
Figure 16a	²⁹ Si CP-MAS NMR spectrum for β-cyclodextrin bonded to Vydac silica hydride (hydrosilation done in 1:1 ethanol/water solvent system).	59
Figure 16b	¹³ C CP-MAS NMR spectrum for β-cyclodextrin bonded to Vydac silica hydride (hydrosilation done in 1:1 ethanol/water solvent system).	60
Figure 17	DRIFT spectrum for β-cyclodextrin bonded to Vydac silica hydride (hydrosilation done in 1:1 ethanol/water solvent system).	62
Figure 18a	²⁹ Si CP-MAS NMR spectrum for β-cyclodextrin bonded to Vydac silica hydride hydrosilation done in 19:1 ethanol/water solvent system).	63
Figure 18b	¹³ C CP-MAS NMR spectrum for β-cyclodextrin bonded to Vydac silica hydride hydrosilation done in 19:1 ethanol/water solvent system).	64
Figure 19	DRIFT spectrum for β-cyclodextrin bonded to Vydac silica hydride (hydrosilation done in 19:1 ethanol/water solvent system).	66

Figure 20	²⁹ Si CP-MAS NMR spectrum for β-cyclodextrin bonded to Vydac silica hydride (hydrosilation done in 3:1 methanol/ethanol solvent system).	67
Figure 21	¹³ C CP-MAS NMR spectrum for β-cyclodextrin bonded to Vydac silica hydride (hydrosilation done in 3:1 methanol/ethanol solvent system).	69
Figure 22	DRIFT spectrum for β-cyclodextrin bonded to Vydac silica hydride (hydrosilation done in 3:1 methanol/ethanol solvent system).	70
Figure 23.	¹³ C CP-MAS NMR spectrum for β-cyclodextrin bonded to Vydac silica hydride (Big Batch).	71
Figure 24.	DRIFT spectrum for β-cyclodextrin bonded to Vydac silica hydride (Big Batch).	72
Figure 25	¹³ C CP-MAS NMR spectrum for β-cyclodextrin bonded to Kromasil silica hydride (Big Batch).	74
Figure 26	²⁹ Si CP-MAS NMR spectrum for β-cyclodextrin bonded to Kromasil silica hydride (Big Batch).	75
Figure 27.	DRIFT spectrum for β-cyclodextrin bonded to Kromasil silica hydride (Big Batch).	76
Figure 28	DRIFT spectrum for β-cyclodextrin bonded to Kromasil silica hydride (Free Radical Mechanism).	78
Figure 29	²⁹ Si CP-MAS NMR spectrum for β-cyclodextrin bonded to Kromasil silica hydride (Free Radical Mechanism).	79
Figure 30.	¹³ C CP-MAS NMR spectrum for β-cyclodextrin bonded to Kromasil silica hydride (Free Radical Mechanism).	80
Figure 31	DRIFT spectrum for reaction product of tert-butyl peroxide and Kromasil silica hydride via free radical mechanism.	82

Figure 32	¹³ C CP-MAS NMR spectrum for the reaction product of tert-butyl peroxide and Kromasil silica hydride via free radical mechanism.	83
Figure 33	¹³ C CP-MAS NMR spectrum for (8S, 9R)-(-)-N-Benzylcinchonidium chloride bonded phases on Kromasil silica.	85
Figure 34	DRIFT spectrum for (8S, 9R)-(-)-N-Benzylcinchonidium chloride bonded to Kromasil silica hydride.	86
Figure 35	²⁹ Si CP-MAS NMR spectrum for (R)-(+)-acryloxy-β,β-dimethyl-γ-butyrolactone bonded to Kromasil silica hydride.	88
Figure 36	¹³ C CP-MAS NMR spectrum for (R)-(+)-acryloxy-β,β-dimethyl-γ-butyrolactone bonded to Kromasil silica hydride.	89
Figure 37	DRIFT spectrum for (R)-(+)-acryloxy-β,β-dimethyl-γ-butyrolactone bonded to Kromasil silica hydride.	90
Figure 38	¹³ C CP-MAS NMR spectrum for (R)-(+)-limonene bonded to Kromasil silica hydride.	92
Figure 39.	DRIFT spectrum for (R)-(+)-limonene bonded to Kromasil silica hydride.	93
Figure 40a	²⁹ Si CP-MAS NMR spectrum for the β-cyclodextrin bonded phase on Kromasil silica (removed from the column after 69 runs).	95
Figure 40b	¹³ C CP-MAS NMR spectrum for the β-cyclodextrin bonded phase on Kromasil silica (removed from the column after 69 runs).	96
Figure 41	DRIFT spectrum for the β-cyclodextrin bonded phase on Kromasil silica (removed from the column after 69 runs).	97
Figure 42	Structure of Benzodiazepines.	99
Figure 43	Hyperchem molecular model of diazepam showing the non-planarity of the molecule.	100

Figure 44	Structures of dansyl-amino acids.	102
Figure 45	Structure of drugs.	103
Figure 46	Reversed phase separation of the optical isomers of temazepam on a β -cyclodextrin modified Vydac silica column (4.6 mm x 150 mm); mobile phase: methanol:water (30:70); flow rate: 0.20 mL/min; temperature: 25°C; UV detection at 254 nm; sample injection: 20 μ L; column pressure :77 bars.	109
Figure 47	Reversed phase separation of the optical isomers of temazepam on a β -cyclodextrin modified Vydac silica column (4.6 mm x 150 mm); mobile phase: methanol:water (10:90); flow rate: 0.18 mL/min; temperature: 25°C; UV detection at 254 nm; sample injection: 20 μ L; column pressure :50 bars.	110
Figure 48	Reversed phase separation of the optical isomers of oxazepam on a β -cyclodextrin modified Vydac silica column (4.6 mm x 150 mm); mobile phase: methanol:water (30:70); flow rate: 0.20 mL/min; temperature: 25°C UV detection at 254 nm; sample injection: 20 μ L; column pressure :77 bars.	111
Figure 49	Reversed phase separation of the optical isomers of temazepam on a β -cyclodextrin modified Kromasil silica column (4.6 mm x 50 mm); mobile phase: methanol:water (50:50); flow rate: 0.20 mL/min; temperature: 25°C UV detection at 254 nm; sample injection: 10 μ L; column pressure :1140 psi.	112
Figure 50	Reversed phase separation of the optical isomers of temazepam on a β -cyclodextrin modified Kromasil column (4.6 mm x 50 mm) Mobile phase: methanol:water (30:70); Flow rate: 0.15 mL/min; temperature: 25°C UV detection at 254 nm; sample injection: 20 μ L; column pressure :14 bars.	113

- Figure 51** Reversed phase separation of the optical isomers of temazepam on a β -cyclodextrin modified Kromasil column (4.6 mm x 50 mm); mobile phase: methanol:water (12:88); flow rate: 0.10 mL/min; temperature: 25°C
UV detection at 254 nm; sample injection: 10 μ L; column pressure :783 psi. 114
- Figure 52** Reversed phase separation of the optical isomers of oxazepam on a β -cyclodextrin modified Kromasil column (4.6 mm x 50 mm); mobile phase: methanol:water (40:60); flow rate: 0.15 mL/min; temperature: 25°C
UV detection at 254 nm; sample injection: 10 μ L; column pressure :755 psi. 115
- Figure 53** Reversed phase separation of the optical isomers of oxazepam on a β -cyclodextrin modified Kromasil column (4.6 mm x 50 mm); mobile phase: methanol:water (30:70); flow rate: 0.15 mL/min; temperature: 25°C; UV detection at 254 nm; sample injection: 20 μ L; column pressure :14 bars. 116
- Figure 54** Reversed phase separation of the optical isomers of temazepam on a β -cyclodextrin modified Kromasil column (46mm x 150mm) Mobile phase: methanol:water (30:70); Flow rate: 0.30ml/min; temperature: 25°C
UV detection at 254nm; sample injection: 10 μ L; column pressure :1425 psi 117
- Figure 55** Reversed phase separation of optical isomers of temazepam on a β -cyclodextrin modified Kromasil column (4.6 mm x 150 mm); mobile phase: methanol:water (20:80); flow rate: 0.30 mL/min; temperature: 25°C; UV detection at 254nm; sample injection: 10 μ L; column pressure :1311 bars. 118
- Figure 56** Reversed phase separation of the optical isomers of oxazepam on a β -cyclodextrin modified Kromasil column (4.6 mm x 150 mm); mobile phase: methanol:water (30:70); flow rate: 0.20 mL/min; temperature: 25°C; UV detection at 254 nm; sample injection: 20 μ L; column pressure:67 bars. 119

Figure 57	Reversed phase separation of the optical isomers of oxazepam on a β -cyclodextrin modified Kromasil column (4.6 mm x 150 mm); mobile phase: methanol:water (10:90); flow rate: 0.15 mL/min; temperature: 25°C; UV detection at 254nm; sample injection: 10 μ L; column pressure :1396 psi.	120
Figure 58	Diagram showing the interactions between (R)-(+)-acryloxy- β , β -dimethyl- γ -butyrolactone and temazepam.	125
Figure 59	A plot of capacity factor (k') Vs % methanol in the mobile phase for the chromatographic studies of benzodiazepines Flow rate: 0.5 mL/min.	127
Figure 60	Reversed phase separation of the optical isomers of dansyl-DL-leucine on a β -cyclodextrin modified Kromasil column (4.6 mm x 150 mm); mobile phase: methanol/water (20:80); flow rate: 0.30mL/min; temperature: 25°C; UV detection at 254nm; sample injection: 10 μ L; column pressure: 1481 psi.	133
Figure 61	Reversed phase separation of the optical isomers of dansyl-DL-leucine on a β -cyclodextrin modified Kromasil column (4.6 mm x 150 mm); mobile phase: methanol/water (10:90); flow rate: 0.20 mL/min; temperature: 25°C; UV detection at 254 nm; sample injection: 10 μ L; column pressure: 59 bars.	134
Figure 62	Reversed phase separation of optical isomers of dansyl-DL-leucine on a β -cyclodextrin modified Kromasil column (4.6 mm x 150 mm); mobile phase: methanol/water (40:60); flow rate: 0.10 mL/min; temperature: 25°C; UV detection at 254 nm; sample injection: 10 μ L; column pressure: 1510 psi.	135
Figure 63	Reversed phase separation of optical isomers of dansyl-DL-leucine on a β -cyclodextrin modified Vydac column (4.6 mm x 150 mm); mobile phase: methanol/water (10:90); flow rate: 0.27 mL/min; temperature: 25°C; UV detection at 254 nm; sample injection: 20 μ L; column pressure: 73 bars.	136
Figure 64	A plot of capacity factor (k') Vs % methanol in the mobile phase for the chromatographic studies of dansyl-DL-amino acids. Flow rate: 0.5 mL/min.	143

- Figure 65** Reversed phase separation of the optical isomers of dansyl-DL-leucine on a β -cyclodextrin modified Kromasil column (4.6 mm x 150 mm); mobile phase: methanol/water (30:70); flow rate: 0.20 mL/min; temperature: 25°C; UV detection at 254 nm; sample injection: 20 μ L; column pressure: 68 bars. 148
- Figure 66** Reversed phase separation of the optical isomers of dansyl-DL-leucine on a β -cyclodextrin modified Kromasil column (4.6 mm x 150 mm); mobile phase: methanol/water (30:70); flow rate: 0.20 mL/min; temperature: 50°C; UV detection at 254 nm; sample injection: 20 μ L; column pressure: 41 bars. 149

List of Tables

Table 1	Physical Properties of native Cyclodextrin	18
Table 2	Properties of Vydac and Kromasil Silica	28
Table 3	Summary of syntheses of chiral stationary phases	32
Table 4	CAS registry numbers of chemicals	34-35
Table 5	Chiral column packed	47
Table 6	The surface coverage and percent carbon of the bonded phases	50
Table 7	Variation of k' for benzodiazepines at different % methanol on β -cyclodextrin modified Kromasil silica chiral stationary phase (4.6 mm x 150 mm)	106
Table 8	Variation of k' for benzodiazepines at different % methanol on β -cyclodextrin modified Vydac silica chiral stationary phase (4.6 mm x 150 mm)	107
Table 9	Variation of k' for benzodiazepines at different % methanol on β -cyclodextrin modified Vydac silica chiral stationary phase (4.6 mm x 50 mm short column)	108
Table 10A	Comparison of separation factor and resolution of oxazepam and temazepam on β -cyclodextrin Kromasil based chiral column, 4.6 mm x 150 mm	122
Table 10B	Comparison of separation factor and resolution of oxazepam and temazepam on β -cyclodextrin Vydac based chiral column, 4.6 mm x 150 mm	122
Table 11	Variation of capacity factor (k') for benzodiazepines at different % methanol in the mobile phase. Flow rate for analysis is 0.5 mL/min	126
Table 12	Chromatographic data for dansyl-amino acids using β -cyclodextrin Kromasil chiral column, 4.6 mm x 150 mm	129
Table 13	Chromatographic data for dansyl-amino acids using β -cyclodextrin Vydac chiral column, 4.6 mm x 150 mm	130

Table 14	Chromatographic data for dansyl-DL-amino acids by using β -cyclodextrin Kromasil chiral column, 4.6 mm x 50 mm (short)	130
Table 15A	Optical resolution and separation factors of dansyl-DL-leucine on β -cyclodextrin Kromasil chiral column, 4.6 mm x 150 mm	139
Table 15B	Optical resolution and separation factors of dansyl-DL-leucine on β -cyclodextrin Vydac chiral column, 4.6 mm x 150 mm	139
Table 15C	Separation of dansyl-DL-amino acids on various β -cyclodextrin stationary phases	140
Table 16	Chromatographic data of dansyl-DL-amino acids on lactone modified Kromasil chiral column, 4.6 mm x 150 mm at flow rate 0.5 mL/min	142
Table 17A	Variation of k' of temazepam, oxazepam and dansyl-DL-leucine at different temperatures on β -cyclodextrin Vydac silica chiral column (4.6 mm x 150 mm)	146
Table 17B	Variation of k' of temazepam, oxazepam and dansyl-DL-leucine at different temperatures on β -cyclodextrin Kromasil silica chiral column (4.6 mm x 150 mm)	146
Table 17C	Variation of k' of temazepam, oxazepam and dansyl-DL-leucine at different temperatures on β -cyclodextrin Kromasil silica chiral column (4.6 mm x 50 mm)	146

Chapter I

INTRODUCTION

A. Chiral Compounds¹

Stereoisomers are isomeric compounds in which the atoms have different spatial arrangements but equivalent bond connectivities. Stereoisomers can be categorized by symmetry into diastereomers and enantiomers. Enantiomers are a pair of compounds that are mirror images of each other and they cannot be superimposable onto each other without any bond cleavage. Compounds of that kind are chiral in nature or they are said to exhibit chirality. Diastereomers are those stereoisomers which are not enantiomeric to each other. A simple example of chiral compound is the one with four different groups attached to a central carbon atom as shown in Figure 1a. The carbon atom is called a chiral center. Figure 1b illustrates a molecule with two chiral centers and it has a total of four stereoisomers. There are two pairs of enantiomers (AB and CD) and each enantiomer is a diastereoisomer of the other pair of enantiomers. Chirality may also result from a variety of situations other than the presence of chiral centers. Figure 2a shows an example of chirality which arises from the hindered free rotation about a single bond due to bulkiness of the neighbor groups. The resulting molecules have benzene rings occupying in different planes and thus enantiomerism occurs. Furthermore, Figure 2b provides an example of a compound in which rings are joined at a single common atom. As inversion at the common atom without bond breaking is impossible, this rigidity of the structure causes the chirality of the molecule.

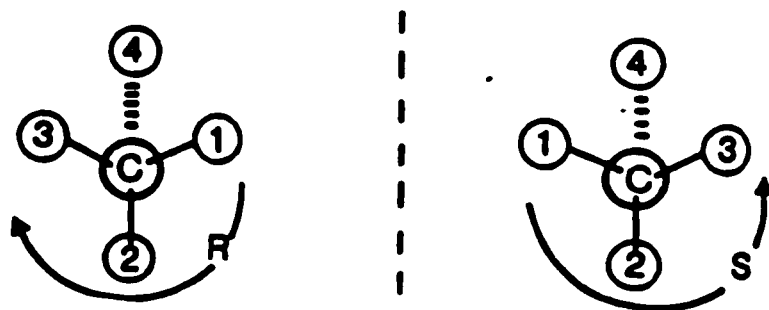


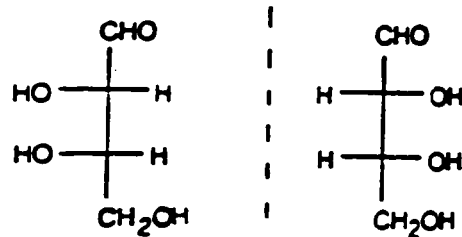
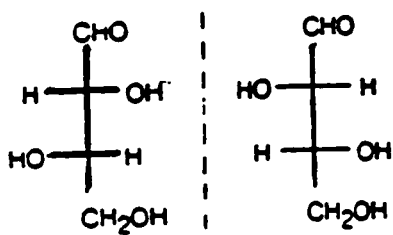
Figure 1a. Schematic diagram showing a pair of enantiomers.

(A)

(B)

(C)

(D)



A and B are enantiomeric pairs

C and D are enantiomeric pairs

Figure 1b. Stereochemistry of Tetroses.

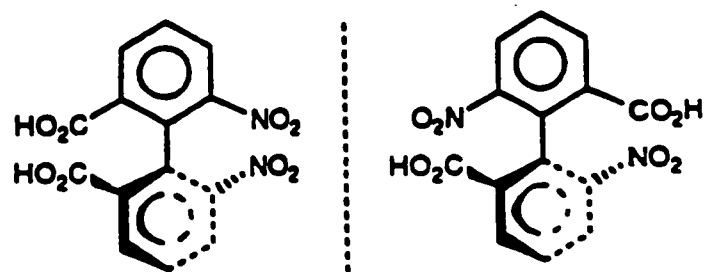


Figure 2a. Molecules that are chiral due to hindered free rotation along a single bond.

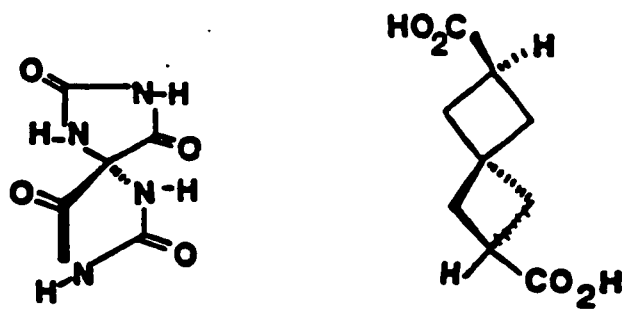


Figure 2b. Chirality arising from the rigidity of the structure.

Enantiomers have identical physical properties (e.g. melting point, boiling point, solubility etc.) and chemical properties with two exceptions:- (1) The pair of enantiomers rotate plane polarized light in opposite directions. (2) They interact differently with other compounds containing chiral centers. The enantiomer which rotates the plane polarized light to the right is designated as dextrorotatory D or (+), meanwhile the isomer which rotates the plane polarized light to the left is termed as laevorotatory L or (-). In contrast, diastereomers have different physical and chemical properties.

B. Importance of Chiral Separation

Chiral separation has become one of the fastest developing areas of scientific research in chiral synthesis, kinetic studies, mechanistic studies, agricultural chemistry, pharmacology and medicine in the last 20 years. Since living systems are chiral in nature, enantiomers will interact differently in biological processes which result in different biological responses and effects. As a consequence, accurate monitoring of the optical purity of pharmaceutical products is critical, otherwise, undesirable toxic and physiological effects may follow. Furthermore, new guidelines of the U.S. Food and Drug Administration in 1992 and similar policies in other countries² state that only one enantiomer of a chiral drug can be brought to the market. This drives the necessity to investigate the pharmacological effects and metabolic pathways of each individual enantiomer separately. Under these circumstances, the enantiomers must separate on a preparative scale. Hence, much effort has been put in the research and development of

chiral separation technology even though it has been recognized as one of the most difficult problems in science.

C. History^{3,4,5} and Development of Chiral Separation

Because enantiomers have similar physical and chemical properties, the separation of chiral compounds is non-trivial and expensive. Early in 1848, Pasteur was able to achieve optical resolution of enantiomers of tartaric acid which could be crystallized in recognized morphological form. In 1952, Schlenk introduced the use of urea inclusion compounds in chiral separation. Urea could be arranged to form two enantiomorphous lattices that have different affinities to enclose the optical isomers. Moreover, in 1949 Dickey demonstrated partial optical resolution by a surface imprinting technique. In his method, a silica gel was produced in the presence of asymmetric molecules which were then extracted leaving "footprints" on the surface. The modified surface had greater affinity towards the enantiomer of one particular configuration and thus chiral separation could be achieved. In another approach, differential enzymatic catalysis could be applied to a microbiological process to produce an excess enantiomeric product. Later, the most popular method of chiral separation was done by derivatizing the enantiomers in a mixture using a chiral reagent to form a set of diastereomers⁴. Because of the differences in the physical properties of the diastereomers, they can be separated by methods such as fractional distillation or fractional crystallization. The separated components were then further reacted with an appropriate reagent to regenerate the enantiomers. However, the

methods described above involve multiple steps with low efficiency. They all normally fail to give a total separation of the enantiomers.

However, the introduction of chromatographic techniques to chiral analysis provides a direct, quick and efficient method for separation. It is a robust technique that can be tailor-made to separate different classes of chiral compounds. With the advent of new technology in chromatographic systems, this method can be extended to a large preparative scale.

In the early stages of development, indirect separation of enantiomers was done by chromatography. The enantiomers were first derivatized on a pre-column containing a chiral selector into diastereomers. Such a pair of diastereomers were then separated by a normal achiral chromatographic column. This method has limited applications because the enantiomeric separation can be contaminated by the derivatizing agent, which leads to inaccurate measurement. Alternatively, a more efficient and widespread chromatographic method is to separate the enantiomers directly by using a chiral stationary phase (CSP) or by adding a chiral selector in the mobile phase. With a chiral additive in the mobile phase, the analytes form transient diastereomeric complexes with the chiral selector. The separation will then be based on the difference in the stabilities of the complexes, differential solvation in the mobile phase or the binding of the complexes to the solid support⁴. On the other hand, separations achieved by chiral stationary phases are determined by the difference in energy between the two diastereomeric complexes formed between the solutes and the CSP⁴. The efficiency of separation will be a result of all the interactions between the stationary phase and the solutes.

In the past 20 years, there have been many studies on various formats of chiral chromatographic separation⁶. Successful separations have been performed by various chromatographic techniques such as thin layer chromatography (TLC), gas chromatography (GC), supercritical fluid liquid chromatography (SFC), high performance liquid chromatography (HPLC) and capillary zone electrophoresis (CZE). Among all the chromatographic techniques, the development of chiral separation by HPLC has grown tremendously. These advances can be attributed to the breakthrough of HPLC technology such as hardware design and the packing techniques as well as the development of chiral stationary phases for HPLC. In addition, HPLC has some important advantages over other separation methods. For example, GC and SFC require high temperature to operate and this may cause racemization or decomposition of chiral compounds. TLC is less reproducible and this method offers lower column efficiency. CZE is presently limited to the analytical scale. As a consequence, HPLC is the most promising chromatographic technique showing the greatest potential for chiral separation.

D. Chromatographic chiral separation by HPLC using chiral stationary phases

1. High Performance Liquid Chromatography

Liquid Chromatography is a technique based on the differential partition of solutes between the mobile phase and the stationary phase. In the older technique of liquid column chromatography, a glass column having dimensions of 1 x 30 cm was filled with a granular solid and the carrier liquid containing the sample was poured through the column⁷. In order to achieve better separation, small particles were used. However, the

drawbacks were slow analysis and long retention time. One way to increase the throughput was to exert a force on the liquid by a pump or gas pressure. It was found that with an increase of pressure from 10 psi to 500 psi, the retention could be decreased from days to minutes⁷. Nowadays, with advanced packing techniques and pumping systems, particles as small as 5 μ m and high pressure can be used. Because of the increased surface area for interactions and the uniformity of the packing, the efficiency for separation is greatly increased. This new format is designated as High Performance Liquid Chromatography (HPLC).

HPLC can be operated in two different modes depending on the relative polarity of the stationary phase and the mobile phase. In normal phase HPLC, the retarding force involves the adsorption of the solute at the hydroxyl groups on a solid support such as silica or alumina. Therefore, polar molecules are held strongly and are eluted later from the column. The stationary phase in this case is more polar than the mobile phase (e.g. n-hexane, chloroform, chloroethane). In the reversed phase mode, the solid support, like silica, is further modified with less polar compounds which render them hydrophobic. The solvent system used is polar in nature such as water, methanol, tetrahydrofuran and acetonitrile. Reversed phase HPLC is now the most important mode in liquid chromatography as a result of the bonding of a great variety of compounds onto the solid support. Bonding of the octadecyl moiety to silica is a commonly used reversed phase material with widespread applications in diverse fields. In this research, separations of chiral compounds are mainly based on hydrophobic interactions between the analytes and the chiral stationary phase, so the analyses are operated in the reversed phase mode using

methanol/water mixtures as the mobile phase. The selectivity, resolution, and retention times depend on the percentage of methanol (as organic modifier), flow rate and temperature.

2. Chiral Recognition and Chiral Stationary Phase

The fundamental mechanism for chiral recognition is the “three point rule” suggested by Dalgliesh in 1952⁸. It states that enantioselectivity can only be achieved when there are three simultaneous interactions between the chiral selector and the solutes. At least one interaction must be dependent on the stereochemistry at the chiral center of the chiral selector and the enantiomers. The degree and the extent of such interactions varies greatly with distances of the effective interactive groups from the stereogenic center and the relative spatial orientation of the interacting groups. An understanding of the recognition mechanism of the CSP is important since it often allows one to predict qualitatively the extent of interaction and the relationship of the elution order to the absolute configurations⁹. With the insight gained from Dalgliesh’s recognition theory, a great variety of chiral stationary phases that are based on different types of interactions have been developed. With various functionalities on the chiral stationary phases, each has its own class of resolvable compounds. This explains why it is worth investigating and developing different chiral stationary phases in order to increase the variety of applications for enantiomeric separation by HPLC. Chiral stationary phases are classified according to the type of solute-CSP complexes formed and the interactions existing between the solutes and the CSP are summarized as follows:-

Chiral ligand exchange chromatography:-

The enantiomeric solutes interact with the ligand which is bonded to the solid support in the presence of metal ions in the mobile phase. This leads to the formation of diastereomeric chelate complexes which are different in energy and so chiral resolution can be achieved. One example of this approach was done by bonding a selector ligand, L-proline, to a solid support as shown in Figure 3¹⁰. In the presence of Cu²⁺ ions, racemates of DL-proline formed transient diastereomeric metal complexes of different stability with the bonded L-proline and copper ion.

Synthetic multiple interaction CSPs (Pirkle type bonded phases)

The solutes and the chiral stationary phase form diastereomeric complexes by various attractive interactions such as π - π interaction, hydrogen-bonding, dipole stacking, hydrophobic interaction, Van der Waals's forces, electrostatic interaction or steric repulsion. Enantioselectivity is achieved if the three point rule is followed. Figure 4 gives an overview of how chiral separation can be achieved by three point interaction. The chiral stationary phase in the diagram possesses a large bulky group (steric interaction), an acidic site and a basic site. Molecules A(+) and A(-) are mirror images of each other bearing a bulky group, an acidic site and a basic site. The enantioselectivity is a consequence of the acidic-basic site interactions and the steric repulsion between the solute and the chiral stationary phase. It can be seen that molecule A(+) has a stronger interaction with the chiral stationary phase and thus it will be retained on the surface for a longer period of time. On the other hand, molecule A(-) has only one site of interaction and thus it will be eluted first from the chiral column.

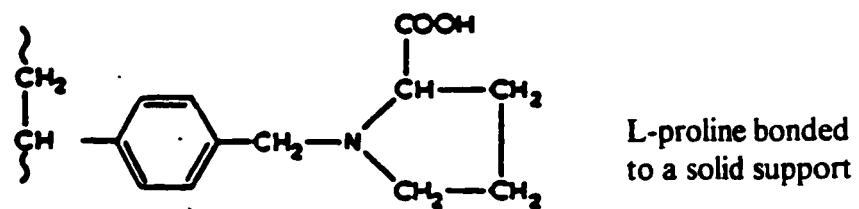


Figure 3. Chiral ligand exchange stationary phase

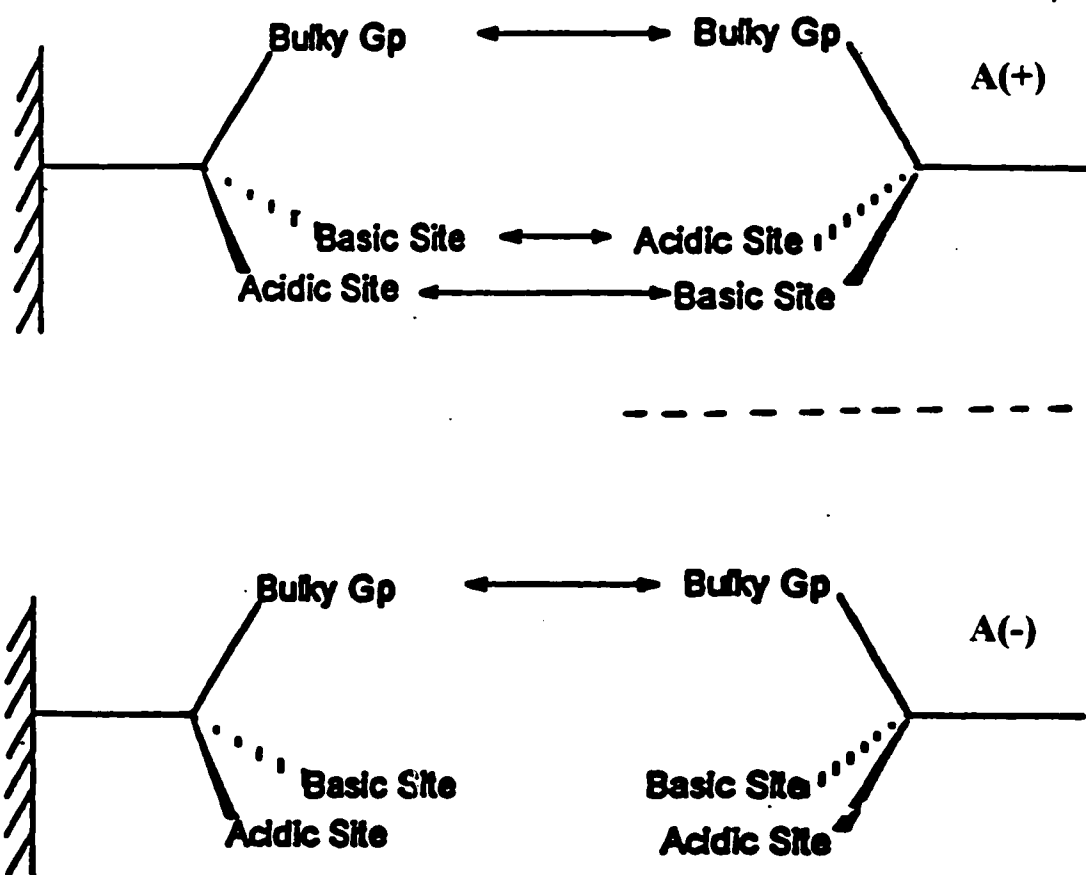


Figure 4. Schematic diagram showing how enantioselectivity can be achieved by three point interaction.

In 1979, Pirkle initially synthesized the first CSP based on multiple interactions¹¹. He bonded chiral anthoyl alcohol to silica and a wide range of racemates such as sulphoxides, lactones and amino acids could be separated. Figure 5a shows the structure of the fluoroalcoholic chiral stationary phase and Figure 5b illustrates the three point interaction between a 3,5-dinitrobenzoyl (DNB) derivative of an amine and the fluoroalcoholic chiral stationary phase. Chiral recognition was achieved by the following three interactions:- (a) the formation of hydrogen bonding between the DNB carbonyl oxygen and the hydroxyl group of the CSP; (b) the acidic-basic sites interaction between the basic group B of the solute and the acidic hydrogen on CSP; and (c) the π - π interaction between the DNB aromatic ring and the aromatic ring system of the CSP. For the other enantiomer of the solute, the DNB aromatic ring and the aromatic ring system of the chial stationary phase are trans to each other and thus the tertiary π - π interaction is unlikely to occur.

Protein CSP

This chiral stationary phase is made by immobilizing protein such as albumin, α -acid glycoprotein and bovin serum albumin (BSA) to a solid support. Since protein has shown strong ability to bind a wide range of compounds including anionic, inorganic as well as organic compounds through interactions such as hydrophobic interaction, electrostatic interaction, hydrogen bonding and charge transfer process. This gives protein a great potential to be developed as a chiral selector. In 1973, Steward and Doherty has successfully immobilized BSA to Sepharose and demonstrated the chiral resolution of

Chiral selector:

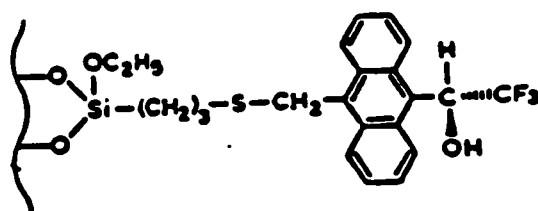


Figure 5a. Structure of fluoroalcoholic chiral stationary phase.

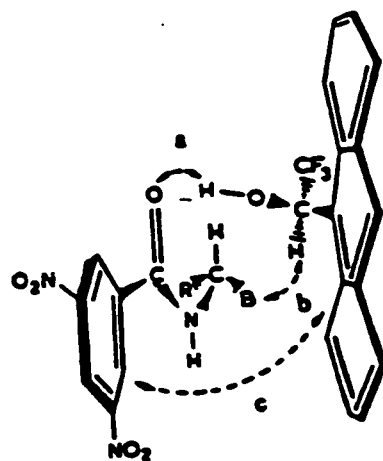


Figure 5b. Diagram showing the three point interaction between a DNB amine molecule and fluoroalcoholic chiral stationary phase.

racemate DL-tryptophan by the BSA chiral stationary phase⁵. The separation is due to the difference in affinity of BSA for the pair of enantiomers. Even though direct optical resolution attained by the enantioselective properties of protein is versatile, this method suffers from low sample capacity and is limited to operation at high pH.

Cellulose CSP

The chiral selector is cellulose or its derivatives. The primary mechanism is due to the formation of an inclusion complex between the solute and the helical structure of the polysaccharides⁵. The enantiomeric inclusion complexes formed interact with the CSP to varying extents so they are eluted at different retention times. Figure 6 illustrates how to prepare cellulose chiral stationary phases on different solid supports via free radical reaction by means of the C=C on the undecenoyl group¹².

Cyclodextrin CSP

Figure 7a shows the structure of native β -cyclodextrin¹³. Cyclodextrin is a cyclic oligosaccharide with a torodial shape, consisting of six or more (D)-(+)-glucose residues in a chair form bonded through α -(1,4) glycoside linkages. The resulting structure is a truncated cone (Figure 7b)¹⁴ with the mouth of cone larger than the base. The mouth is surrounded by hydroxyl groups of the C-2 and C-3 carbons in an anti-clockwise direction. The primary hydroxyl groups are located at the base of the cyclodextrin in a clockwise direction. Because the primary hydroxyl groups are free to move, the base is partially blocked. Due to the orientation of the glucose units, there are no hydroxyl groups in the interior, so cyclodextrin has a hydrophobic cavity with hydrophilic edges. The interior

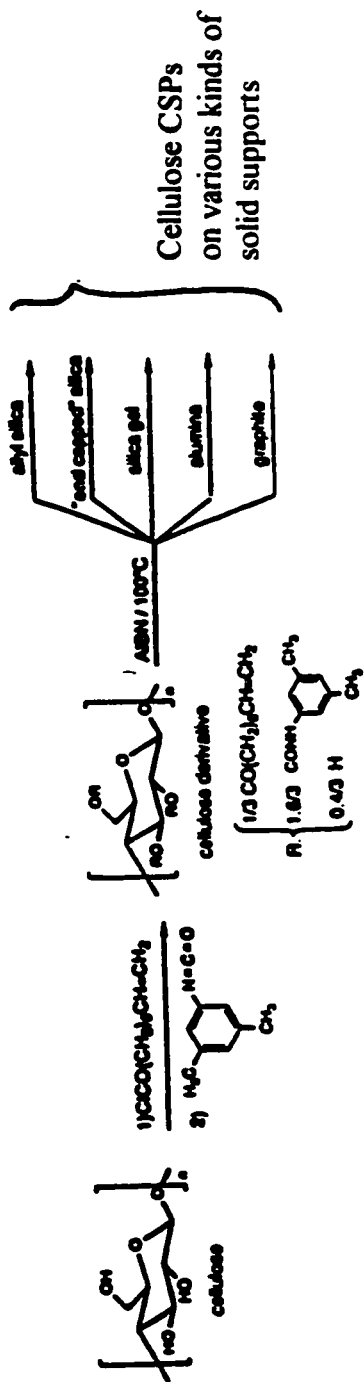


Figure 6. Preparation of cellulose CSP.

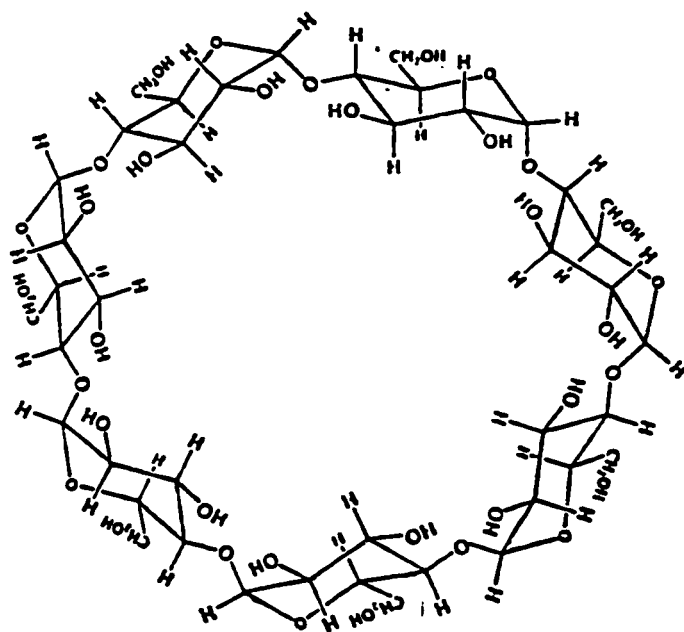


Figure 7a. Structure of native β -cyclodextrin.

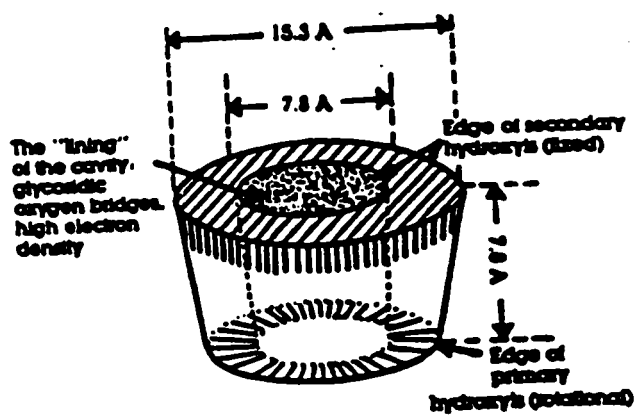


Figure 7b. Geometry of β -cyclodextrin.

cavity of cyclodextrin consists of two rings of the C-H skeleton and one ring glycosidic oxygen. The size of the interior cavity is proportional to the number of glucose units in the cyclodextrin. Typical physical properties of cyclodextrin are listed in Table 1.

Table 1. Physical Properties of native Cyclodextrin¹³

Cyclodextrin	Number of glucose unit	Molecular weight	Cavity Dimension (Diameter), A		
			External	Internal	Depth
α -cyclodextrin	6	973	13.7	5.7	7.8
β -cyclodextrin	7	1135	15.3	7.8	7.8
γ -cyclodextrin	8	1297	16.9	9.5	7.8

Chiral recognition by cyclodextrin requires the solutes entering into the hydrophobic cavity to form guest-host inclusion complexes¹³⁻¹⁶. This process involves interaction between the non-polar part of the solutes with the hydrophobic cavity. The associative forces between the polar hydroxyl groups at the rim of the cyclodextrin with the solutes also play a significant role to enantioselectively differentiate between the two enantiomers^{17,18}. In addition, further interaction such as dipole stacking, steric repulsion or hydrogen bonding between the solute and the cyclodextrin are necessary to achieve chiral resolution. The chiral nature of cyclodextrin accounts for the difference in free energy of the pair of diastereomers formed. As a result, the size, polarity and the shape of the analytes are critical factors responsible for the different stability of the inclusion complexes¹⁹.

Based on the size of various cyclodextrins, it was found that α -cyclodextrin works best with simple six-membered ring molecules. β -cyclodextrin accommodates molecules

of the size of biphenyl or naphthyl whereas γ -cyclodextrin can include large polyaromatic pyrene-types of compounds¹³.

Figure 8 shows the structures of chiral selectors that were chosen to study in this research. First, 2-hydroxy-3-methacryloyloxypropyl- β -cyclodextrin (substituted β -CD) is a new product from Wacker Chemical (USA) Company. It is a β -cyclodextrin molecule with partially derivatized hydroxyl groups. Figure 9a and Figure 9b are the DRIFT spectrum and the ¹³C CP-MAS NMR spectrum of the substituted cyclodextrin respectively. Such modification can increase the depth of the cone. In some cases, the modification may enhance the extent of interaction of the solutes with the reactive site on the cyclodextrin. In the other cases, it may block the mouth of the cyclodextrin and thus eliminating some or all of the hydrogen bonding between the solutes and the CSP. This modification changes the nature of the inclusion complexes and causes significant differences in selectivity^{20,21}. The enantioselectivity of this particular cyclodextrin on various dansyl-DL-amino acids, benzodiazepines and drugs was investigated in this work.

The second type of chiral selectors under study are classical Pirkle type bonded phases including (R)-(+)-acryloxy- β,β -dimethyl- γ -butyrolactone (LACT), (R)-(+)-limonene (LIM) and (8S,9R)-(-)-N-benzylcinchonidium chloride (BENZ). These three compounds are very useful materials for organic synthesis and optical isomers of these three compounds have been separated previously. As chiral separation by using CSP has a

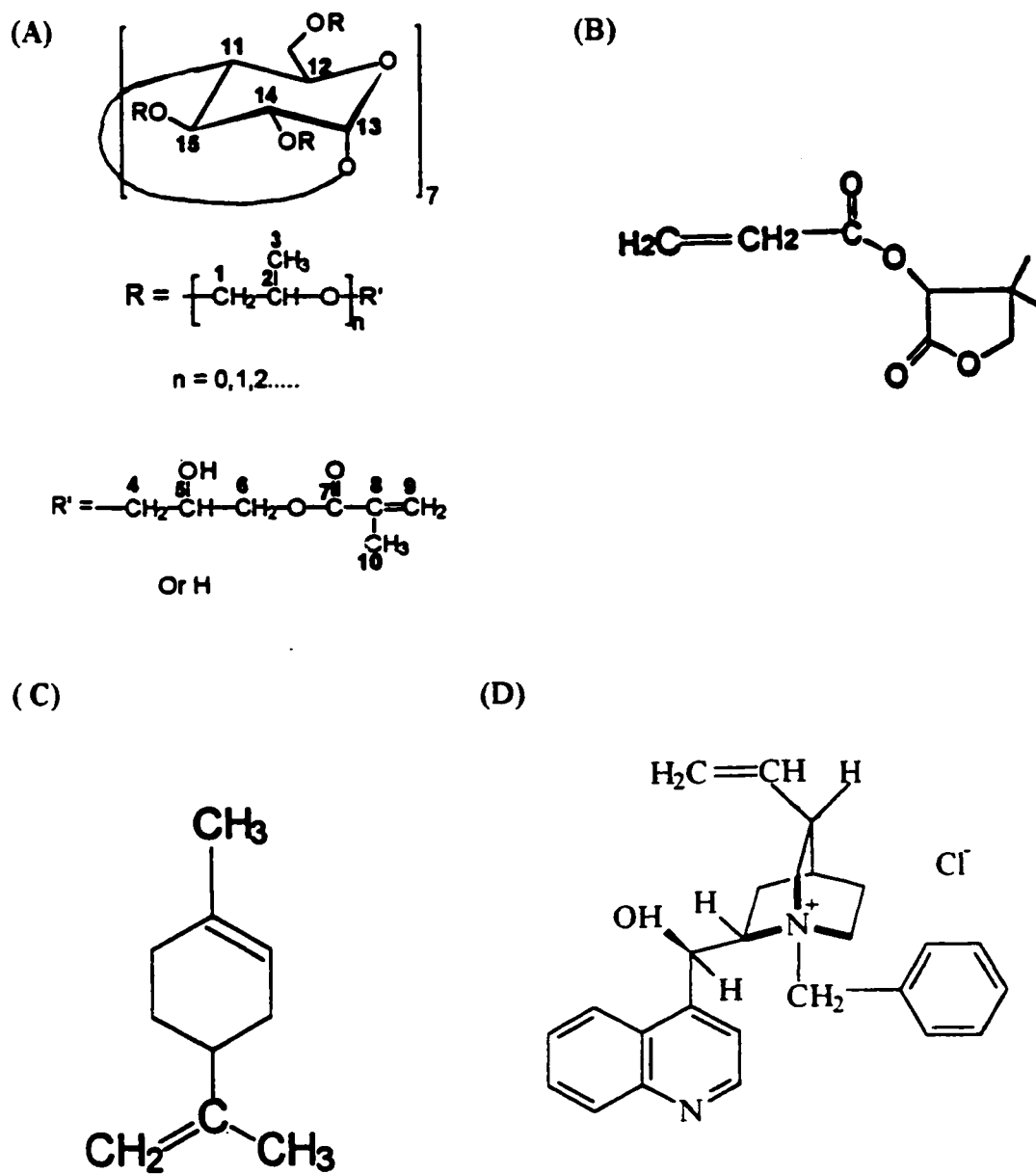


Figure 8. Structure of chiral selectors.

- (A) 2-hydroxy-3-methacryloyloxy-propyl- β -cyclodextrin
 (B) (R)-(+)-Acryloxy- β,β -dimethyl- γ -butyrolactone
 (C) (R)-(+)-Limonene
 (D) (8S, 9R)-(-)-N-benzylcinchonidinium chloride

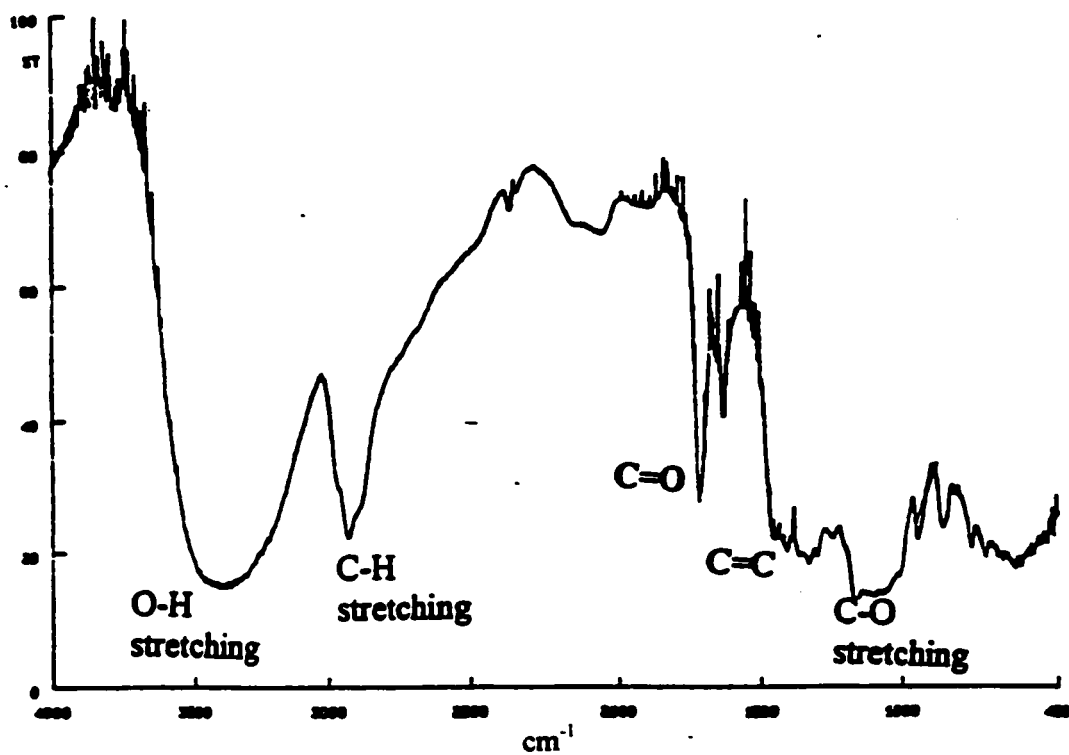


Figure 9a. DRIFT Spectrum for 2-hydroxy-3-methacryloyloxy-propyl- β -cyclodextrin.

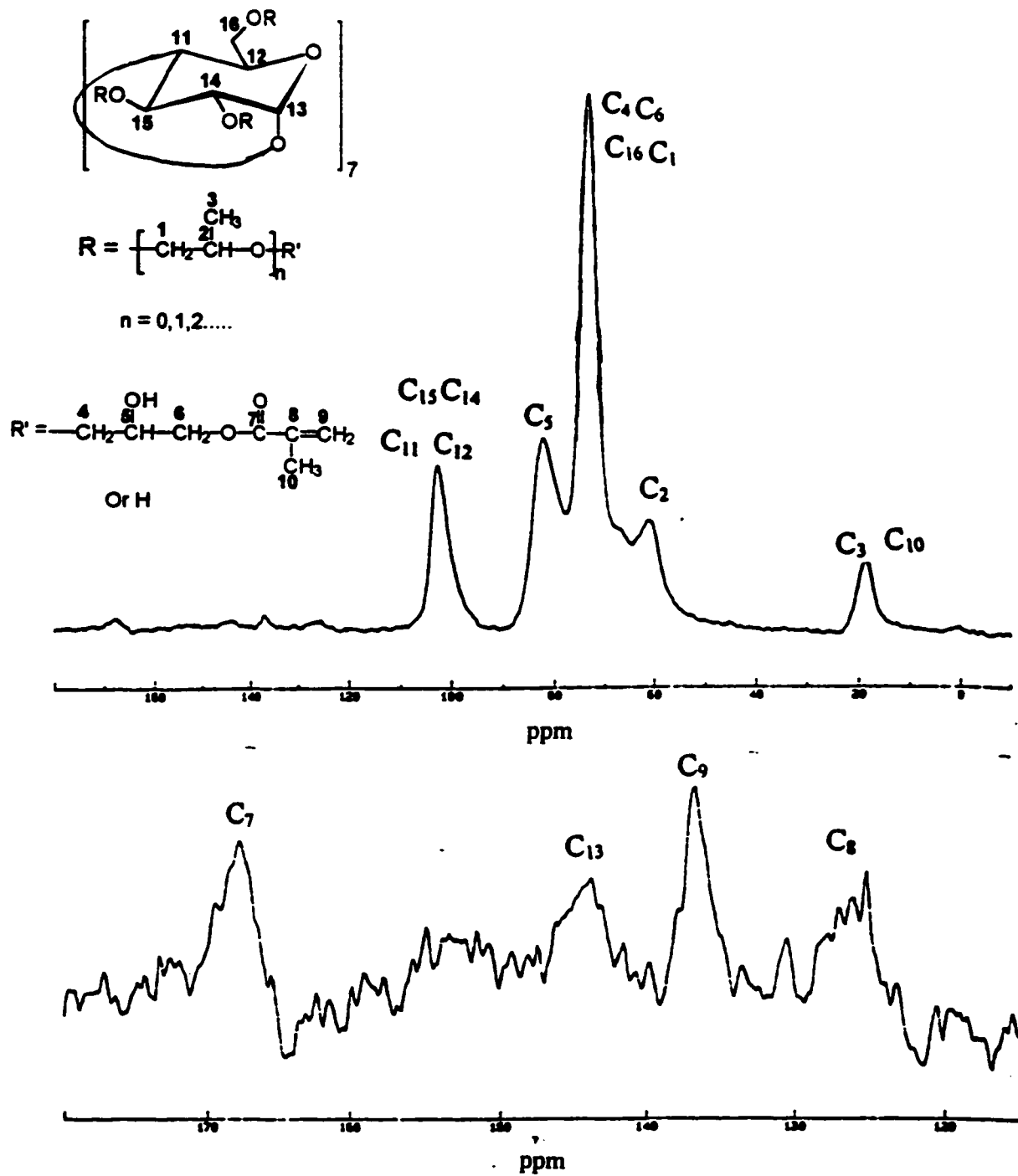
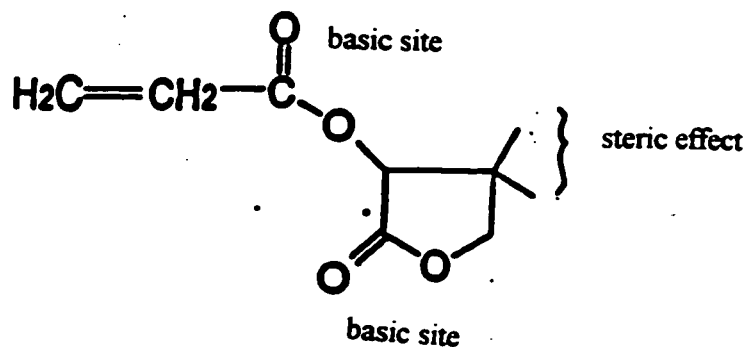


Figure 9b. ^{13}C CP-MAS NMR spectrum for 2-hydroxy-3-methacryloyloxy-propyl- β -cyclodextrin.

reciprocal relationship, the use of these three compounds as CSP materials is worth investigating. The chiral recognition of these type of phases is determined by multiple interactions between the stationary phases and the solutes. The major interaction sites include basic sites, acidic sites, steric interaction sites, sites for electrostatic interaction, π -basic aromatic rings and π -acidic rings⁹. The presence of the aromatic rings can provide for π - π interaction between the bonded phases and the solutes. Acidic sites are due to the presence of acidic hydrogen which can form intermolecular hydrogen bonding. In conjunction with acidic hydrogens, the basic sites such as sulfinyl oxygen, hydroxyl groups, ether oxygen or amino groups are needed for intermolecular hydrogen bonding. Electrostatic interactions occur at either charged groups as well as permanent or induced dipoles whereas steric interactions exist between large bulky groups.

The interactive sites of the three Pirkle-type of chiral selectors used in the study are shown in Figure 10. In the case of LACT, it can be seen that the existence of the cyclic oxygen, carbonyl oxygen, ester oxygen and the crowded methyl substitutes at the β position of the lactone are potential sites of interaction²²⁻²⁴. It is possible to separate compounds with features consisting of acidic hydrogens and bulky groups. For BENZ, the aromatic ring A and the aromatic system B are electron rich π systems which work best with solutes having similar π aromatic systems. In this way, there will be significant π - π interactions which are essential for chiral recognition. In addition, the hydroxyl group attached to one of the stereogenic centers is another potential acidic site that can form hydrogen bonding with the basic site from solute. Finally, the positively charged nitrogen

(A) (R)-(+)-acryloxy- β,β -dimethyl- γ -butyrolactone



(B) (R)-(+)-Limonene (C) (8S,9R)-(-)-N-benzylcinchonidinium chloride

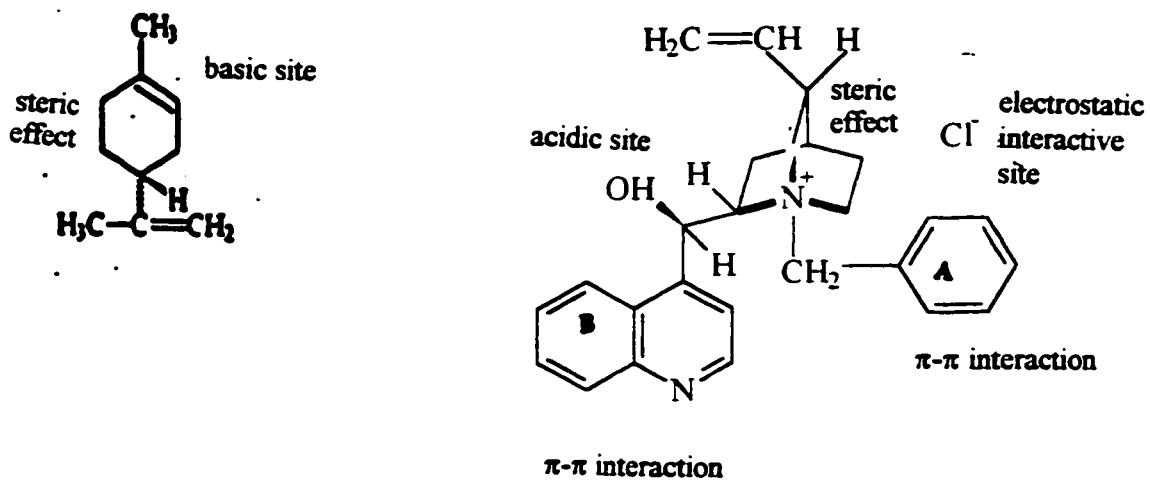


Figure 10. Possible interaction sites of the chiral selectors.

stereogenic center may introduce an electrostatic interactive site. Lastly, LIM is a relatively a small molecule so it is more accessible to interact with the silica surface in order to achieve a high bonded phase density. This increases the hydrophobic interaction between the solutes and this chiral selector in reversed phase chromatography. Moreover, the C=C bond in the six membered ring is an electron rich site for the second interaction and the bulky six membered ring itself may possibly introduce steric interactions with solutes.

E. Synthesis of Chiral Stationary Phases

1. The Solid Support - Silica Gel

The success and the progress of development in liquid chromatography is highly dependent on the quality of the solid support. The most commonly and widely used support material is silica gel. The structure of silica gel is shown in Figure 11. It has a rigid, stable and porous structure²⁵. The existence of accessible silanol (Si-OH) groups and a large surface area make it easy to convert silica into a wide variety of bonded phases materials. Since silica has been studied for several decades, a wide variety of particle sizes and pore diameters are available commercially. It also provides high efficiency in separation and it is reasonably priced.

Silica has different roles in the chromatographic separation processes. On the surface of the silica, there are different types of Si-OH groups. The most reactive one is the silanol group which determines the reactivity and the surface properties of silica²⁵.

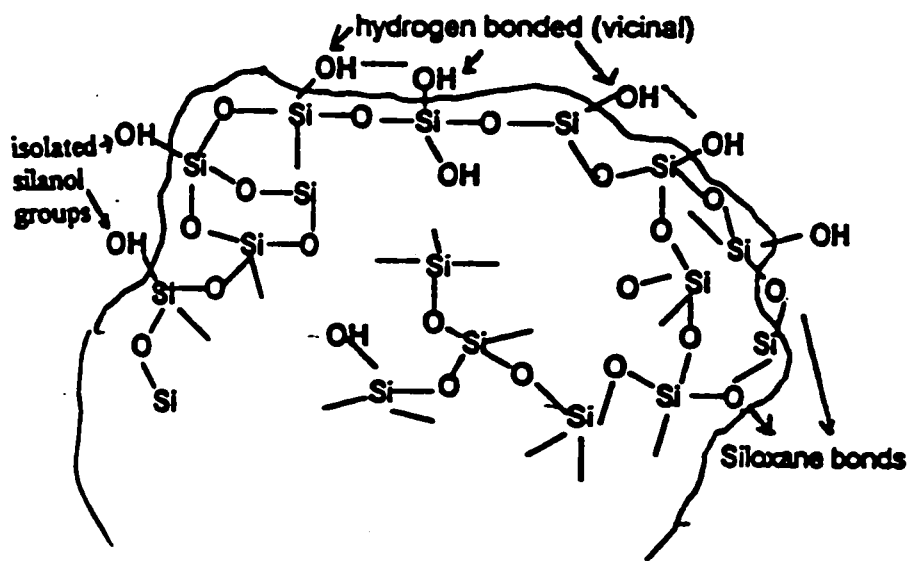


Figure 11. Structure of silica.

With silica as a solid support, there will be direct interaction between the solute and the reactive polar groups on the silica surface. In addition, the characteristics of the bonded phases are affected by the porosity, specific surface area and the particle size of the silica. As a result, the effectiveness of the separation is indirectly affected by the underlying silica support²⁶. By modifying silica with molecules of different polarities, it can be employed in both normal and reverse phase HPLC for different types of separations. Because of the steric hinderance of the bulky organic groups, it has been estimated that the maximum amount of modifiable silanol groups²⁶ on the silica surface is about 8 $\mu\text{mol}/\text{m}^2$ with the optimum surface coverage²⁶ that can be reached upon modification about is 4.5 $\mu\text{mol}/\text{m}^2$. Therefore, even after silica has been modified, there are still silanol groups left on the surface, which may account for the tailing effect and loss of resolution on separation. In chiral separations, the presence of reactive silanol groups may cause non-enantioselective interactions with the solutes resulting in a reduction of enantiomeric resolution.

In this study, two different types of silica, Vydac and Kromasil, are used as the solid support. The properties of both kinds of silica are listed below in Table 2. The particle size of Vydac silica is larger and it has a smaller surface area (per gram), so the percentage of bonded phase surface coverage or the extent of interaction with the solutes will be different from Kromasil. Through the modification of the two different kinds of silica, it is possible to evaluate the effect of the surface area of the solid support on the quality of the bonded phases and thus the efficiency of separations.

Table 2. Properties of Vydac and Kromasil Silica .

Silica	particle size	pore size	surface area
Kromasil silica	5.0 μm	100 A	340 m^2/g
Vydac silica	6.5 μm	300 A	106 m^2/g

2. Methods for Synthesis of Bonded Phases

Due to the improvement of modifications on silica surfaces for HPLC, the stability and the reproducibility of chemically bonded stationary phases has been greatly increased and their applications have been extended further. The bonding of organic moieties to silica is based on the chemistry of the silanol groups on the surface. The first reported successful modification involved esterification of the silanol group by an alcohol²⁷ as shown in Figure 12a. The Si-O-C bond linkages formed are hydrolytically unstable and so such a modified silica stationary phase cannot be used for aqueous mobile phases.

Organosilanization is another well-established method used for the attachment of an organic moiety to silica. It can be carried out by reacting silica with a organosilating reagent $\text{X-SiR}_1\text{R}_2$ to form a monomeric or polymeric layer of organic bonded phases²⁷⁻²⁹ as shown in Figure 12b. The resulting form of the bonded phases depends on the experimental conditions and it has been proved that it is more reproducible to control the conditions for the synthesis of the monomeric layers. In organosilanization, new Si-O-Si-C bond linkages are formed which are hydrolytically unstable at pHs smaller than 2 or greater than 8. It often gives relatively lower organic surface coverage. As a consequence, there will be a significant number of silanol groups left on the surface. This

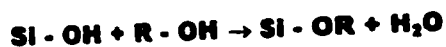


Figure 12a. Esterification of silanol group by alcohol.

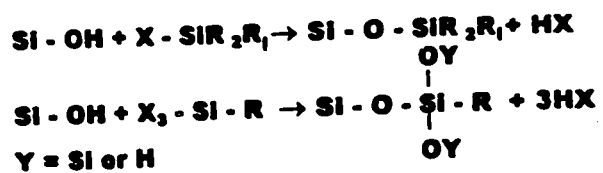


Figure 12b. Organosilanization

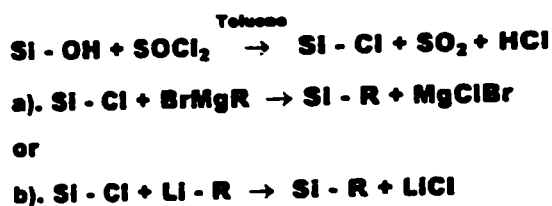


Figure 12c. Modification by chlorination/organometallic reaction.

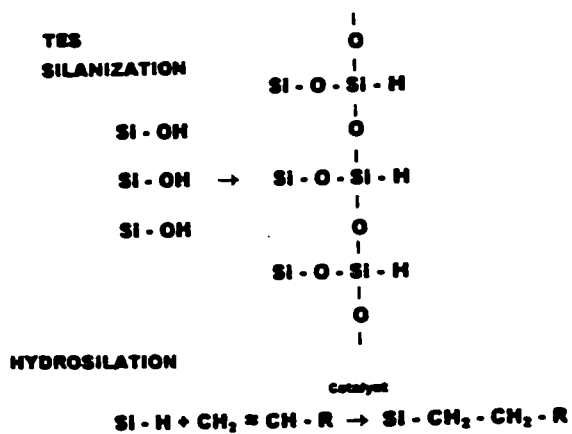


Figure 12d. TES silanization and hydrosilation.

accounts for the residual adsorption and tailing observed, thus the efficiency of the column will be reduced.

To improve surface coverage and stability, methods of producing a direct Si-C bond have been developed. One strategy is to employ a chlorinating reagent such as thionyl chloride followed by reaction with a Grignard reagent or an organometallic compound (Figure 12c). The organic moiety is then bonded to the silica surface through a direct Si-C linkage which is hydrolytically stable^{27,28,30,31}. However, this process is a two step synthesis which is more difficult compared to the traditional organosilanization method. Furthermore, the reaction conditions have to be absolutely dry because the Grignard reagent is very sensitive to moisture and the chlorinated surface can also be hydrolysed easily.

A better approach which results in reproducible modification with reasonable carbon coverage is shown in Figure 12d. This method involves the conversion of the Si-OH (silanol) groups on silica by triethoxysilane (TES silanization) to a hydride-based surface³²⁻³⁴. The Si-H is then reacted with a terminal olefin in the presence of the catalyst to give a direct Si-C bond. One common catalyst used is hexachloroplatinic acid (Speier's catalyst)³¹. The second step is similar to the electrophilic addition reaction of alkene chemistry and so it is called hydrosilation. The resulting addition product has an anti-Markovnikov configuration²⁸. The formation of the Si-C bond is more stable compared to the Si-O-Si-C linkage. This allows the stationary phase prepared by TES silanization/hydrosilation to be used under more aggressive mobile phase conditions. The greater bonded phase stability leads to a longer column life and better precision in retention. In

this research work, the TES silanization / hydrosilation method was adopted for the synthesis of the chiral stationary phases. Therefore, the chiral selectors chosen all possess a terminal olefin.

Even though hydrosilation of the hydride-based bonded intermediate has shown promising results in the preparation of the chemically bonded phases, there are two drawbacks. First, there may be reduction of the catalytic metal complex which leads to the deposition of metal on the surface of the silica³⁵. Second, the attachment of the organic moiety to the surface involves the formation of an intermediate complex, which may cause steric hinderance in the bonding process thus lowering the possibility of interaction between the silanol and the olefin. Instead of using a metal complex as a catalyst, hydrosilation can be performed via a free radical mechanism³⁶. There have been preliminary studies showing that quite a wide variety of functional groups can be bonded to the silica surface with a small degree of polymerization. The resulting modified surface is comparable to that synthesized by metal complex hydrosilation. Two common free radical initiators that can be used are AIBN and tert-butyl peroxide.

Because of the reasons listed above, the synthesis of a β -CD chiral stationary phase could also be done via a free-radical mechanism using tert-butyl peroxide as the initiator. In the previous study, only straight chain olefins or diols have been used to explore the feasibility of hydrosilation via the free radical mechanism. Thus, the applicability of such a mechanism can be further extended through the study of the attachment of a huge cyclic molecule like β -CD to the silica hydride surface.

In summary, the various syntheses of chiral bonded phases attempted in this study are shown in Table 3 below:-

Table 3. Summary of syntheses of chiral stationary phases

Chiral selector	Synthesis method
Cyclodextrin on Vydac silica	TES silanization/hydrosilation by Speier's catalyst
Cyclodextrin on Kromasil silica	TES silanization/hydrosilation by Speier's catalyst
Cyclodextrin on Kromasil silica	TES silanization/hydrosilation via free radical mechanism using tertbutyl peroxide
(R)-(+) Acryloxy- β,β -dimethyl- γ -butyrolactone on Kromasil silica	TES silanization/hydrosilation by Speier's catalyst
(8S,9R)-(-)-N-Benzylcinchonidium chloride on Kromasil silica	TES silanization/ hydrosilation via Speier's catalyst
(R)-(+)- Limonene on Kromasil silica	TES silanization/hydrosilation via Speier's catalyst

F. Goal

The goal of this project was to synthesize different chiral stationary phases and to study their applications for enantiomeric separations by HPLC. The chiral selectors that were chosen for study include 2-hydroxy-3-methacryloyloxypropyl- β -cyclodextrin (substituted β -CD), (R)-(+)-acryloxy- β,β -dimethyl- γ -butyrolactone (LACT), (R)-(+)-Limonene (LIM) and (8S,9R)-(-)- N- Benzylcinchonidium chloride (BENZ). The structures of the chiral selectors studied are shown in Figure 8. This research is divided into three parts: (1) Synthesis of the chiral stationary phases using the modification of the silica surface by TES silanization followed by hydrosilation of the chiral selector on the

surface . (2) Characterization of the modified silica surface by spectroscopic techniques (Cross Polarization Magic Angle Spinning Nuclear Magnetic Resonance Spectroscopy and Diffuse Reflectance Infrared Fourier Transform Spectroscopy) and elemental analysis. (3) Investigation of applications of the newly synthesized CSPs for the separation of dansyl-DL-amino acids, drugs and benzodiazepines by reversed phased HPLC using a methanol/water mobile phase system.

Chapter II

EXPERIMENTAL

A. Materials

1. Chemicals

The Chemical Abstracts Service (CAS) registry numbers of all the compounds used in the synthesis of bonded phases and the chromatographic studies are listed in Table 4.

Table 4. CAS registry numbers of chemicals

Chemical Name	CAS Registry Numbers
Beta W7 MAHP 0.1/0.4 Lodextrin (β -CD)	no CAS number assigned
(R)-(+)- Acryloxy- β , β -dimethyl- γ -butyrolactone	[1020-96-60-6]
(R)-(+)- Limonene	[5989-54-8]
(8S,9R)-(-)- N- Benzylcinchonidium chloride	[69257-04]
Chlorodoazepoxide	[58-25-3]
Chloroplatinic acid hexahydrate	[16941-12-1]
Clenbuterol	[21898-19-1]
Clonazepam	[1622-61-3]
Dansyl-DL-Leucine	[102783-70-0]
Dansyl-DL-Methionine	[42808-13-9]
Dansyl-DL-Norvaline	[102783-76-6]
Dansyl-DL-Phenylalanine	[42808-06-0]
Dansyl-DL-Threonine	[24540-66-9]
Dansyl-DL-Tryptophan	[102703-324]

Chemical Name	CAS Registry Number
Dansyl-DL-Serine	[42808-14-0]
Dansyl-DL-Valine	[84540-670]
Diethyl ether	[60-29-7]
Dioxane	[17647-74-4]
Ethanol	[64-17-5]
Hydrochloric acid	[7647-01-0]
DL-Homatropine	[51-56-9]
Isopropanol	[67-63-0]
Methanol	[67-56-1]
Nitrazepam	[146-22-5]
Oxazepam	[604-75-1]
Terbutaline	[23031-32-5]
Tert-butyl peroxide	[110-05-4]
Temazepam	[849-50-4]
Tetrahydrofuran	[109-99-8]
Toluene	[108-88-33]
Triethoxysilane (TES)	[998-30-1]
Tropicamide	[1508-75-4]

2. Materials for Synthesis of Bonded Phases

The silica supports are Vydac TP106 Batch#7 (particle diameter:6.5um, pore diameter:300A. specific surface area: 106 m²/g), a product from The Separations Group (Hesperia, CA) and Kromasil (Lot#AT0112, particle diameter: 5.0 μm, pore diameter: 100A, specific surface area: 340 m²/g). The silica was first modified by triethoxysilane (Aldrich Chemical Co., Milwaukee, WI, Lot #CN00401CN) with 2.3M hydrochloric acid

in dioxane (Aldrich Chemical Co., Milwaukee, WI) to form a hydride silica intermediate. Afterwards, the hydride material was reacted with the chiral selectors. One of the chiral selectors, 2-hydroxy-3-methacryloyloxypropyl- β -cyclodextrin, is a new product from Germany (Wacker Chemical Co., Norwalk, CT). The other chiral selectors (R)-(+)-limonene, (8S, 9R)-(-)-N-benzylcinchonidinium chloride and (R)-(+)-acroyloxy- β , β -dimethyl- γ -butyrolactone were purchased from Alrich Chemical Co. (Milwaukee, WI). Chloroplatinic acid hexahydrate (Strem Chemicals, Newburyport, MS) in 2-propanol (Aldrich Chemical Co., Milwaukee, WI) was used in catalytic hydrosilation. For free radical hydrosilation, tert-butylperoxide (Aldrich Chemical Co., Milwaukee, WI) was used. Absolute methanol (General Chemicals, Pittsburg, CA), absolute ethanol (Shield Chemical Co., Rossville, CA), toluene (Fisher Scientific, Fair Lawn, NJ), and diethyl ether (Fisher Scientific, Fair Lawn, NJ) were also obtained in reagent grades for the washing steps.

B. Synthesis Procedures

1. Preparation of Speier's Catalyst

A 10 mM hexachloroplatinic acid was used as the catalyst in the hydrosilation. Because the compound is highly reactive, it was opened under nitrogen atmosphere and about 0.0400 g of the solid hexachloroplatinic acid hexahydrate was weighed and dissolved in 100.00 mL of 2-propanol in a volumetric flask. The resulting solution was thoroughly-mixed and kept in the freezer.

2. Preparation of 1.0mM Triethoxysilane (TES)

Because Triethoxysilane (5.326 mM) can polymerize easily upon exposure to air, the preparation was carried out in a glove box which provides an inert nitrogen atmosphere. All of the apparatus was dried in the oven for 3 hours before the preparation. Initially, all the dried glassware and required reagents were put in the glove box which was then sealed. To create an inert environment (N_2), the air inside the glove box was evacuated by vacuum and then it was flushed with nitrogen gas. The flushing process was repeated three times to ensure the environment was inert. In order to prepare 45.00 mL of 1.0 mM TES, 8.45 mL of 5.326 mM TES were measured and mixed with 36.55 mL of dioxane in the nitrogen glove box. The 5.326 mM TES reagent was further flushed with nitrogen gas before it was sealed and it was put in a dessicator for storage.

3. Preparation of silica hydride³⁴

a. Vydac Silica hydride

All the apparatus was dried in the oven overnight. Silica hydride was prepared by refluxing Vydac silica (CAT#101TPB6.5) with 1.0 mM Triethoxysilane (TES) in the presence of 2.3 mM hydrochloric acid in dioxane as the solvent.

A portion of 9.9809 g of Vydac silica was transferred to a 500 mL three-necked round bottom flask equipped with a West condenser, addition funnel and a thermometer. A portion of 245.00 mL of dioxane was added followed by 10.00 mL of 2.3 mM HCl solution. The mixture was stirred and heated under reflux at 93.0°C for about 1 hour. Then, 45.00 mL of 1.0 mM TES was added dropwise from an equalized pressure addition funnel to the reaction flask over a period of 25 to 30 minutes. After completing the

addition of TES solution, the reaction mixture was further refluxed at 93°C for another hour. The final silica hydride product was then poured into four centrifuge tubes and centrifuged for 10 minutes at 1500 r.p.m. using an IEC-HN-S system. The supernatant dioxane was poured off and the sample was further washed to remove the impurities.

The final product, Vydac hydride, was washed two times with tetrahydrofuran, two times with 1:1 V/V tetrahydrofuran/water mixture and finally two times with diethyl ether. In the washing procedure, about 15 mL of the washing solvent was added to the centrifuge tubes and the mixture was stirred gently for 10 minutes. They were then centrifuged at 1500 r.p.m for 10 minutes. Afterwards, the washing solvent was poured off and another washing solvent was added until the sample was finally washed with diethyl ether. Finally, the sample was dried in the hood to allow diethyl ether to evaporate and then it was put in vacuum oven at 110°C overnight.

b. Kromasil silica hydride

The same procedure as for the synthesis of Vydac silica hydride was used. Because Kromasil silica has a large surface area (340m²/g), the amount of 1.0 mM TES used was three times as the amount used in the synthesis of Vydac silica hydride for the same amount of silica.

In the preparation of Kromasil silica hydride, 5.0102 g of Kromasil silica was heated in 392 mL of dioxane under reflux for one hour. Then, 72 mL of 1.0 mM TES was added dropwise into the reaction flask over a period of 25 to 30 minutes. The reaction continued for one more hour after the addition of TES. Upon the completion of the reaction, dioxane was decanted and the sample was washed three times with

tetrahydrofuran, three times with a 1:1 V/V tetrahydrofuran/water mixture and three times with diethyl ether. Finally, the sample was dried in the hood to remove the traces of ether and the final product was put in the vacuum oven overnight before further spectroscopic characterization was carried out.

4. Preparation of Chiral bonded phases³⁴

In this research, all four chiral selectors chosen for study have a terminal double bond and so hydrosilation either by Speier's catalyst or by free radical addition can be used in the synthesis of the bonded phases.

a. Synthesis of β -cyclodextrin bonded chiral stationary phase on Kromasil silica hydride using Speier's catalyst

A portion of 5.1929 g of Kromasil silica hydride was dried in a vacuum oven overnight before the modification was carried out. All the necessary glassware was rinsed with methanol and deionized water and put in the oven overnight.

The experimental set up consisted of a 150 mL three necked round bottom flask equipped with a west condenser, a thermometer and a nitrogen venting system. A drying tube was further connected to the top of the west condenser to preclude moisture. Then, 3.1120 g of β -cyclodextrin was dissolved in 90.00 mL of a 3:1 V/V methanol/ethanol solvent system and added to the flask followed by 1200.00 μ L of Speier's catalyst. The mixture was then heated to 70°C under reflux for about 1 hour and the dried 5.1929g of Kromasil silica was added to the flask. The system was then flushed with a slow stream of

nitrogen gas for about 5 seconds and the reaction was allowed to proceed for 5 days at 70°C.

After the reaction was complete, the mixture was poured into four centrifuge tubes and they were centrifuged at 1500 r.p.m for about 10 minutes. The supernatant solvent was poured off and the sample was further washed four times with a 3:1 V/V methanol/ethanol mixture and four times with diethyl ether. The washed sample was then dried in the hood to evaporate off the ether and then dried in a vacuum oven overnight.

b. Synthesis of β -cyclodextrin bonded chiral stationary phase on Kromasil silica using free radical tert-butyl peroxide.³⁶

A portion of 0.6990 g of Kromasil hydride was put in a vacuum oven overnight and all the glassware was put in the oven for drying.

A 50 mL three-necked round bottom flask was equipped with a thermometer, west condenser and a stopper. 0.3006 g of β -cyclodextrin was dissolved in 15.00 mL of a 3:1 V/V methanol/ethanol solvent system. The solution was added into the reaction flask followed by 36 μ L of tert-butyl peroxide. The mixture was heated under reflux at 68°C for one hour. Then 0.6990 g of dried Kromasil hydride was added and the system was flushed with nitrogen gas for 5 seconds. The solution was further heated under reflux for 5 days.

After 5 days, the solvent was poured off and the sample was washed four times with 15 mL of 3:1 V/V methanol/ethanol and four times with 15 mL of diethyl ether.

The washed product was put in a hood overnight to evaporate the ether and the final sample was dried in a vacuum oven.

c. Synthesis of β -cyclodextrin bonded chiral stationary phase on Vydac silica hydride using Speier's catalyst.

The experimental set up, procedure and conditions were the same as for Kromasil hydride (Section 4a). In this synthesis, 2.6037 g of Vydac silica hydride was reacted with 1.5222 g of β -cyclodextrin in the presence of 300.00 μ L of Speier's catalyst in 60.00 mL of a 3:1 V/V methanol/ethanol solvent system. The final product was washed four times with 15 mL of a 3:1 V/V methanol/ethanol mixture and four times with 15 mL of diethyl ether. The washed sample was placed in a hood overnight to remove the ether and then put in a vacuum oven overnight.

d. Synthesis of (R)-(+)-acryloxy- β,β -dimethyl- γ -butyrolactone chiral bonded stationary phase on Kromail silica hydride

A portion of 2.8046 g of Kromasil silica hydride was dried in a vacuum oven overnight before the modification was carried out. All the necessary glassware was rinsed with methanol and deionized water and put in an oven overnight.

In a 150 mL three necked round bottom flask which was equipped with a West condenser, a thermometer and a nitrogen venting system, 3.9 mL of (R)-(+)-acryloxy- β,β -dimethyl- γ -butyrolactone was mixed with 40.82 mL of toluene. In addition, 4.75 mL of Speier's catalyst was added to the flask. The top end of the West condenser was connected to a drying tube to exclude moisture. The mixture was then heated to 80°C

under reflux for about 1 hour. Afterwards, 2.8046 g of dried Kromasil hydride was added to the flask. The system was then flushed with a slow stream of nitrogen gas for about 5 seconds and the reaction was allowed to proceed for 5 days at 80°C.

After the reaction was completed, the mixture was poured into four centrifuge tubes and they were centrifuged at 1500 r.p.m for about 10 minutes. The supernatant toluene solvent was poured off and the sample was further washed three times with 15 mL of toluene, three times with 15ml of tetrahydrofuran , three times with 15 mL of a 1:1 V/V tetrahydrofuran/water and finally three times with 15 mL of diethyl ether. The washed sample was placed in a hood to evaporate the ether and then dried in the vacuum oven overnight.

e. Synthesis of (8S,9R)-(-)-N-benzylcinchonidium chloride chiral stationary phase on Kromasil silica hydride

A portion of 0.3250 g of Kromasil silica hydride was dried in a vacuum oven overnight before the modification was carried out. All the necessary glasswares was rinsed with methanol and deionized water and put in an oven overnight.

In a 50 mL three necked round bottom flask which was equipped with a West condenser, a thermometer and a nitrogen venting system, 0.4181 g of (8S,9R)-(-)-N-benzylcinchonidium chloride was dissolved in 15.00 mL of 3:1 V/V methanol/ethanol. Then, 180 µL of Speier's catalyst was added to the flask. The top end of the West condenser was connected to a drying tube to exclude moisture. The mixture was then heated to 68°C under reflux for about 1 hour. Next, dried 0.3250 g of dried Kromasil hydride was added to the flask. The system was then flushed with a slow stream of

nitrogen gas for about 5 seconds and the reaction was allowed to proceed for 5 days at 68°C.

After the reaction was completed, the mixture was poured into four centrifuge tubes and they were centrifuged at 1500 r.p.m for about 10 minutes. The supernatant toluene solvent was poured off and the sample was further washed three times with 15 mL of a 3:1 V/V methanol/ethanol mixture and finally three times with 15 mL of diethyl ether. The washed sample was then placed in a hood to evaporate off the ether and then dried in a vacuum oven overnight.

f. Synthesis of (R)-(+)-Limonene chiral bonded stationary phase on Kromasil silica hydride

A portion of 0.4419 g of Kromasil silica hydride was dried in a vacuum oven overnight before the modification was carried out. All the necessary glassware was rinsed with methanol and deionized water and put in an oven overnight.

In a 50 mL three necked round bottom flask which was equipped with a West condenser, a thermometer and a nitrogen venting system, 1.50 mL of (R)-(+)-limonene was mixed with 20.00 mL of toluene. Next, 400 µL of Speier's catalyst was added to the flask. The top end of the West condenser was connected to a drying tube to exclude moisture. The mixture was then heated to 100°C under reflux for about 1 hour. Then, 2.8046 g of dried Kromasil hydride was added to the flask. The system was then flushed with a slow stream of nitrogen gas for about 5 seconds and the reaction was allowed to proceed for 5 days at 100°C.

After the reaction was completed, the mixture was poured into four centrifuge tubes and they were centrifuged at 1500 r.p.m for about 10 minutes. The supernatant toluene solvent was poured off and the sample was further washed three times with 15 mL of toluene, three times with 15 mL of tetrahydrofuran, three times with 15 mL of 1:1 V/V tetrahydrofuran/water and finally three times with 15 mL of diethyl ether. The washed sample was then placed in a hood to evaporate the ether and then dried in a vacuum oven overnight.

C. Instrumentation and Operating Procedures

1. Diffuse Reflectance Infrared Fourier Transform Spectrometry (DRIFT)

The infrared spectra of all the bonded phase silica samples and the reactants were run on a Perkin Elmer Model 1800 FT-IR Spectrophotometer (Norwalk, CT). The spectrophotometer consists of a demountable sample compartment, a laser infrared light source, an interferometer and a deuterated triglycine sulfate (DTGS) detector. In order to increase the sensitivity of the output, the signal was obtained in the diffuse reflectance mode. The sample was mixed with an equal weight portion of spectral grade potassium bromide and the final mixture was placed in a small 2mm diameter x 2mm depth sample cup. A uniform and flat top sample surface can be achieved by smoothing the surface using a glass plate. After placing the sample in the compartment, the whole system is purged with nitrogen gas at 55-65 psi for about 15-30 minutes depending on the humidity in the laboratory. A pure sample of KBr is run as the reference background signal. Each spectrum was scanned 100 times at a resolution of 2 cm^{-1} from 4000 cm^{-1} to 450 cm^{-1} .

The signal intensity was normalized to 100% transmittance. The data signal was analyzed by a Perkin Elmer Series 7500 Professional Computer and the final spectra were plotted by a Hewlett Packard 7475A Plotter (Palo Alto, CA).

2. Cross-Polarization Magic Angle Spinning Nuclear Magnetic Resonance Spectroscopy (CP-MAS NMR)

The CP MAS C-13 and Si-29 NMR spectra were obtained on a Bruker (Billerica, MS) MSL 300 Mhz spectrometer. The cross polarization technique is employed to transfer the resonance nuclear spin energy from proton to carbon and silicon in order to increase the sensitivity of detection. In addition, the sample is spun at a magic angle so that narrow lines are obtained. The solid samples were placed in ZrO₂ double bearing rotor and spun at a frequency of 4700-5200Hz. The signals were obtained with a 5-msec contact time and 5-μsec repetition rate. Pulse widths for ¹³C and ²⁹Si were 6.5-μsec and 5.0-μsec respectively. The probe temperature was maintained at 20 ±2 °C. The chemical shifts in ¹³C spectra were referenced to an the external glycine standard while those in the ²⁹Si spectra were referenced to an external polyhydridosiloxane sample.

3. Elemental Analysis

The bonded phase silica samples were sent to Desert Analytics (Tucson, AZ) for the determination of percentage carbon. Such a determination is based on the results from the combustion analysis of the sample³⁷. Then the surface coverage, α_R, of the bonded groups (organic moiety) can be calculated from the percentage carbon as follows³⁸:-

$$\alpha_R (\mu\text{mol}/\text{m}^2) = 10^6 P_c / (100 M_c n_c - P_c M_R) S_{\text{BET}}$$

where P_c is the carbon percentage difference between the modified silica bonded phases and the silica hydride; n_c is the number of the carbon atoms in the bonded groups; M_c and M_R are the the molar mass of carbon and the bonded molecules respectively, and S_{BET} is the specific surface area of the silica/hydride substrate determined by the Brunauer, Emmet and Teller nitrogen adsorption method.

In the calculation of the surface coverage for substituted β -cyclodextrin, we can take an average of 58 carbons per cyclodextrin molecule, which is based on the substitution of one methacryloyloxy group and three hydroxy-propyl groups attached to one cyclodextrin molecule.

4. Column Packing

All bonded phases were packed into stainless steel columns supplied by Alltech, Deerfield, IL. In the column packing procedure, about 1.8 grams of the bonded silica was added to a 9:1 V/V tetrachloromethane/methanol mixture to form a homogeneous suspension. The column was attached to a Haskell Pump (Burbank, CA) column packer. The suspension was then poured into the reservoir of the column packer and the column was packed at 6000 psi pressure using nitrogen. Filtered HPLC grade methanol was used as the solvent for packing. The packed column was allowed to remain at high pressure for about 30 minutes to ensure uniformity of packing. Four different columns were packed for this research and the details are listed in Table 5 below:-

Table 5: Chiral column packed

Bonded silica stationary phase	stainless steel column dimension
Kromasil Silica modified with β -cyclodextrin	internal diameter 4.6mm x 150mm
Kromasil Silica modified with β -cyclodextrin	internal diameter 4.6mm x 50mm (short)
Vydac Silica modified with β -cyclodextrin	internal diameter 4.6mm x 150mm
Kromasil Silica modified with Lactone	internal diameter 4.6mm x 150mm

5. High Performance Liquid Chromatography

Two HPLC systems were used in testing the applications of the newly developed chiral stationary phase. All the preliminary analyses were done on a Hitachi system while the temperature effects on the chiral separations were carried out on a Perkin Elmer system. The Hitachi HPLC system consisted of a tertiary pumping system, a Hitachi L-6200, where the mobile phases are mixed and pumped through the column to the detector. The flow rate for the analysis varied from 0.06 mL/min to 0.50 mL/min depending on the back pressure of the column and the retention of the samples. The samples were injected through a six-valve injector port (7125NS, Rheodyne) with a 10 μ L sample loop and were detected by a UV-Visible multi-wavelength detector (Hitachi L-4000). All the measurements in this research were made at 254nm and recorded on a Chromatojet intergrator manufactured by Spectra-Physics.

The Perkin Elmer (Norwalk, CT) HPLC system was equipped with a Series 200LC Pump and a Perkin Elmer LC295 Multi-wavelength UV-visible detector. The chromatograms were plotted on a Hewlett Packard Model 3395 Integrator. The samples

were injected through a Rheodyne 7125 six port injector with a 20 μ L sample loop. The flow rate for all the analyses done on 4.6mm x 150mm columns using the Perkin Elmer HPLC system was 0.20 mL/min with a mobile phase system consisting of 30% MEOH/70% H₂O. In the case of the short column (46mm x 50mm), the flow rate was set at 0.15 mL/min. Temperature effect studies were done by putting the column in a thermostated jacket (Fiatron, CH30). Only the most promising separations obtained in the preliminary studies were further analyzed at 40°C, 50°C and 60°C.

For all the analyses, the solvents were degassed by using compressed helium at a flow rate of 50 mL/min through a sparging system manufactured by Spectra Physics. This procedure can prevent the formation of any air bubbles in the tubing. In the analyses, a mixture of methanol (Fisher Scientific, Fair Lawn, NJ) and deionized water was used as the mobile phase. The solvent was first filtered through a 0.20 μ m nylon membrane to remove any fine particles that may cause damage to the column before it is loaded into the solvent reservoirs. Equilibration of new columns involved flushing with methanol overnight at a flow rate of 0.01 mL/min. Also, in order to extend the column life, they were flushed with methanol for 10 minutes at a flow rate of 0.1 -0.2 mL/min at the end of the day.

Chapter III

RESULTS AND DISCUSSION

In this research study, attachment of the chiral selectors with a terminal olefinic group to a silica hydride intermediate was done via hydrosilation. An alternate method of synthesis by free radical initiation was also investigated. The success of the bonding processes was evaluated by elemental analysis, DRIFT spectroscopy and CP-MAS NMR spectra. Preliminary chromatographic studies on the successfully synthesized chiral stationary phases were carried out by reversed phase HPLC using a methanol/water mobile phase. The samples, which included dansyl-DL-amino acids, benzodiazepines, clenbuterol, DL-homatropine, tropicamide, terbutaline, were chosen for study as representative chiral compounds that have already been separated on similar types of commercial columns.

A. Elemental Analysis Results

From the percentage carbon analyses, surface coverage, α_R , can be calculated, which indicates quantitatively how well the silica surface was modified by the chiral selectors. A greater surface coverage means more of the organic moiety (chiral selector) has been successfully bonded to the surface and thus better performance will be expected. The surface coverage of the chiral bonded phases in this research is summarized in Table 6 shown below:-

Table 6: The surface coverage and percent carbon of the bonded phases

Chiral stationary phase	Surface Coverage, α ($\mu\text{mol}/\text{m}^2$)	Percent Carbon (% by mass)
β -cyclodextrin on Vydac Silica	0.67	4.51
β -cyclodextrin on Kromasil Silica	0.57	10.57
(R)-(+)- Acryloxy- β,β -dimethyl- γ -butyrolactone on Kromasil silica	1.42	4.79
(R)-(+)- Limonene on Kromasil silica	2.53	9.25
(8S,9R)-(-)- N- Benzylcinchonidium chloride on Kromasil silica	0.26	2.70
β -cyclodextrin on Vydac Silica (big batch for column packing)	0.58	3.96
β -cyclodextrin on Kromasil Silica (Big batch for column packing)	0.36	7.33
(R)-(+)- Acryloxy- β,β -dimethyl- γ -butyrolactone on Kromasil silica (big batch for column packing)	1.27	4.34

The calculated surface coverage of the four β -cyclodextrin samples, all in the range of 0.36-0.67 $\mu\text{mol}/\text{m}^2$, are less than 10% of the maximum surface modifiable silanol groups (8 $\mu\text{mol}/\text{m}^2$). However, this small value is not unreasonable because the substituted cyclodextrin is a very large oligosaccharide molecule with a molecular weight of about 1400 g/mol. Besides, the surface coverages for the (R)-(+)-acryloxy- β,β -dimethyl- γ -butyrolactone and (R)-(+)-limonene are satisfactory. The small surface coverage obtained for (8S,9R)-(-)- N- benzylcinchonidium chloride indicates the extent of

the hydrosilation was very small for this compound. This might be explained by the bulkiness of the molecule near the olefin carbons or perhaps because it is a charged species (ionic) which may affect the efficiency of the hydrosilation reaction.

B. Spectroscopic analysis for the confirmation of the bonding of the chiral selector on the silica

1. Success of TES silanization

a. CP-MAS NMR spectra

Figures 13a and 13b are ^{29}Si CP-MAS NMR spectra for the Kromasil silica hydride and Vydac silica hydride intermediate respectively. In the Kromasil silica hydride NMR spectrum, the peak at -110 ppm refers to the silicon atoms attached to the siloxane backbone and the peak at -101 ppm represents silicon atoms with surface hydroxyl groups. The intense peak at -84 ppm refers to silicon bonded to hydrogen whereas the peak at -74 ppm is due to a silicon with both a hydrogen and a hydroxyl group^{28,34,39,40}. The presence of the peaks at -84 ppm and -74 ppm indicate the success of the silanization process since they are the result of an Si-H bond in the compound. On the other hand, we can tell that the conversion of silanol groups to Si-H by TES silanization is not complete because of the presence of the peak at -101 ppm due to the Si-OH group³⁹. The incompleteness of the process is probably due to the presence of small pores far from the surface which create steric hinderance for the reaction between silica and the silanization agent. From the relative intensities of the peaks at -84 ppm and -110 ppm, it can be concluded that the extent of the reaction is sufficient.

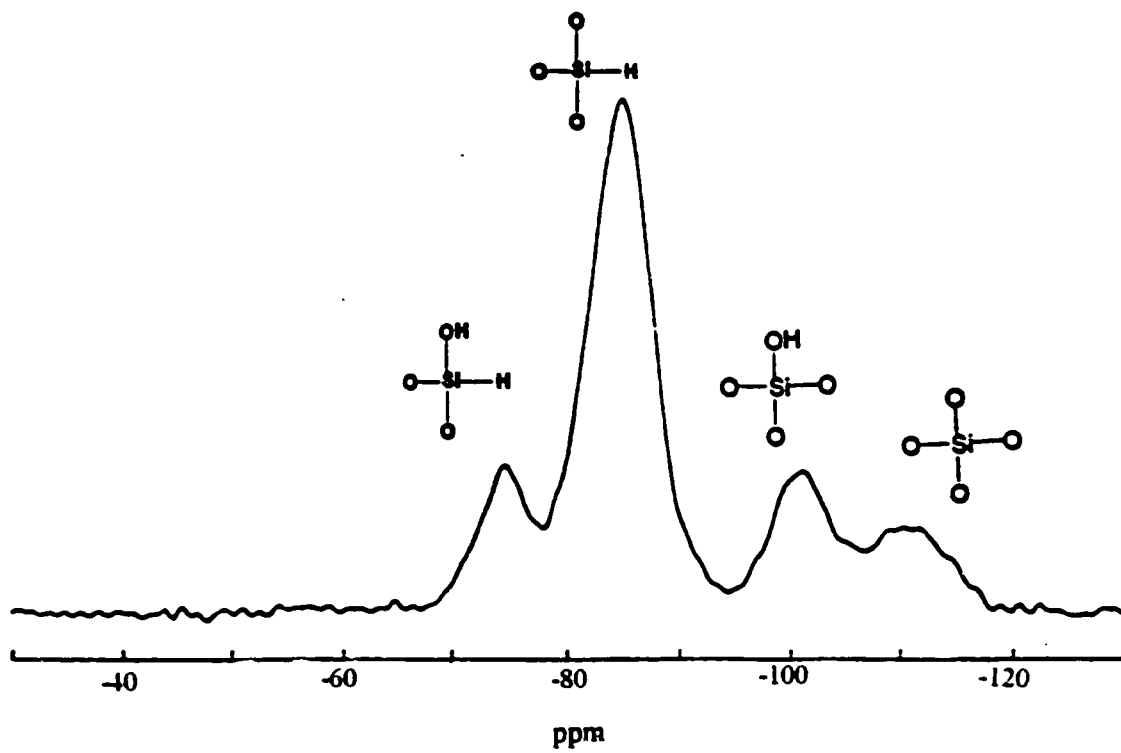


Figure 13a. ^{29}Si CP-MAS NMR spectrum for Kromasil silica hydride.

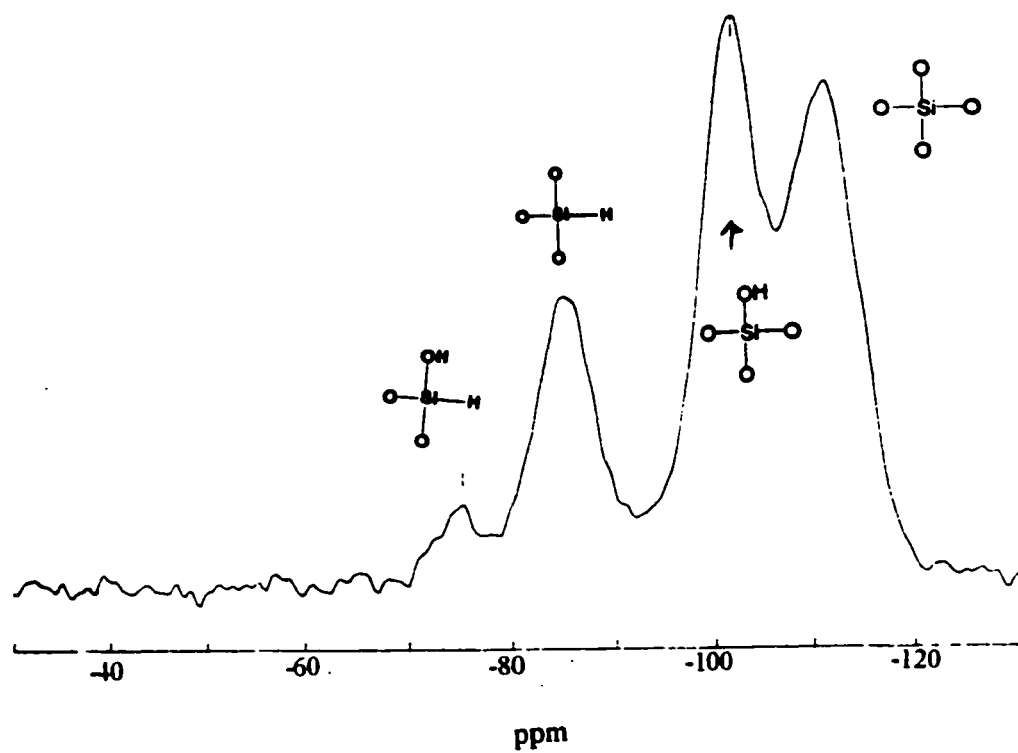


Figure 13b. ^{29}Si CP-MAS NMR spectrum for Vydac silica hydride.

Similar peak assignments can be made for Vydac silica hydride as shown in Figure 13b. The presence of the peak at -85 ppm, which is due to the $\text{O}_3\text{-Si-H}$ group proves the success of the silanization process. At the same time, the peak at -101 ppm shows the incomplete conversion of Si-OH to S-H. The relative peak intensities at -85 ppm and at -101 ppm indicate that there are more silanol groups than Si-H groups existing within the structure. In comparison to Kromasil silica hydride, the efficiency of conversion from Si-OH to Si-H by TES silanization for Vydac silica seems to be lower. This is attributed to a greater percentage of small pores producing severe steric hinderance in the TES reaction.

Fig 14 is a ^{13}C CP-MAS NMR spectrum for Vydac silica hydride. It has a very a low signal to noise ratio despite many scans. Under these conditions, there are no significant peaks due to carbon except two signals at 15 ppm and 58 ppm. These peaks can be assigned to the residual TES $-\text{OCH}_2$ and TES $-\text{CH}_3$ groups respectively³⁹.

b. DRIFT spectra

The success of the silanization of Kromasil silica and Vydac silica can be also seen in the DRIFT spectra shown in Figure 15a and Figure 15b respectively. The intense peaks at about 2250 cm^{-1} in both spectra are due to Si-H bond stretching^{28,34,39,41}, which is strong evidence for the existence of Si-H groups on the surface. Consistent with the NMR spectra, a peak in the range of 3550 cm^{-1} to 3750 cm^{-1} due to O-H stretching of the Si-O-H group⁴¹ shows the presence of residual silanol groups which have not been converted to Si-H on the surface.

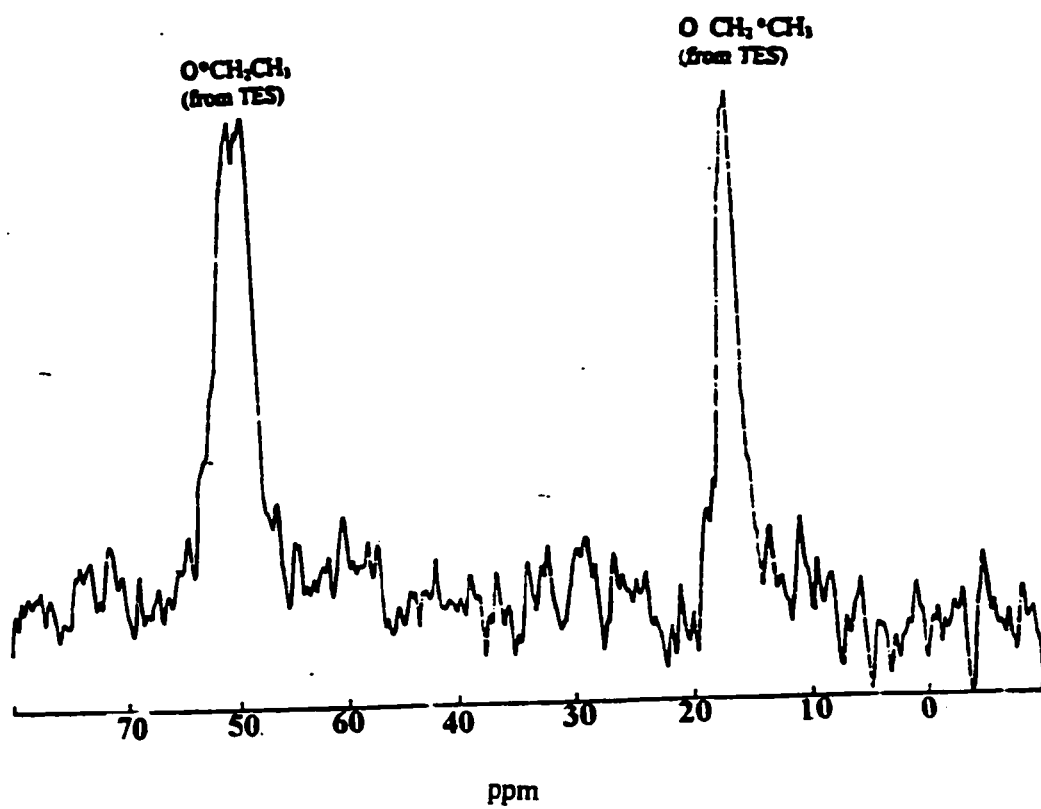


Figure 14. ^{13}C CP-MAS NMR spectrum for Vydac silica hydride.

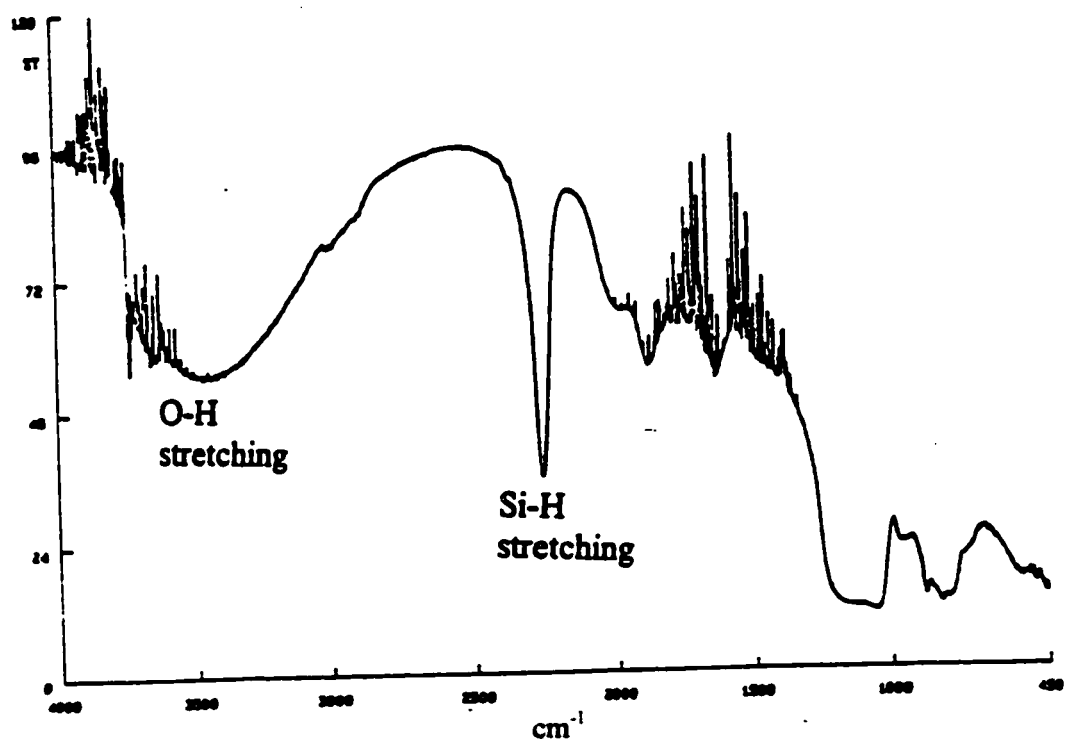


Figure 15a. DRIFT spectrum for Kromasil silica hydride.

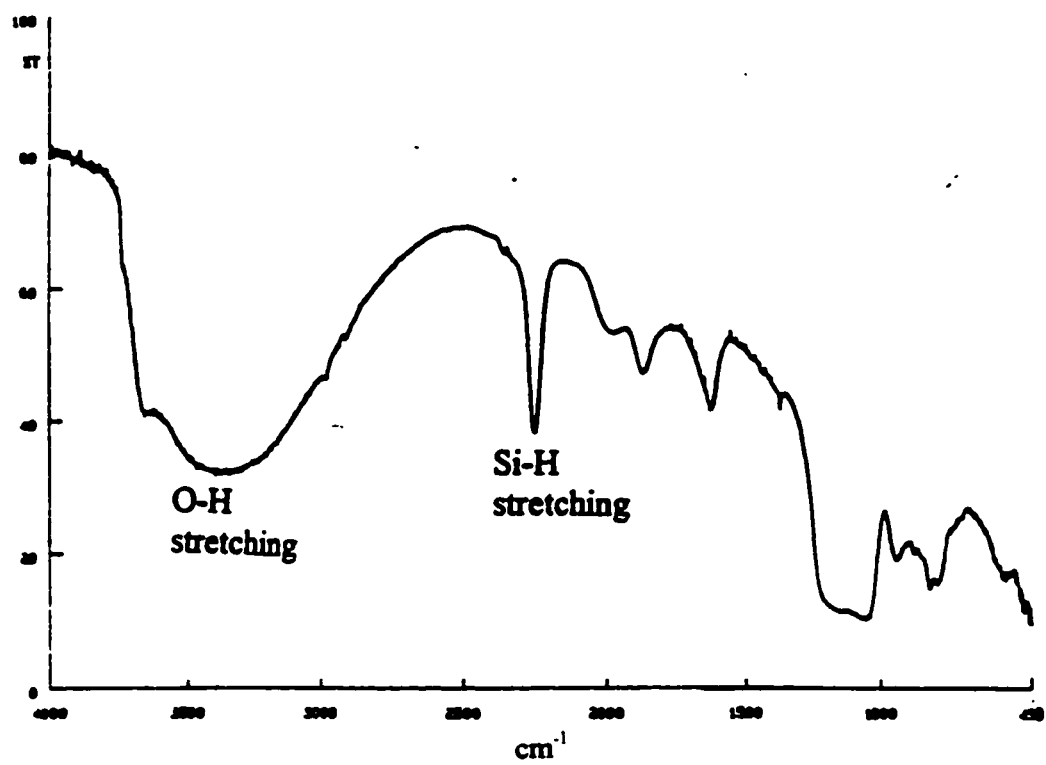


Figure 15b. DRIFT spectrum for Vydac silica hydride.

2. Hydrosilation of β -cyclodextrin on silica hydride intermediate by Speier's catalyst

The extent of bonding for the organic moiety by hydrosilation on silica hydride depends greatly on both the concentration of the organic moiety and the availability of the Si-H groups on the surface. In the hydrosilation of a silica hydride intermediate, a non-polar solvent is more favorable since Si-H can be hydrolyzed at high pH. However, it was found that β -cyclodextrin is not soluble in any non-polar solvent but has a high solubility in water. Other than that, it is sparingly soluble in alcohols such as methanol and ethanol. Hence, in the hydrosilation of silica hydride by β -cyclodextrin, several solvent systems were tested in order to obtain optimized conditions for the bonding. Through the spectroscopic analysis discussed in the following part of this section, the effects of the solvent system on the extent or the success of bonding will be interpreted and explained.

a. Hydrosilation of β -cyclodextrin in 1:1 ethanol/water solvent system on Vydac hydride

In the ^{29}Si CP-MAS NMR spectra (Figure 16a), it was observed that there is a significant decrease in the intensity of the peak at -85 ppm as compared to Figure 13b. In addition, the small peak located at -75 ppm disappeared in this spectrum. It seems that a significant amount of the Si-H was removed after the hydrosilation reaction and this is one possible sign for the success of the bonding. However, in the ^{13}C CP-MAS NMR spectrum (Figure 16b), only two peaks are observed and they are the residual peaks due to TES. Hence, we can confirm that there is no significant bonding between the β -

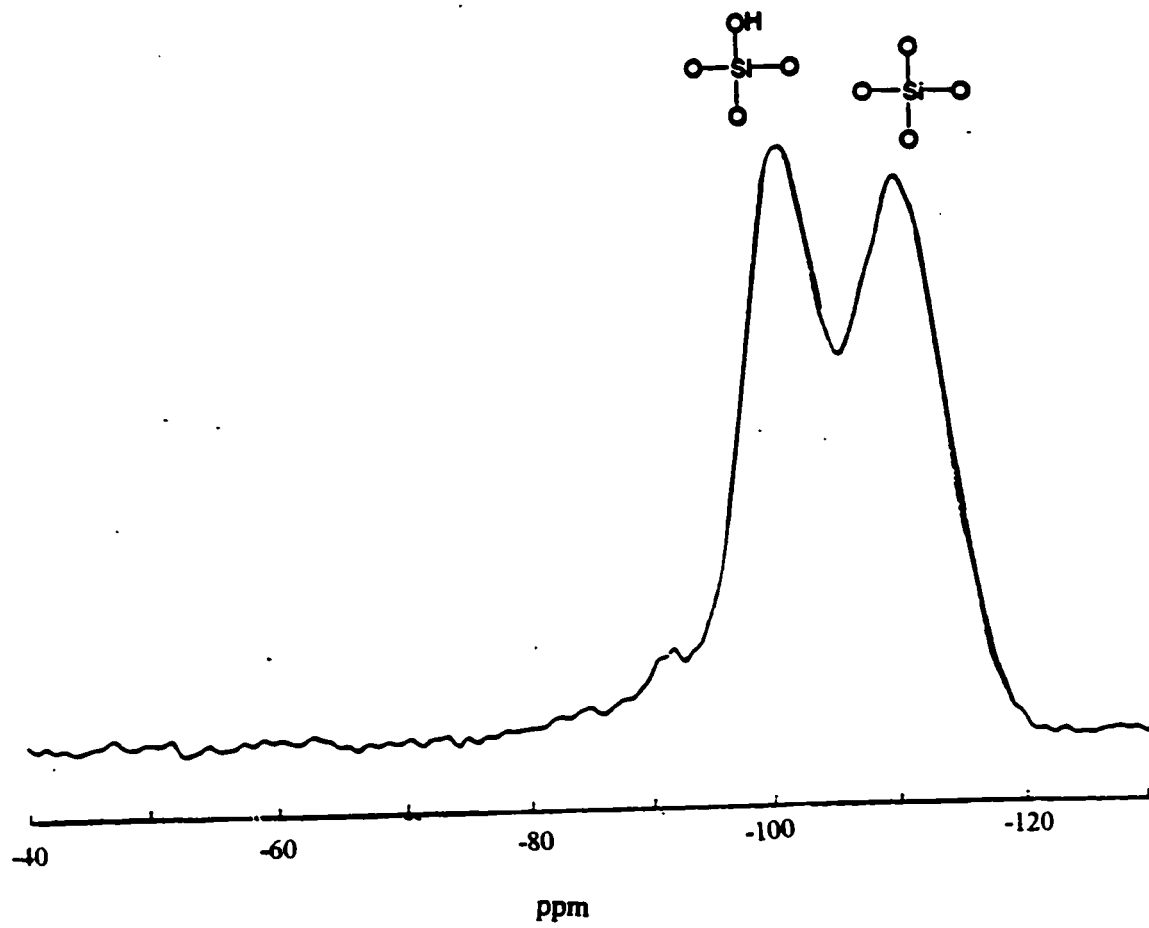


Figure 16a. ^{29}Si CP-MAS NMR spectrum for β -cyclodextrin bonded to Vydac silica hydride (hydrosilation done in 1:1 ethanol/water solvent system).

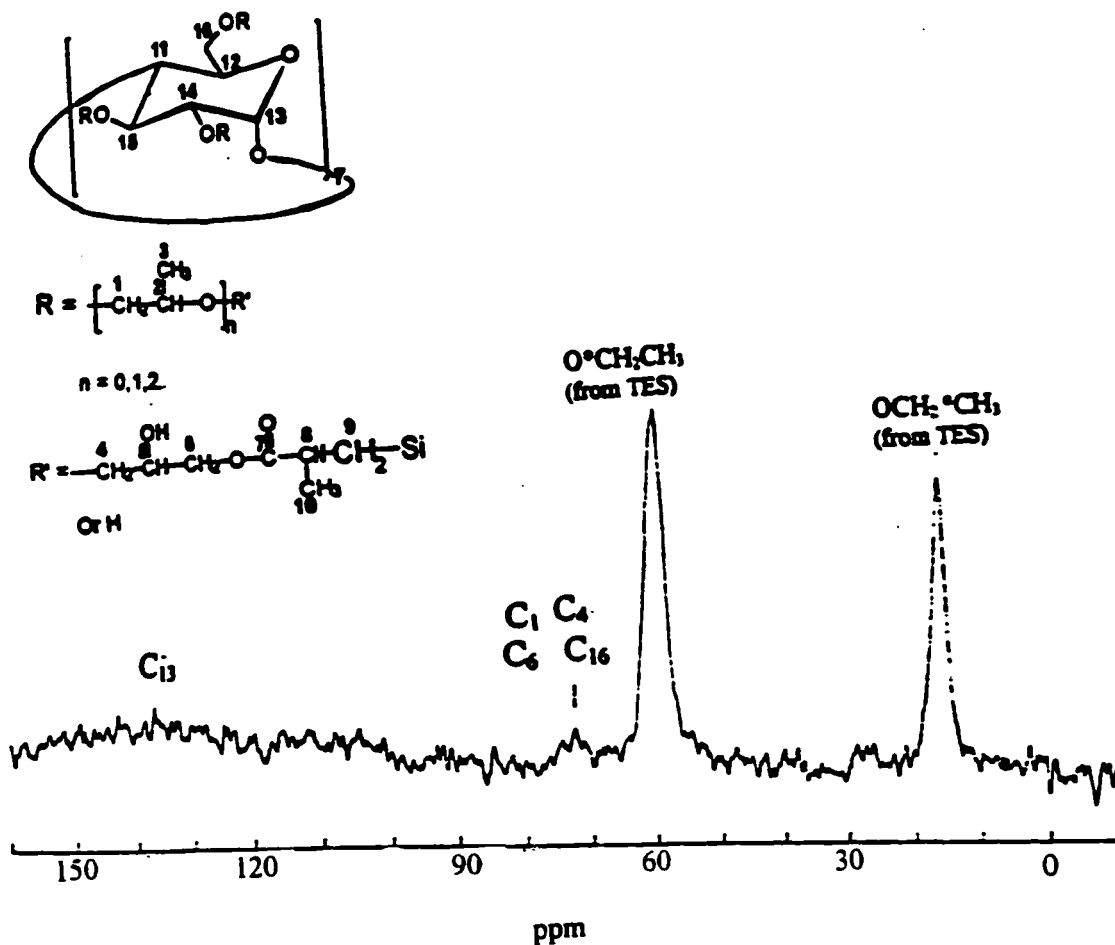


Figure 16b. ^{13}C CP-MAS NMR spectrum for β -cyclodextrin bonded to Vydac silica hydride (hydrosilation done in 1:1 ethanol/water solvent system).

cyclodextrin and the hydride surface. Moreover, two significant features in the DRIFT spectrum (Figure 17) further show the failure to bond the cyclodextrin. First, there is no obvious peak due to C-H bond stretch in the region of 2900 cm^{-1} to 3100 cm^{-1} ^{28,41} and second, the absence of a peak near 1750 cm^{-1} , which is an intense absorption peak that appears in the β -cyclodextrin spectrum (Figure 9a). These results indicate that there is no significant attachment of the chiral selector to the surface. The failure in the hydrosilation may be due to extensive hydrolysis of the Si-H by water or ethanol and thus there would be no Si-H bond available for the attachment. This is consistent with the fact that there is a significant decrease in the peak intensity due to Si-H in both ^{13}C CP-MAS NMR spectrum and the DRIFT spectrum. As a consequence, a solvent system with a low percentage of water was used for hydrosilation to improve the reaction conditions.

b. Hydrosilation of β -cyclodextrin in 19:1 ethanol/water solvent system on Vydac silica hydride

In the ^{29}Si CP-MAS NMR spectrum (Figure 18a), the peak intensity at -85 ppm is greatly diminished and no peak is observed at -75 ppm. Further evaluation of the ^{13}C CP-MAS NMR spectrum (Figure 18b) shows two small peaks at 72 ppm and 101 ppm which are due to the presence of $\text{HO-C}^*(\text{C})_2$ and $\text{O-C}^*(\text{C})_2\text{H}$ of the β -cyclodextrin molecule respectively. This indicates that with a decrease in the water content in the solvent, less Si-H bond is hydrolyzed and thus it makes modification of the silica hydride surface with the chiral selector more likely to take place. However, the large decrease in the intensity of the

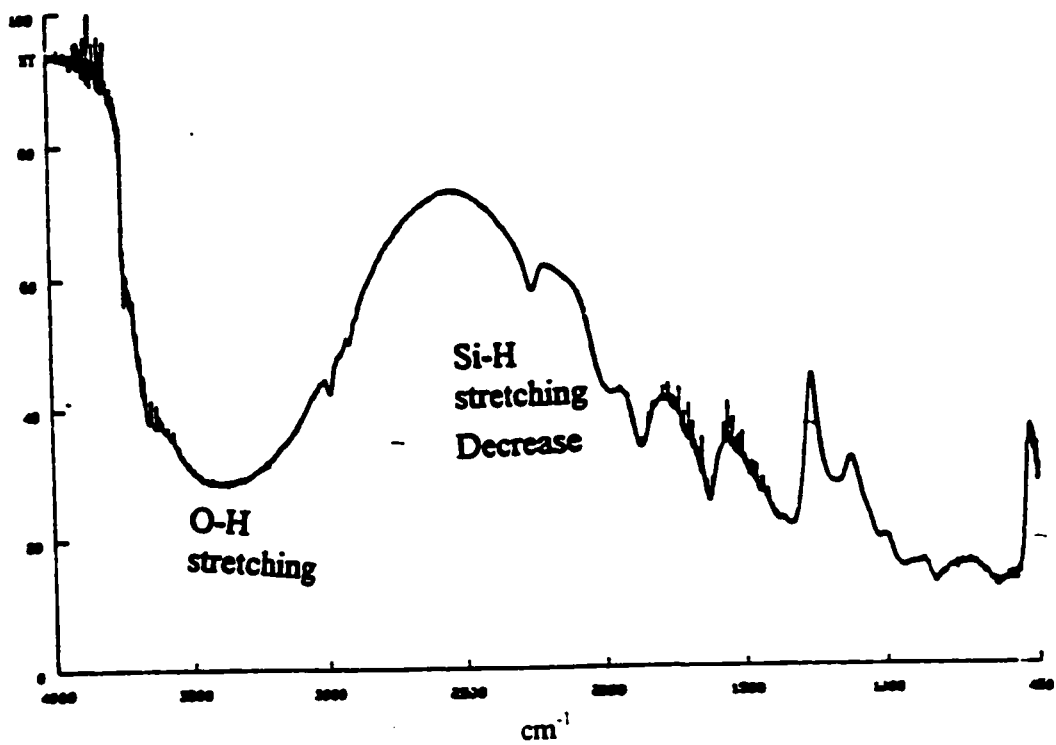


Figure 17. DRIFT spectrum for β -cyclodextrin bonded to Vydac silica hydride (hydrosilation done in 1:1 ethanol/water solvent system).

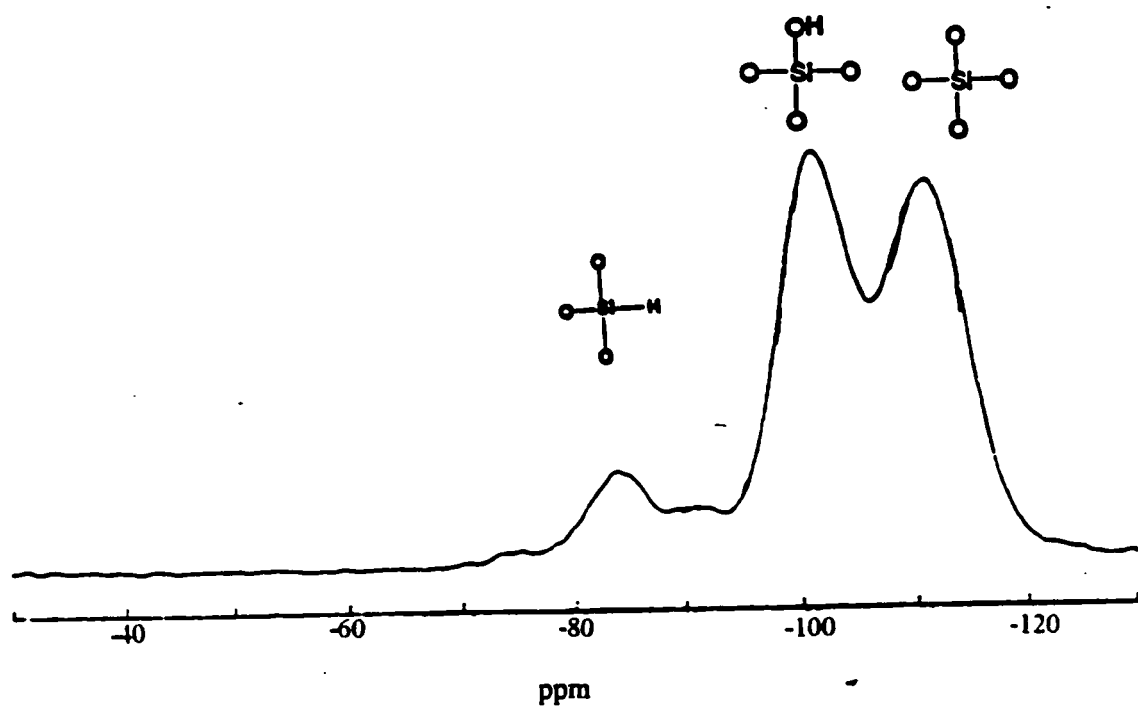


Figure 18a. ^{29}Si CP-MAS NMR spectrum for β -cyclodextrin bonded to Vydac silica hydride (hydrosilation done in 19:1 ethanol/water solvent system).

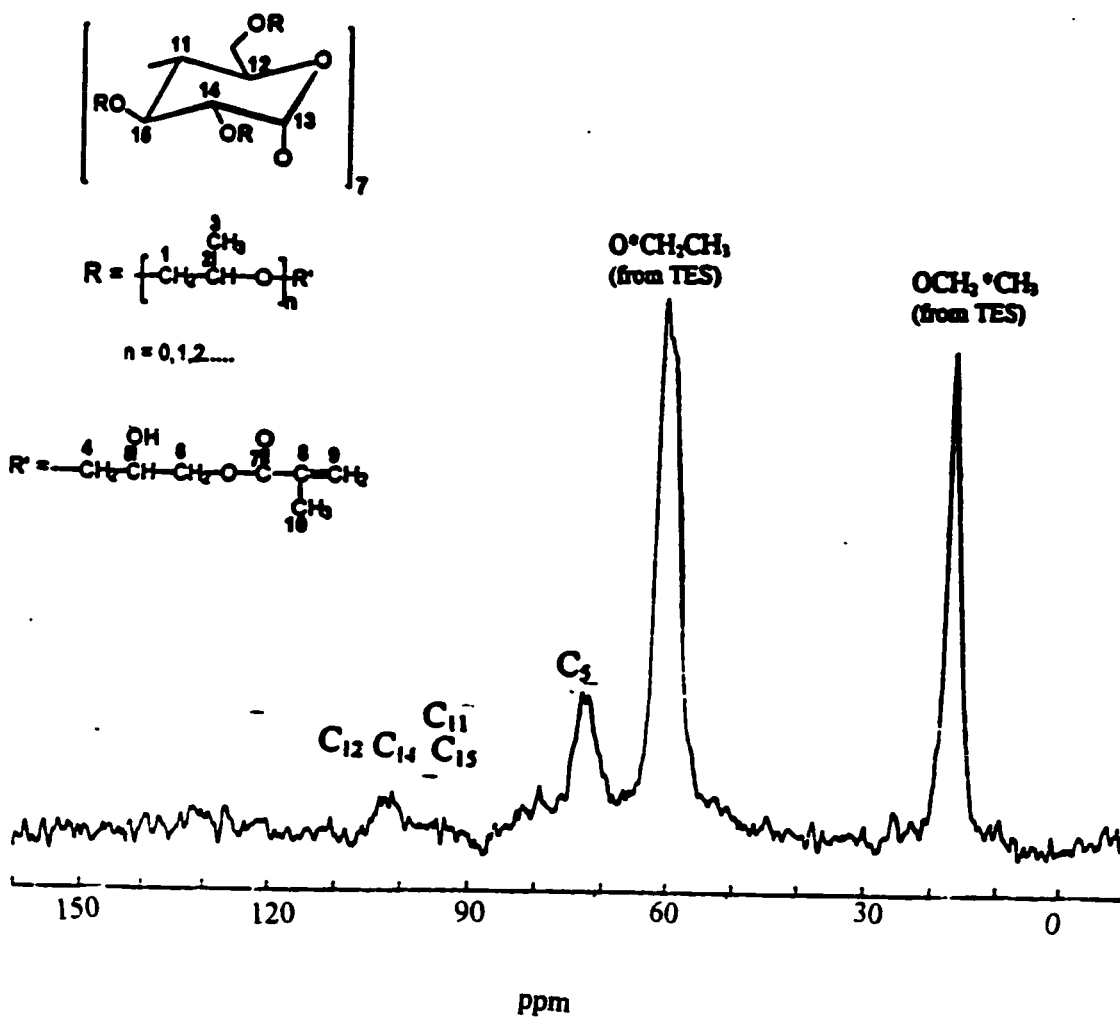


Figure 18b. ^{13}C CP-MAS NMR spectrum for β -cyclodextrin bonded to Vydac silica hydride hydrosilation done in 19:1 ethanol/water solvent system).

peak due to Si-H indicates that most of the Si-H bonds are still hydrolyzed rather than being reacted with the chiral selector. So in order to increase the extent of hydrosilation, it is necessary to choose a solvent system which is free of water.

The NMR results are consistent with the DRIFT spectrum (Figure 19), in which, there is a smaller decrease in the intensity of the Si-H bond stretching at 2250 cm^{-1} as compared to the case using the 1:1 ethanol/water solvent system. Also, the bonding of the chiral selector on the silica hydride surface can also be detected from the appearance of a small peak due to C-H bond stretching just below 3000 cm^{-1} which indicates that there is certain degree of attachment of organic moiety to the surface. However, the absence of the characteristic peak near 1750 cm^{-1} due to β -cyclodextrin tells that the bonding is not very extensive. Under these circumstances, it was necessary to repeat the synthesis by choosing a methanol/ethanol solvent system in which a reasonable amount of β -cyclodextrin can be dissolved.

c. Hydrosilation of β -cyclodextrin in 3:1 methanol/ethanol solvent system on Vydac silica

Figure 20 shows the ^{29}Si CP-MAS NMR spectrum for the bonded phase. There is a decrease in intensity of the peaks at -84 ppm and -74 ppm showing that there is a change in the amount of Si-H bonded to the surface. To further confirm if the decrease in the number of Si-H groups on the surface is due to the success of conversion from Si-H to Si-C attachment in hydrosilation, additional spectroscopic data is necessary. From the ^{13}C

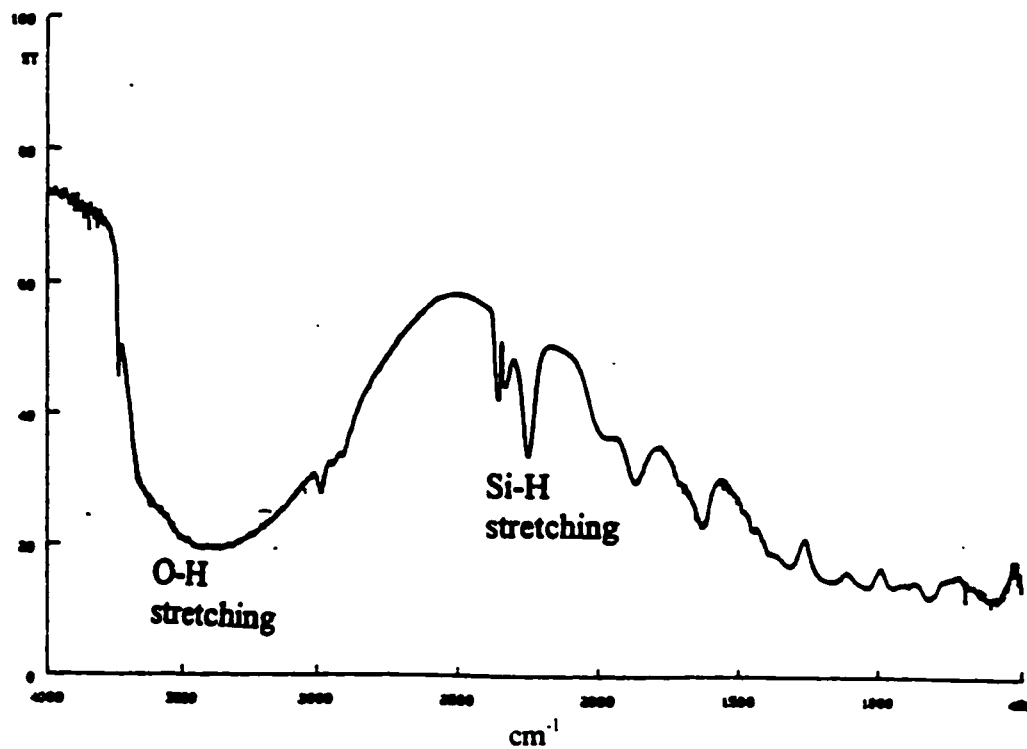


Figure 19. DRIFT spectrum for β -cyclodextrin bonded to Vydac silica hydride (hydrosilation done in 19:1 ethanol/water solvent system).

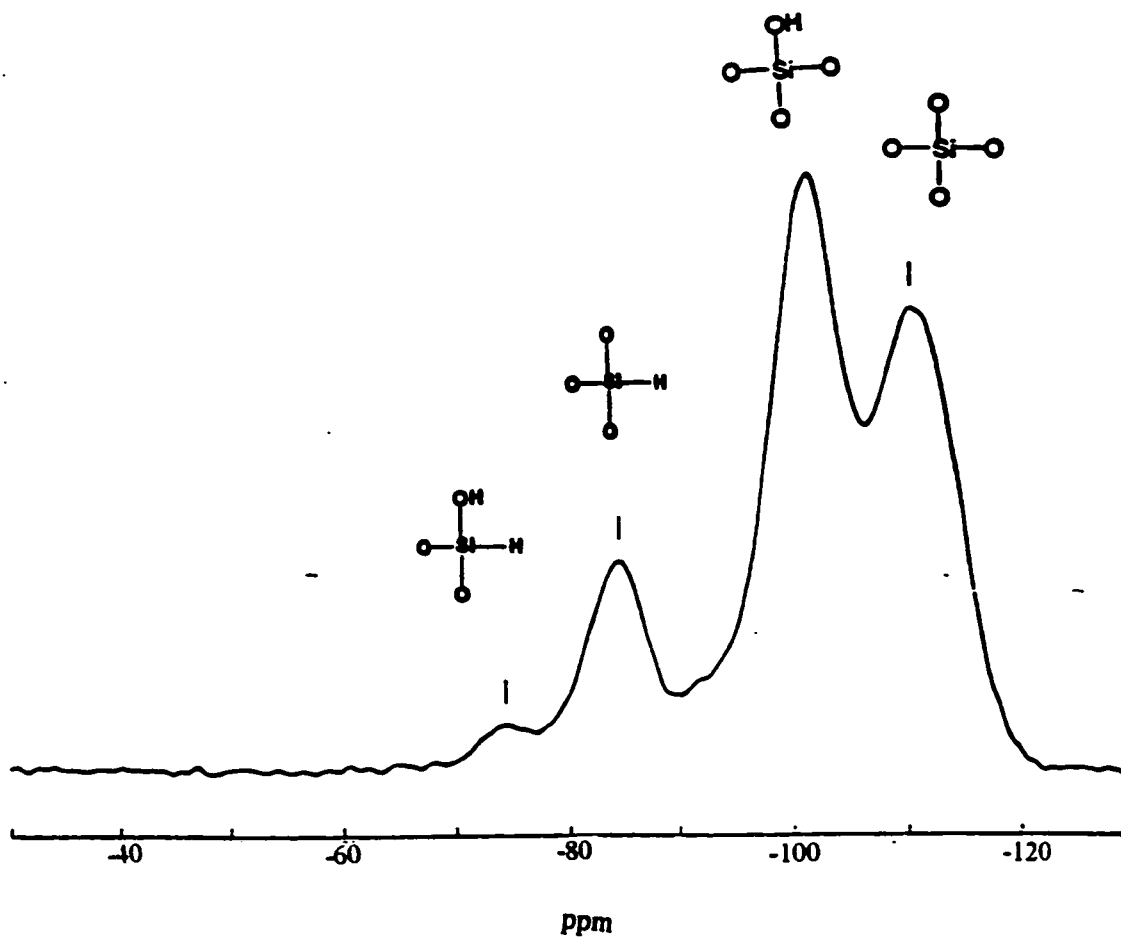


Figure 20. ^{29}Si CP-MAS NMR spectrum for β -cyclodextrin bonded to Vydac silica hydride (hydrosilation done in 3:1 methanol/ethanol solvent system)

CP-MAS NMR spectrum (Figure 21), we can confirm the success of the hydrosilation for three reasons. First, the pattern obtained is almost a mirror of the spectrum for β -cyclodextrin (Figure 9a) with two additional peaks at 50 ppm and 45 ppm. The peak at 45 ppm is due to the methine carbon while the peak at 50 ppm is likely to be from solvent trapped inside the pores of the silica surface⁴¹. Second, there is no obvious peak in the region of 120 ppm - 140 ppm because the olefin carbon has been successfully hydrosilated. Finally, the small bump at about 2 ppm is an indication of the existence of a Si-C bond, whose motion is usually restricted and thus it is difficult to detect in the spectrum.

In the DRIFT spectrum (Figure 22), the decrease in the intensity of the peak at 2250 cm^{-1} can be attributed to the conversion of Si-H groups to a Si-C bond. In addition, the appearance of peaks in the region from 2875 cm^{-1} to 3000 cm^{-1} also confirms the success of the synthesis of bonded phase because they are due to the C-H bond stretching in the chiral selector molecule. Also, a sharp small peak at 1750 cm^{-1} gives additional evidence to confirm the success of the hydrosilation.

Figure 23 and Figure 24 are the ^{13}C CP-MAS NMR spectrum and DRIFT spectrum for the big batch of β -cyclodextrin modified Vydac silica hydride via hydrosilation in the 3:1 methanol/ethanol solvent system. The same assignment of peaks can be done as in Figure 20 and Figure 21. Both spectroscopic methods strongly suggest that there has been successful hydrosilation of β -cyclodextrin on the Vydac silica hydride surface.

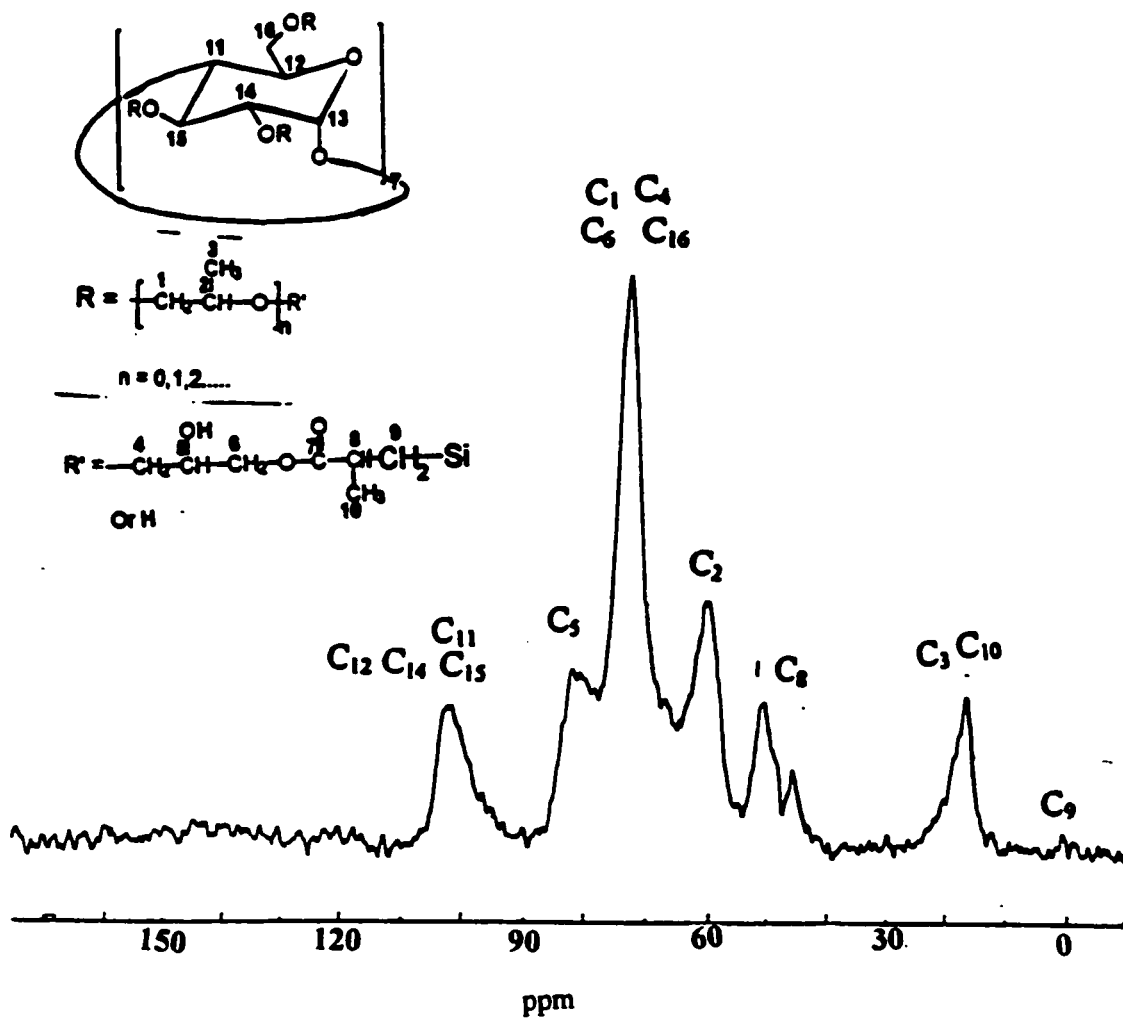


Figure 21. ^{13}C CP-MAS NMR spectrum for β -cyclodextrin bonded to Vydac silica hydride (hydrosilation done in 3:1 methanol/ethanol solvent system).

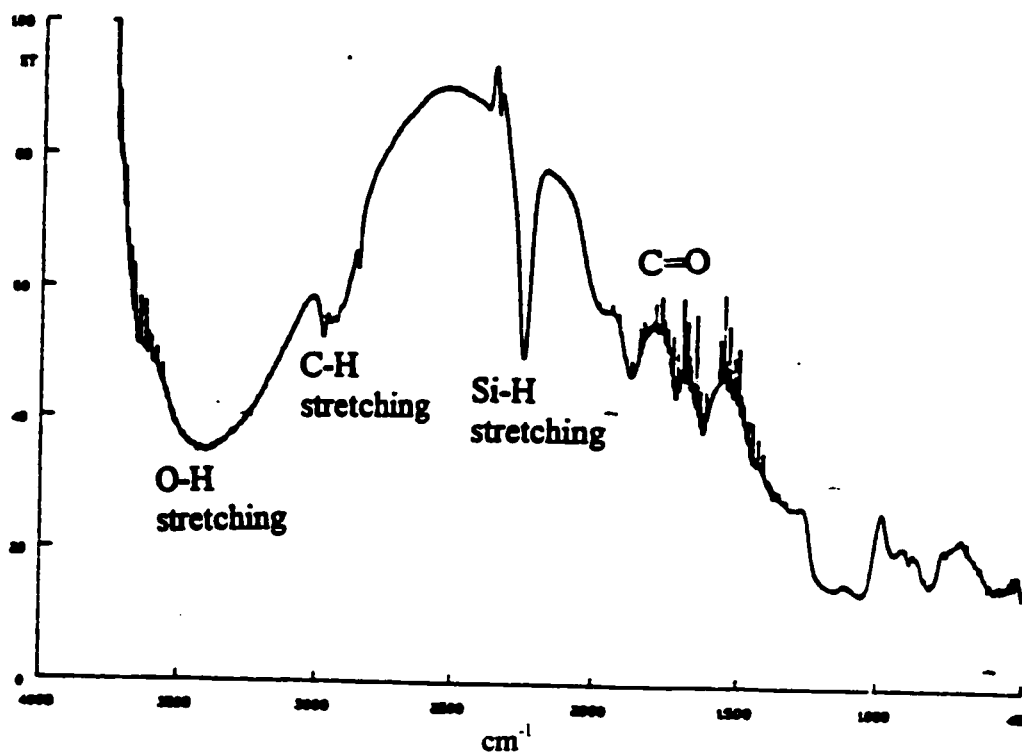


Figure 22. DRIFT spectrum for β -cyclodextrin bonded to Vydac silica hydride (hydrosilation done in 3:1 methanol/ethanol solvent system).

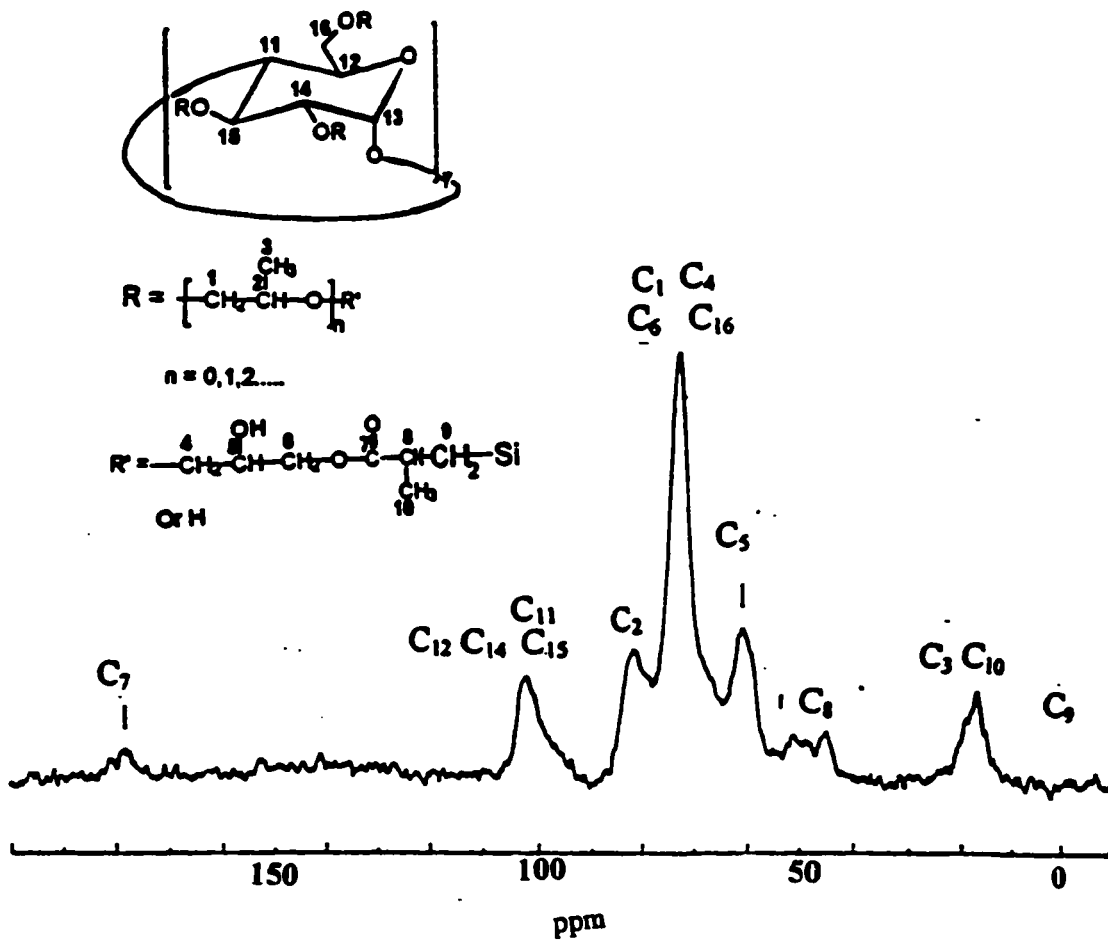


Figure 23. ^{13}C CP-MAS NMR spectrum for β -cyclodextrin bonded to Vydac silica hydride (Big Batch).

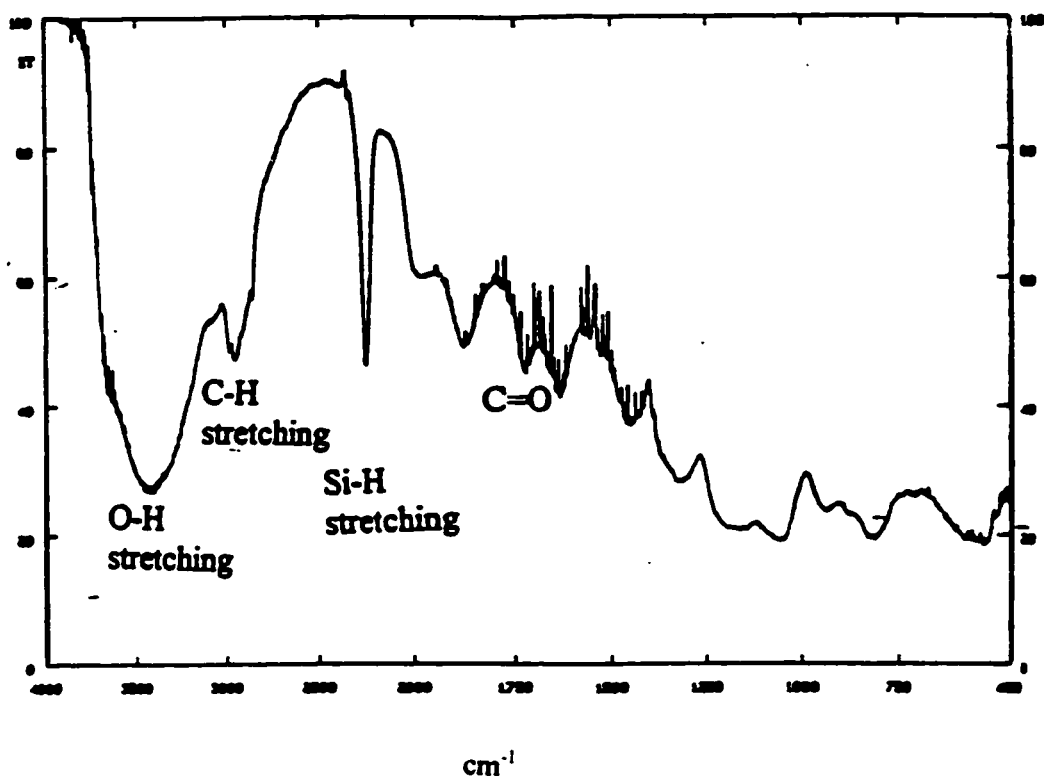
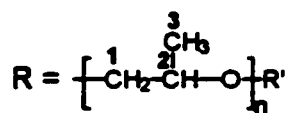
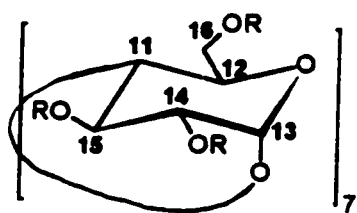


Figure 24. DRIFT spectrum for β -cyclodextrin bonded to Vydac silica hydride (Big Batch).

d. Hydrosilation of β -cyclodextrin on Kromasil silica in 3:1 methanol/ethanol solvent system

The pattern shown in the ^{13}C CP-MAS NMR spectrum (Figure 25) is similar to the spectrum of β -cyclodextrin with an additional peak at 45 ppm which is due to a methine carbon. This result suggests the success of attachment of the chiral selector to the silica hydride surface. Furthermore, in the ^{29}Si CP-MAS NMR spectrum (Figure 26), the relative intensity of the peak at -84 ppm decreases because of the modification of Si-H by the chiral selector. In addition, the DRIFT spectrum of the product (Figure 27) has a decrease in Si-H peak intensity at 2250 cm^{-1} and the appearance of peaks due to C-H bond stretching from 2875 cm^{-1} to 3000 cm^{-1} which also prove the attachment of β -cyclodextrin to the Kromasil silica hydride surface. Another strong indication of the bonding in the DRIFT spectrum is the peak at 1750 cm^{-1} which is due to the symmetric stretch of C=O in the chiral selector. In the fingerprint region below 1500 cm^{-1} , it is difficult to identify the bond stretching due to C-O groups or the bending due to methyl or methylene groups because the peaks are not well-resolved. Overall, the spectral information in conjunction with the elemental analysis suggests that β -cyclodextrin has been successfully bonded to the silica hydride surface so that the modified chiral stationary phase can be packed into a column for preliminary chromatographic studies.



$n = 0, 1, 2, \dots$

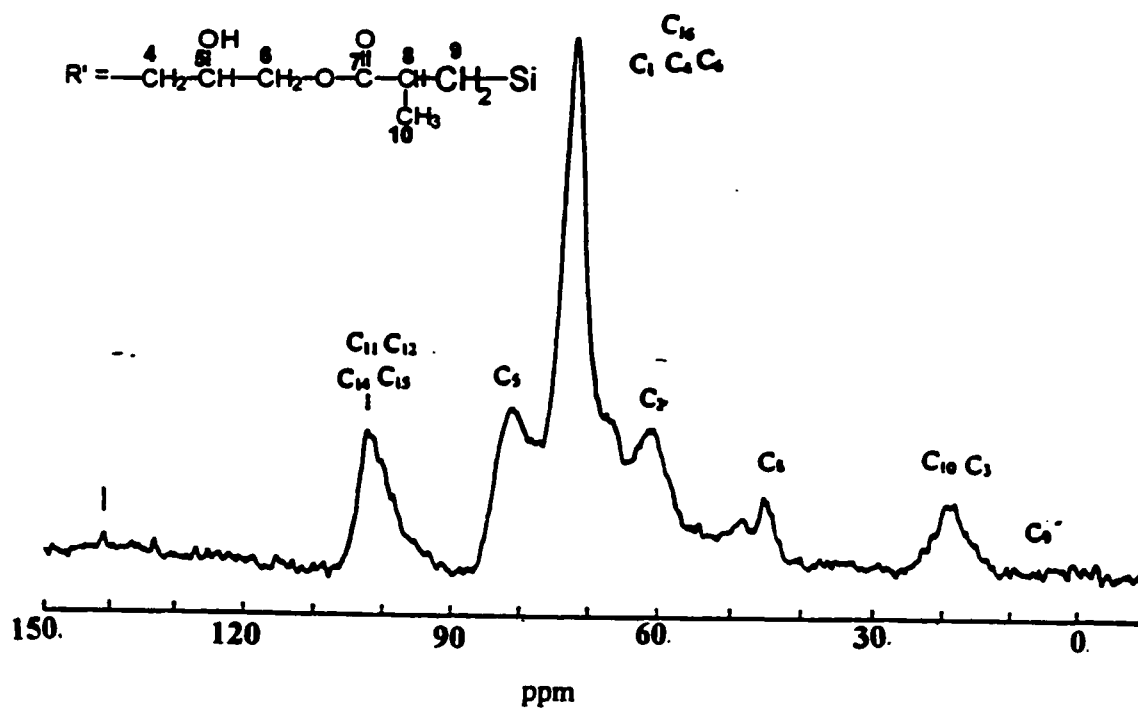


Figure 25. ^{13}C CP-MAS NMR spectrum for β -cyclodextrin bonded to Kromasil silica hydride (Big Batch).

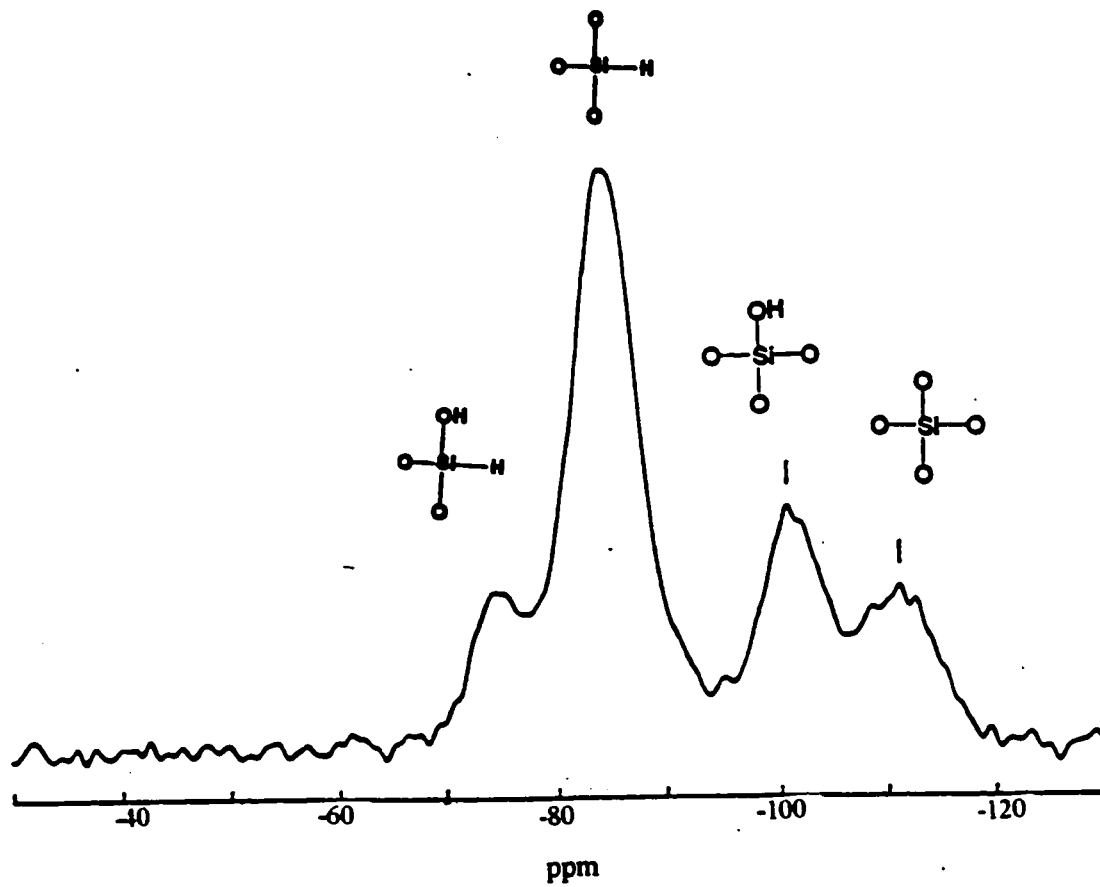


Figure 26. ^{29}Si CP-MAS NMR spectrum for β -cyclodextrin bonded to Kromasil silica hydride (Big Batch).

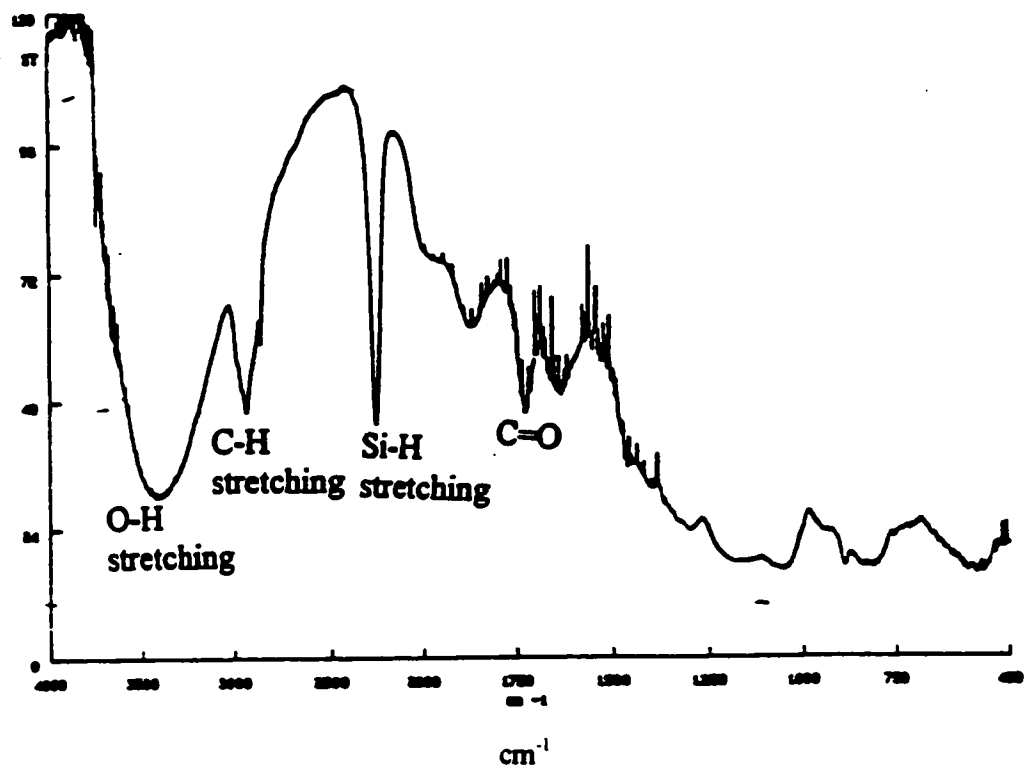


Figure 27. DRIFT spectrum for β -cyclodextrin bonded to Kromasil silica hydride (Big Batch).

3. Hydrosilation of β -cyclodextrin on Kromasil silica hydride via free radical initiation

Based on the DRIFT spectrum shown in Figure 28, the bonding of the chiral selector on the surface of the silica hydride can be confirmed by three features. First of all, the decrease in intensity of Si-H bond stretching peak at 2250 cm^{-1} indicates the replacement of the hydride in the reaction. Furthermore, the appearance of C-H bond stretching between 2800 cm^{-1} to 3000 cm^{-1} and the intense C=O bond at 1750 cm^{-1} strongly indicate that β -cyclodextrin molecules have been bonded to the surface. Additional supporting evidence are the peaks seen in the region between 1250 cm^{-1} to 1500 cm^{-1} , which are due to the bending of $-\text{CH}_3$ or $-\text{CH}_2$ bonds.

From the ^{29}Si CP-MAS NMR spectrum (Figure 29), it can be seen that there is a decrease in the intensity of the peak due to Si-H at -84 ppm which indicates that the bonding between the silicon hydride and the β -cyclodextrin was successful. However, there is an additional peak appeared at -94 ppm which is not identified. This may probably be due to the formation of an intermediate compound or by product during the reaction. Referring to the ^{13}C CP-MAS NMR spectrum (Figure 30), characteristic peaks due to β -cyclodextrin are observed indicating the attachment of β -cyclodextrin moiety on the surface. Similarly, there is an additional peak at 48 ppm , which may be accounted by the formation of an unidentified intermediate with the silicon atoms on the surface. One possible explanation of the formation of the intermediate may be due the attachment of the tert-butyl free radical to the silica surface through the formation of the Si-O-O-C bond.

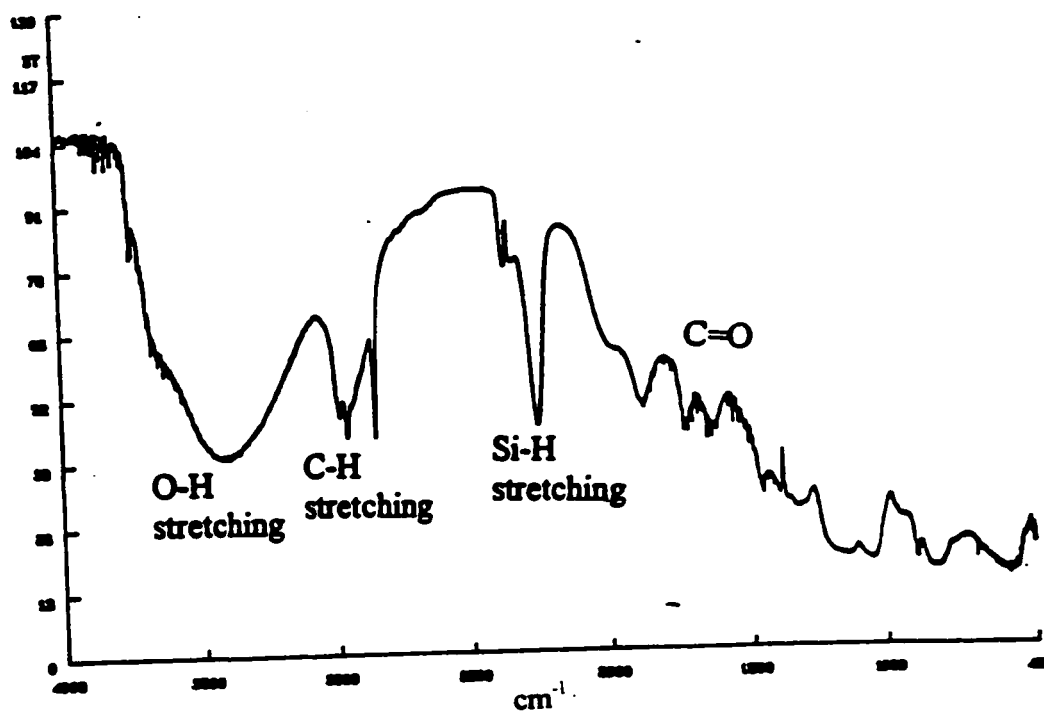


Figure 28. DRIFT spectrum for β -cyclodextrin bonded to Kromasil silica hydride (Free Radical Mechanism).

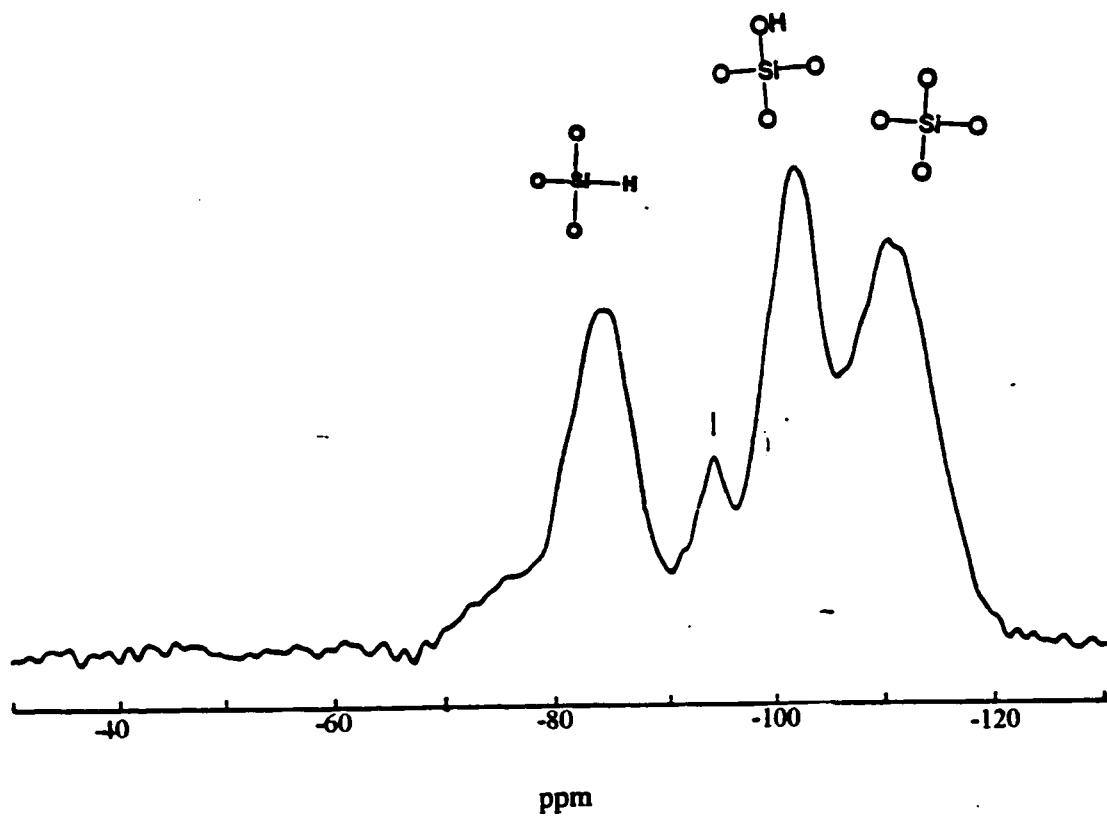


Figure 29. ^{29}Si CP-MAS NMR spectrum for β -cyclodextrin bonded to Kromasil silica hydride (Free Radical Mechanism).

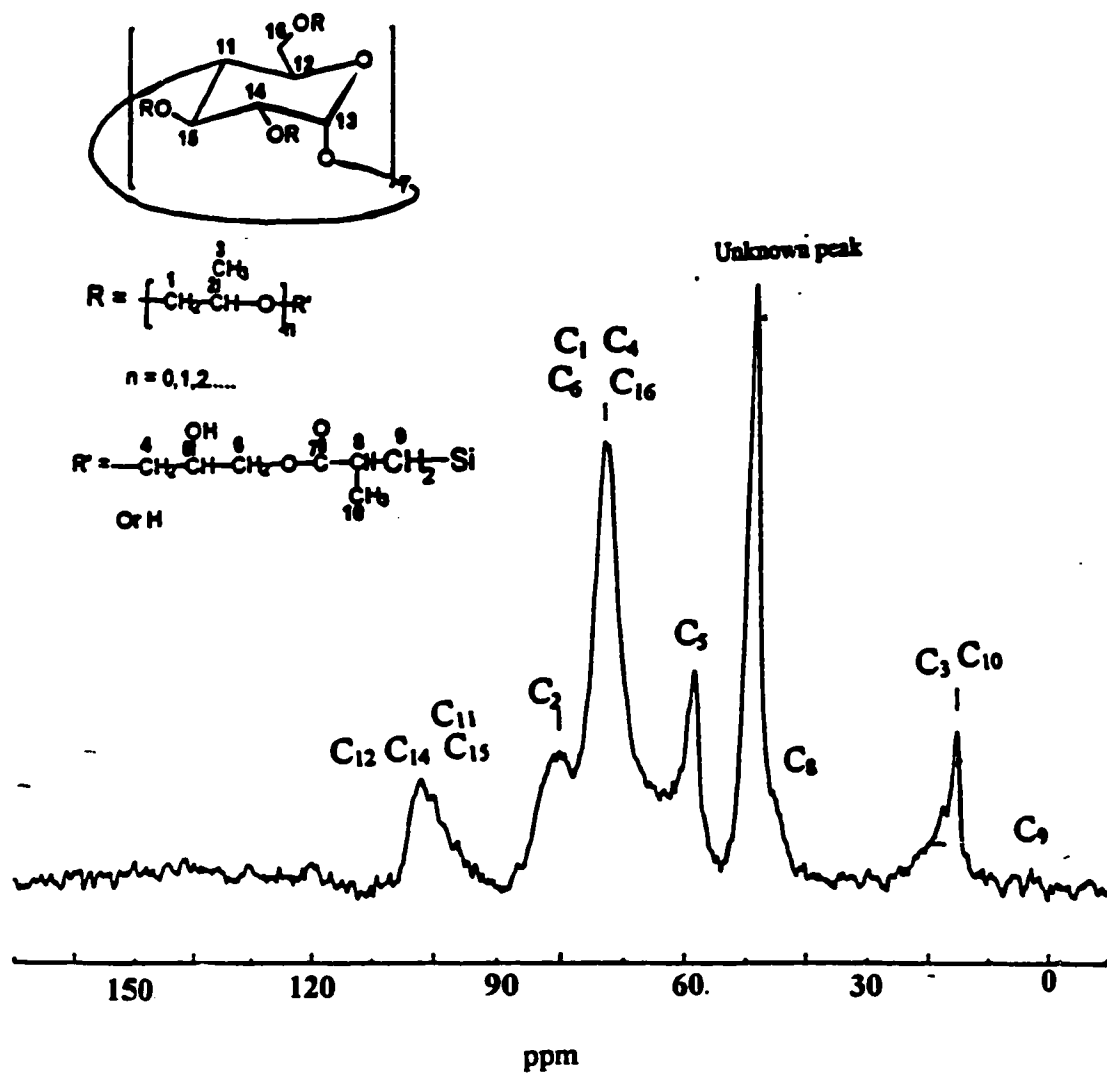


Figure 30. ¹³C CP-MAS NMR spectrum for β-cyclodextrin bonded to Kromasil silica hydride (Free Radical Mechanism).

To further confirm such a possibility, tert-butyl peroxide was allowed to react with the silica hydride intermediate under the same conditions as the hydrosilation. The final product was then examined and characterized by both CP-MAS NMR techniques and DRIFT analysis.

Figure 31 and Figure 32 are the DRIFT spectrum and ^{13}C CP-MAS NMR spectrum of the reaction product of tert-butyl peroxide and the silica hydride respectively. From the DRIFT spectrum, the presence of C-H stretching between 2800 cm^{-1} and 3000 cm^{-1} and the decrease in the intensity of the Si-H bond stretching at 2250 cm^{-1} suggest that there is attachment between the free radical and the silica hydride through the cleavage of Si-H bond. From the ^{13}C NMR spectrum, besides the two peaks at 60 ppm and 15 ppm, which are due to the residual TES molecules adhered on the surface, there is another peak located at 48 ppm. This peak can be reasonably assigned as $-\text{OC}^*(\text{CH}_3)_3$ from tert-butyl peroxide. Its position is the result of three methyl groups which are electron releasing and causing the chemical shift of the central carbon shift upfield as compared to the $\text{OC}^*\text{H}_2\text{CH}_3$ in TES. These results show that the free radical could react on the silica hydride surface in addition to the expected bonding of the chiral selector. Since the effect of such an intermediate on chromatographic chiral separations is unknown, the method of hydrosilation via free radical was no longer used in the later part of the research.

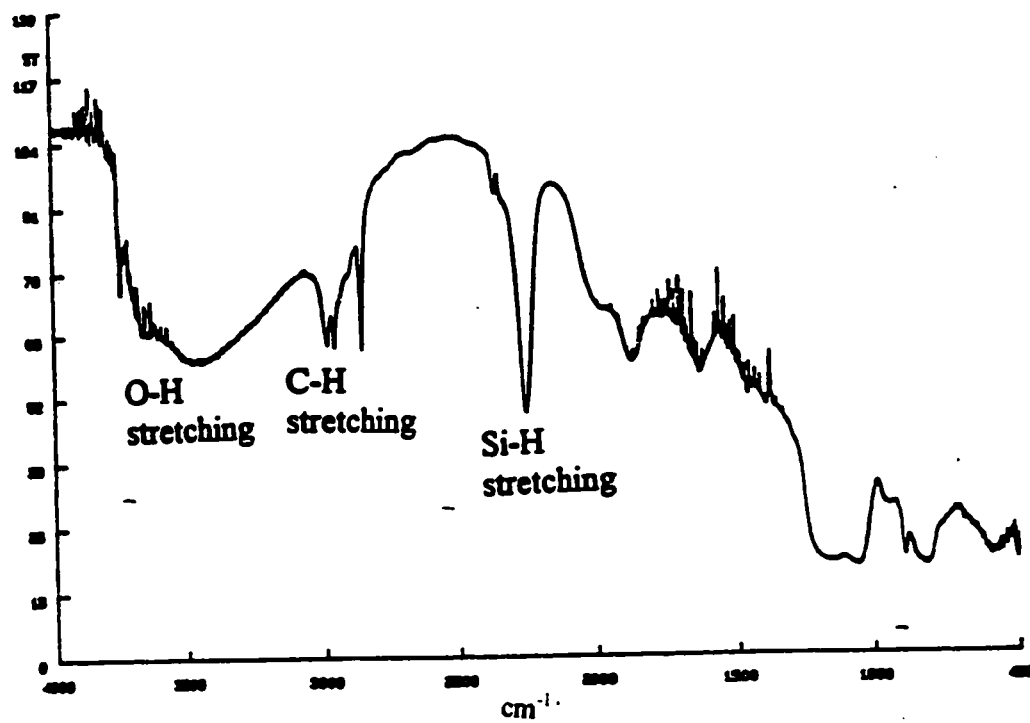


Figure 31. DRIFT spectrum for reaction product of tert-butyl peroxide and Kromasil silica hydride via free radical mechanism.

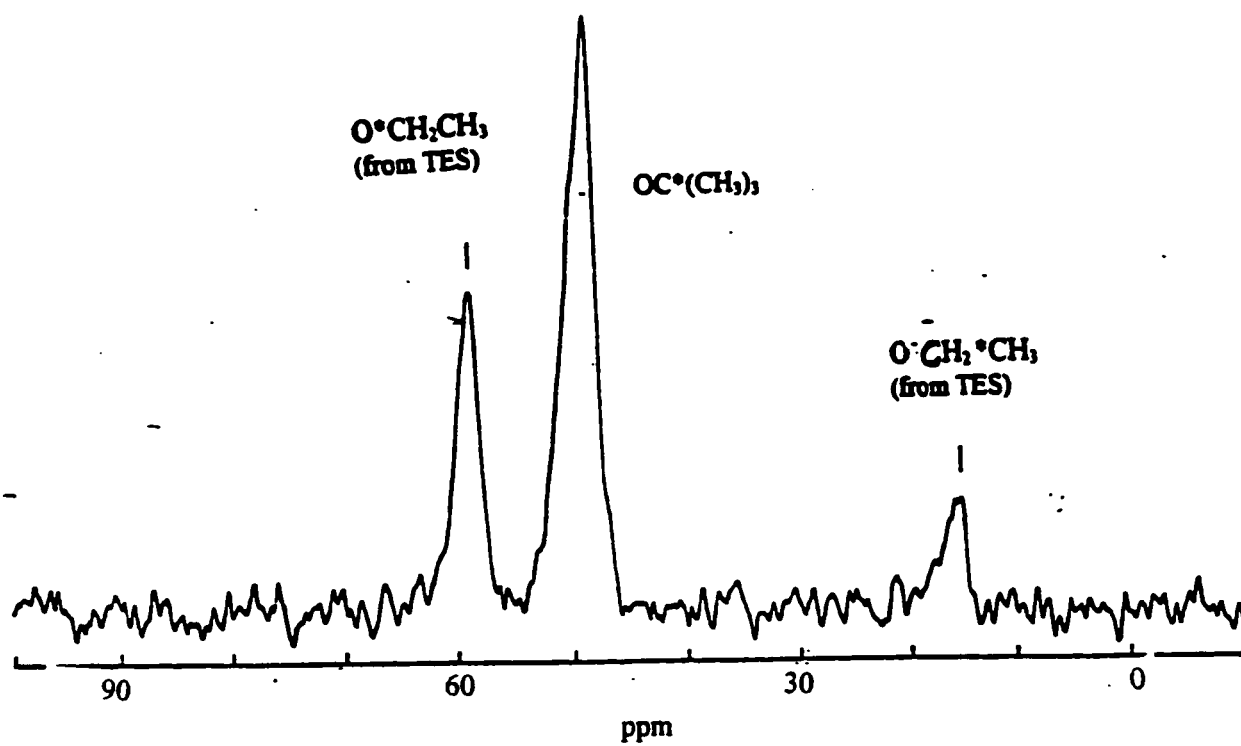


Figure 32. ^{13}C CP-MAS NMR spectrum for the reaction product of tert-butyl peroxide and Kromasil silica hydride via free radical mechanism.

4. Hydrosilation of (8S,9R)-(-)-N-benzylcinchonidium chloride (BENZ) on Kromasil silica hydride using Speier's Catalyst

Figure 33 is the ^{13}C CP-MAS NMR of the final product of the reaction between the chiral selector BENZ and the silica hydride. The absence of an intense peak due to aromatic carbons in the region between 120 ppm and 140 ppm is a sign of failure of the hydrosilation. In addition, no characteristic peaks due to a carbon attached to hydroxyl group, a carbon attached to nitrogen and methylene carbons are observed. The extra peak observed at -49 ppm is a typical resonance for $-\text{OCH}_3$ and one possible source for its existence is from the methanol/ethanol solvent mixture which might absorb in the pores of the silica matrix.

In the DRIFT spectrum (Figure 34), no vibrational band showing the functional groups in BENZ are observed. For instance, peaks due to aromatic $\text{C}=\text{C}$ in the region near 1650 cm^{-1} to about 1700 cm^{-1} should appear in the spectrum if the bonding is successful. Moreover, the Si-H peak intensity at 2250 cm^{-1} is similar to the Kromasil silica hydride spectrum (Figure 15a) suggesting that hydrosilation doesn't occur under these experimental conditions. From both the frequency and the shape of the C-H bond stretching in the region between 2800 cm^{-1} and 2950 cm^{-1} , it can be concluded that the bands are due to aliphatic C-H bonds. These peaks are probably due to the methanol/ethanol solvent mixture from the reaction.

The failure of hydrosilation is probably due to the bulkiness of the molecule near the olefin carbons. The presence of the bulky groups introduce steric hinderance and thus lowering the efficiency of the attachment.

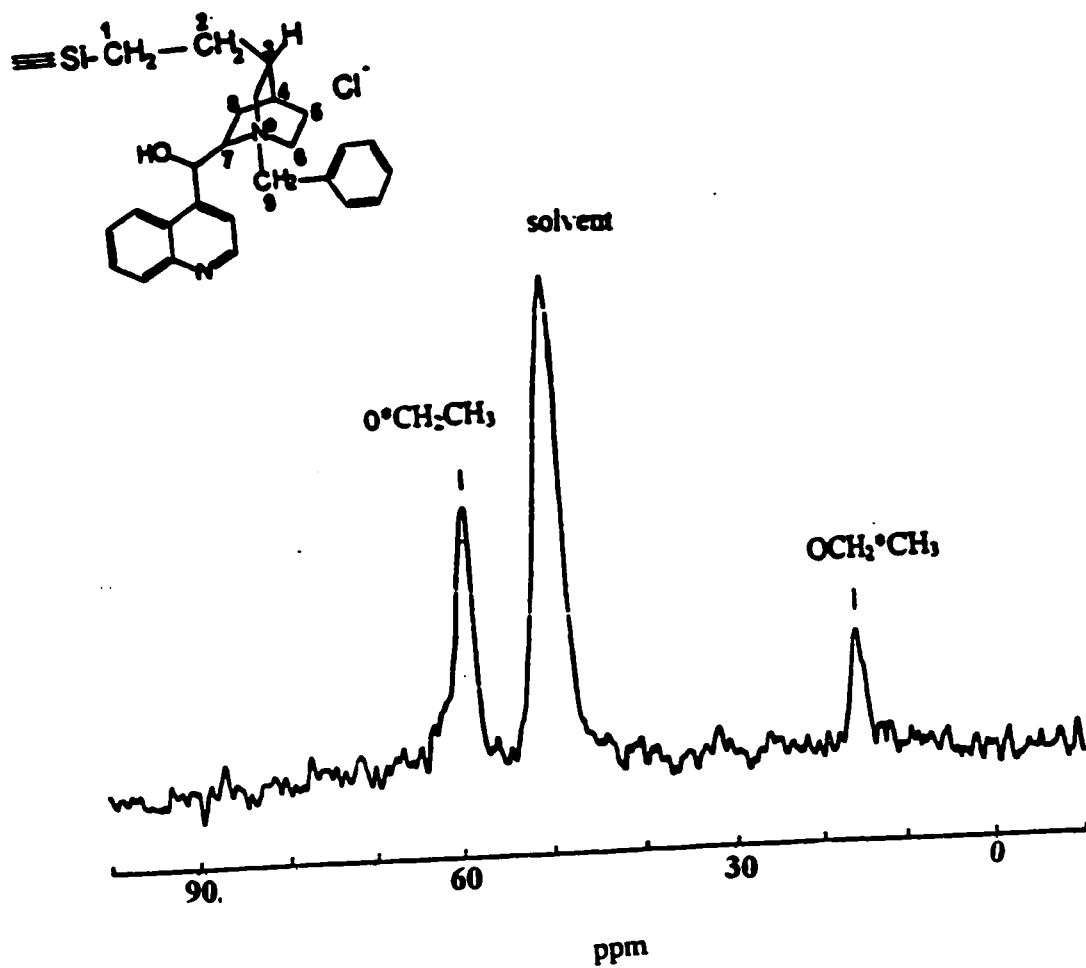


Figure 33. ¹³C CP-MAS NMR spectrum for (8S, 9R)-(-)-N-benzylcinchonidinium chloride bonded phase on Kromasil silica.

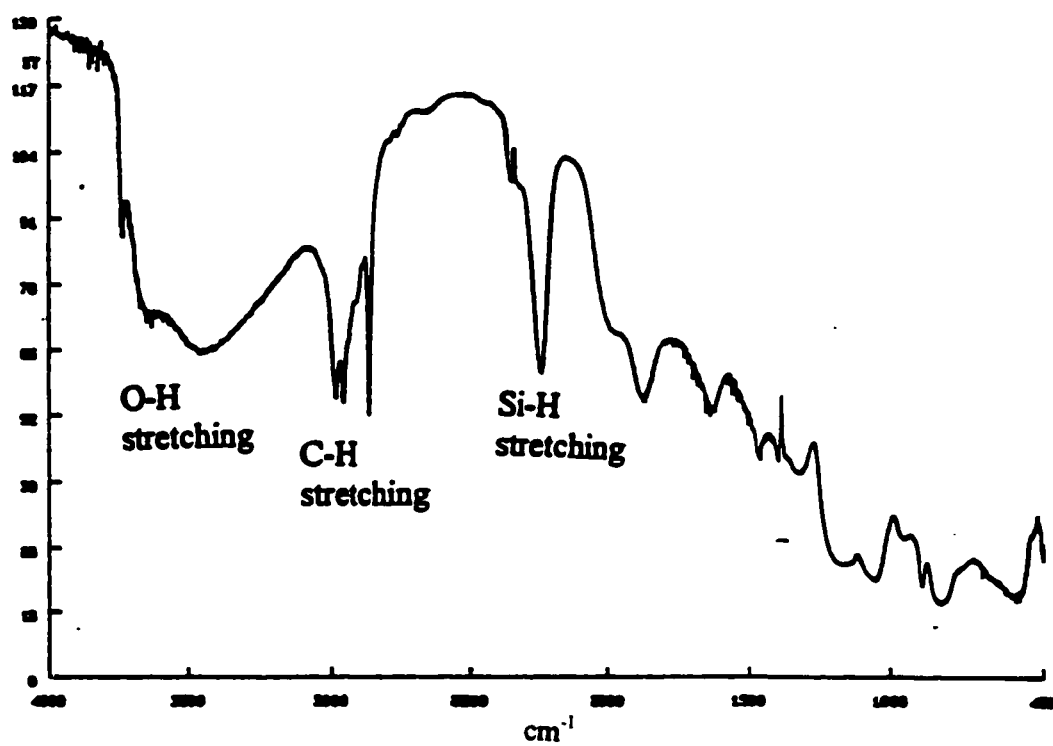


Figure 34. DRIFT spectrum for (8S, 9R)-(-)-N-benzylcinchonidium chloride bonded to Kromasil silica hydride.

5. Hydrosilation of (R)-(+)-acryloxy- β , β -dimethyl- γ -butyrolactone on Kromasil silica hydride using Speier's catalyst

Compared to the ^{29}Si CP-MAS NMR spectrum (Figure 35) with the original Kromasil silica hydride (Figure 13a), the intensity of the Si-H peak at -83 ppm for the bonded phase has diminished. The formation of a single Si-C linkage by cleavage at the Si-H bond should show a peak at -65 ppm³⁹. However, the presence of C=O bond in the vicinity will lead to an upfield shift to about -90 ppm. As a result, the small bump observed in the spectrum at -90 ppm shows the formation of a Si-C single bond confirming the success of the bonding.

Attachment of the lactone to the surface of the silica hydride can be further characterized by ^{13}C CP-MAS NMR spectroscopy. The assignments of all the peaks are shown in Figure 36. The broad peak at 170 ppm is due to the two carbonyl carbons. The peaks at 76 ppm and 66 ppm are due to the two C-O carbons at C4 and C6 position of the lactone ring respectively. The quaternary carbon located at the β position is observed at 40 ppm. The peaks in the upfield region between 17 ppm to 22 ppm are due to the methyl carbon and methylene carbons. Finally, a significant indication of the success of forming a Si-C linkage is the presence of the small peak at 7 ppm.

Furthermore, some features in the DRIFT spectrum (Figure 37) confirm the bonding of the lactone with the silica hydride. The decrease in Si-H bond stretching at 2250 cm^{-1} indicates that some of the hydride has been cleaved and the appearance of C-H bond stretching from 2750 cm^{-1} to 3000 cm^{-1} is due to the success of the attachment of the

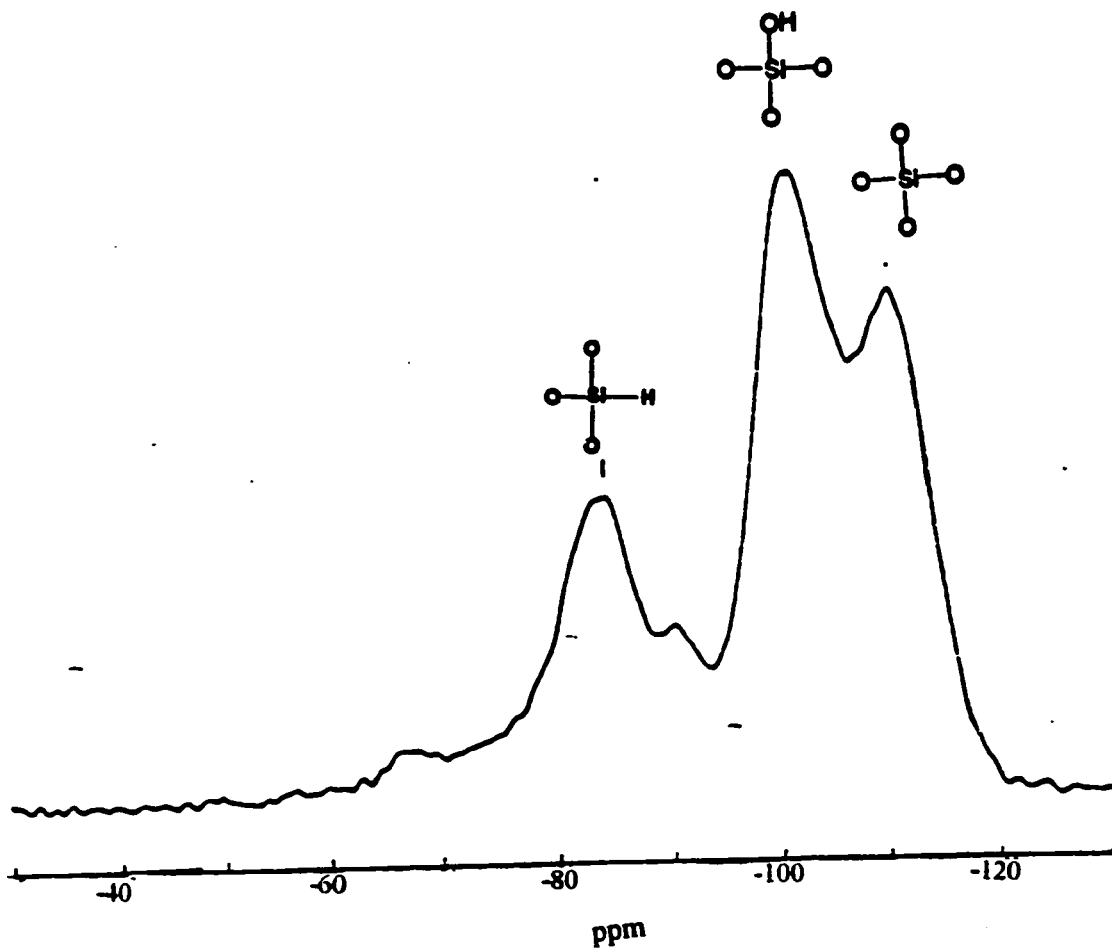


Figure 35. ^{29}Si CP-MAS NMR spectrum for (R)-(+)-acryloxy- β,β -dimethyl- γ -butyrolactone bonded to Kromasil silica hydride.

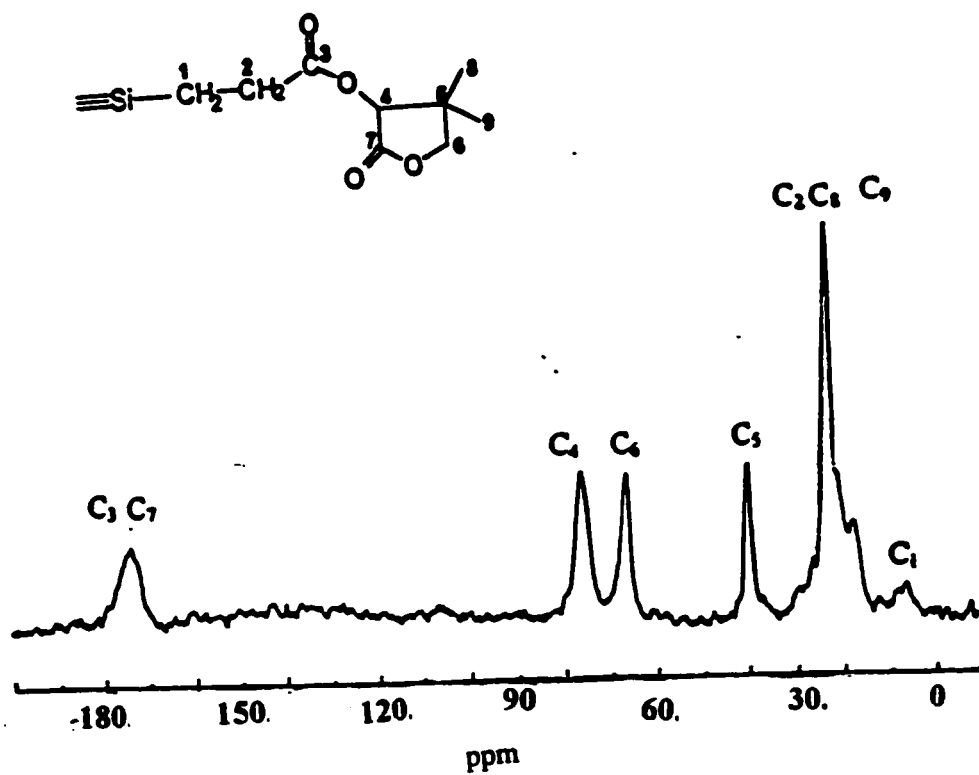


Figure 36. ¹³C CP-MAS NMR spectrum for (R)-(+)-acryloxy-β,β-dimethyl-γ-butyrolactone bonded to Kromasil silica hydride.

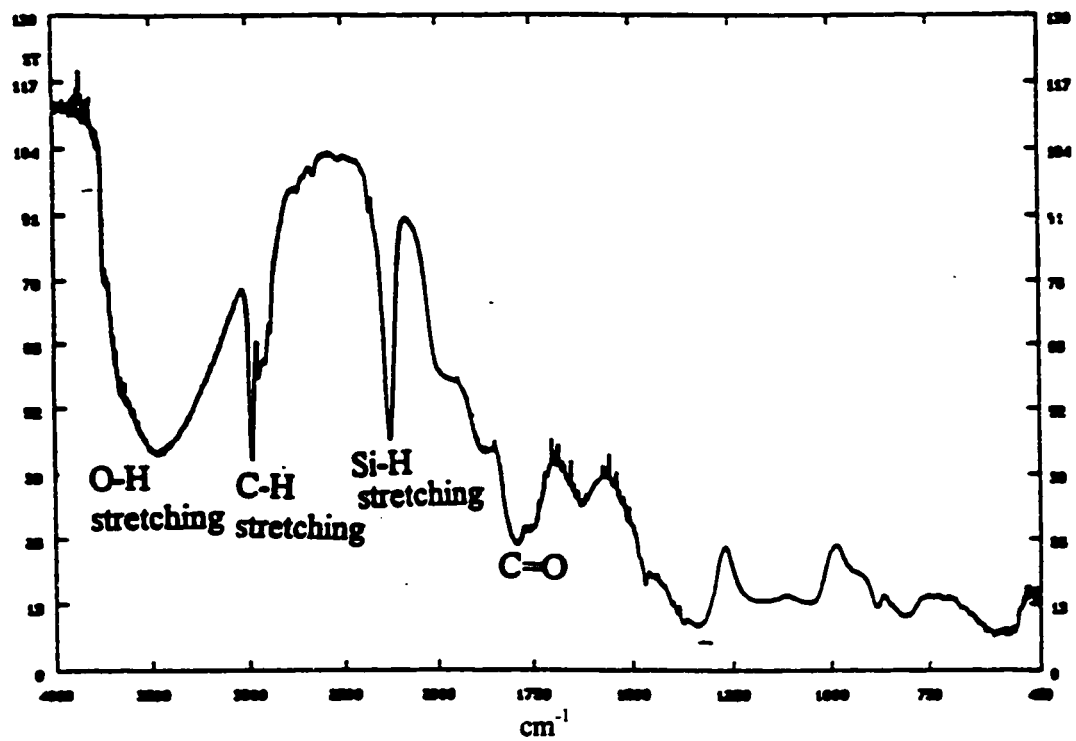


Figure 37. DRIFT spectrum for (R)-(+)-acryloxy- β,β -dimethyl- γ -butyrolactone bonded to Kromasil silica hydride.

organic moiety to the silica material. Moreover, the intense peak at 1750 cm^{-1} is a good indication of the presence of C=O bonds and the unresolved peaks lying between 1250 cm^{-1} and 1500 cm^{-1} are due to the bending of CH_3 groups or CH_2 groups. Based on the spectroscopic studies, it can be concluded that the bonding of (R)-(+)-acryloxy- β,β -dimethyl- γ -butyrolactone on Kromasil silica hydride was successful. Hence, this synthesized chiral stationary phase was packed into a column for further chromatographic studies.

6. Hydrosilation of (R)-(+)-limonene on Kromasil hydride by Speier's catalyst

The characterization of this bonded silica material by ^{13}C CP-MAS NMR spectrum (Figure 38) can confirm the success of the hydrosilation from the following features. The two peaks at 132 ppm and 127 ppm are due to the two olefin carbons in the six - membered rings while the broad peak at 68 ppm is due to the two methylene carbons (C4 and C7) right next to the deshielding region of C=C bond. The two tertiary carbons at the C2 and C10 positions have peaks at 40 ppm and 36 ppm respectively. The carbon at the C10 position is slightly upfield as compared to that at C2 because the carbon in the ring is closer in proximity to the electron cloud of the C=C and thus it is more shielded. The intense peaks observed at 20 ppm and 23 ppm are due to the remaining methylene carbon (C8) and methyl groups (C3 and C9).

From the DRIFT spectrum illustrated in Figure 39, both the intense C-H stretching peaks in the range of 2800 cm^{-1} to 3000 cm^{-1} and the C=C stretching peak at 1750 cm^{-1} are indications of the presence of (R)-(+)-limonene on the silica surface. Simultaneously,

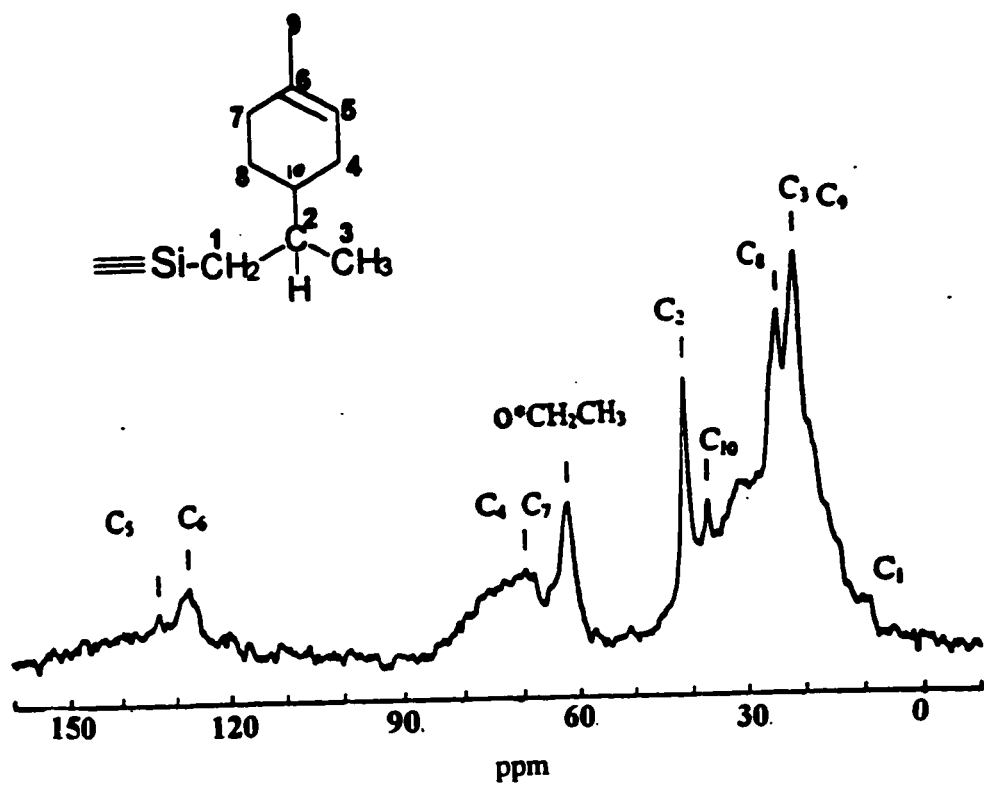


Figure 38 ^{13}C CP-MAS NMR spectrum for (R)-(+)-limonene bonded to Kromasil silica hydride.

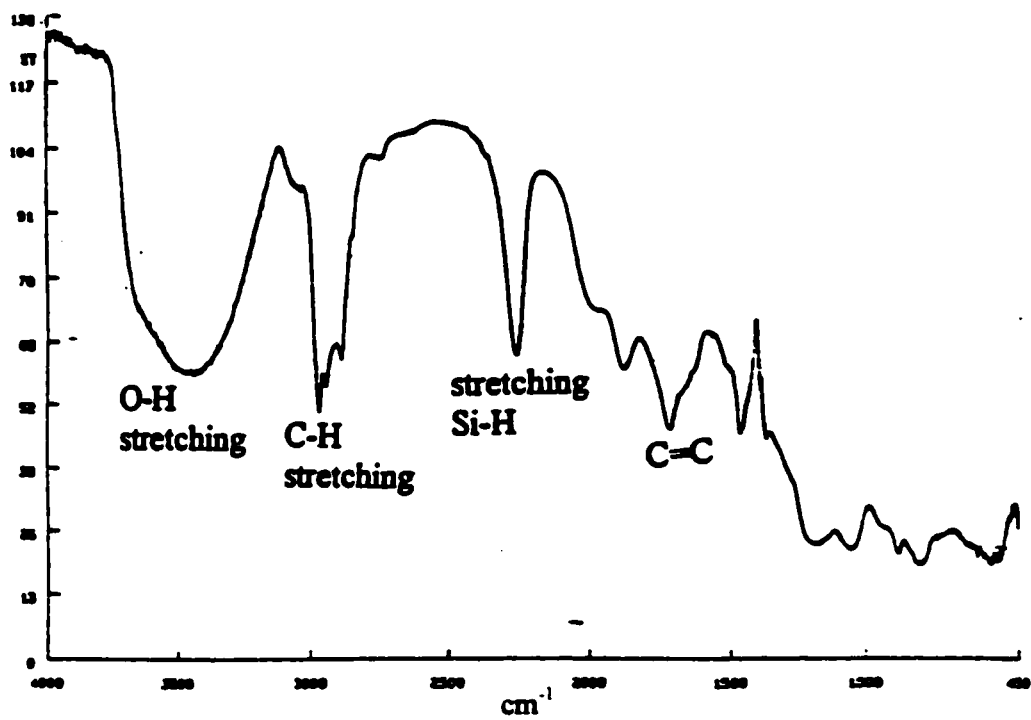


Figure 39. DRIFT spectrum for (R)-(+)-limonene bonded to Kromasil silica hydride.

the decrease in peak intensity of the vibration due to Si-H stretching at 2250 cm^{-1} gives evidence that the bonding of the chiral selector was done via the cleavage of the Si-H bond.

C. Spectroscopic studies on the stability of β -cyclodextrin modified Kromasil silica chiral stationary phase

The use of β -cyclodextrin chiral stationary phases always gave high back pressure in chromatographic studies. It was suspected that the bonded phase was unstable and the chiral selector might have deteriorated. After 69 chromatographic runs, the packed chiral stationary phase was removed from the column and the silica material was studied spectroscopically by ^{29}Si CP-MAS NMR, ^{13}C CP-MAS NMR and DRIFT spectroscopy.

Figure 40a and Figure 40b are the ^{29}Si CP-MAS NMR and ^{13}C CP-MAS NMR spectra respectively. Compared to the spectra of the freshly prepared bonded phase (Figures 25 and 26), the patterns shown are very similar except there is a significant decrease in the intensity of the Si-H peak in the ^{29}Si CP-MAS NMR spectrum. It is actually not surprising because most of the Si-H groups should have hydrolyzed after considerable contact with the mobile phase mixture of water/methanol. Similarly, the same assignment as the original material (Figure 27) can be done in DRIFT spectrum (Figure 41) except the intensity of the peak due to Si-H bond stretching decreases for the same reason. As a consequence, it can be concluded that the bonded material remained qualitatively the same after 69 runs and so the high back pressure in the chromatographic studies was not due to the deterioration of the bonded phase. With a thorough check of

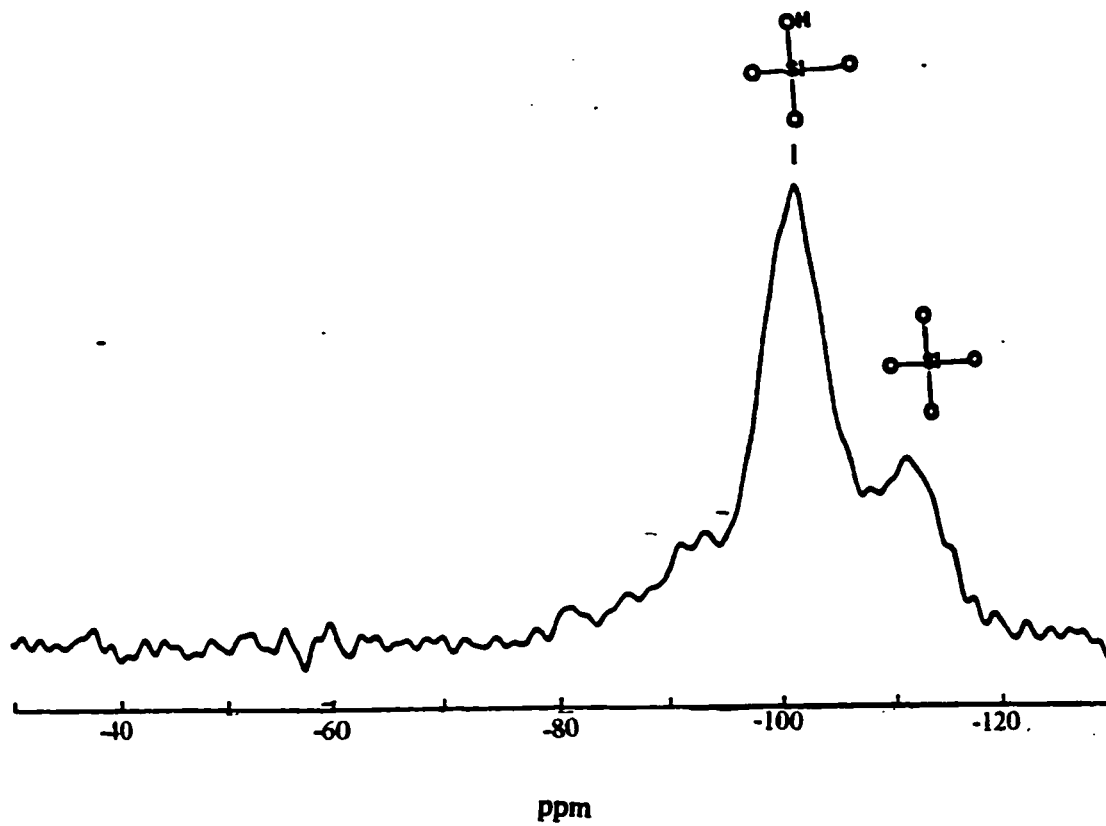


Figure 40a. ^{29}Si CP-MAS NMR spectrum for the β -cyclodextrin bonded phase on Kromasil silica (removed from the column after 69 runs).

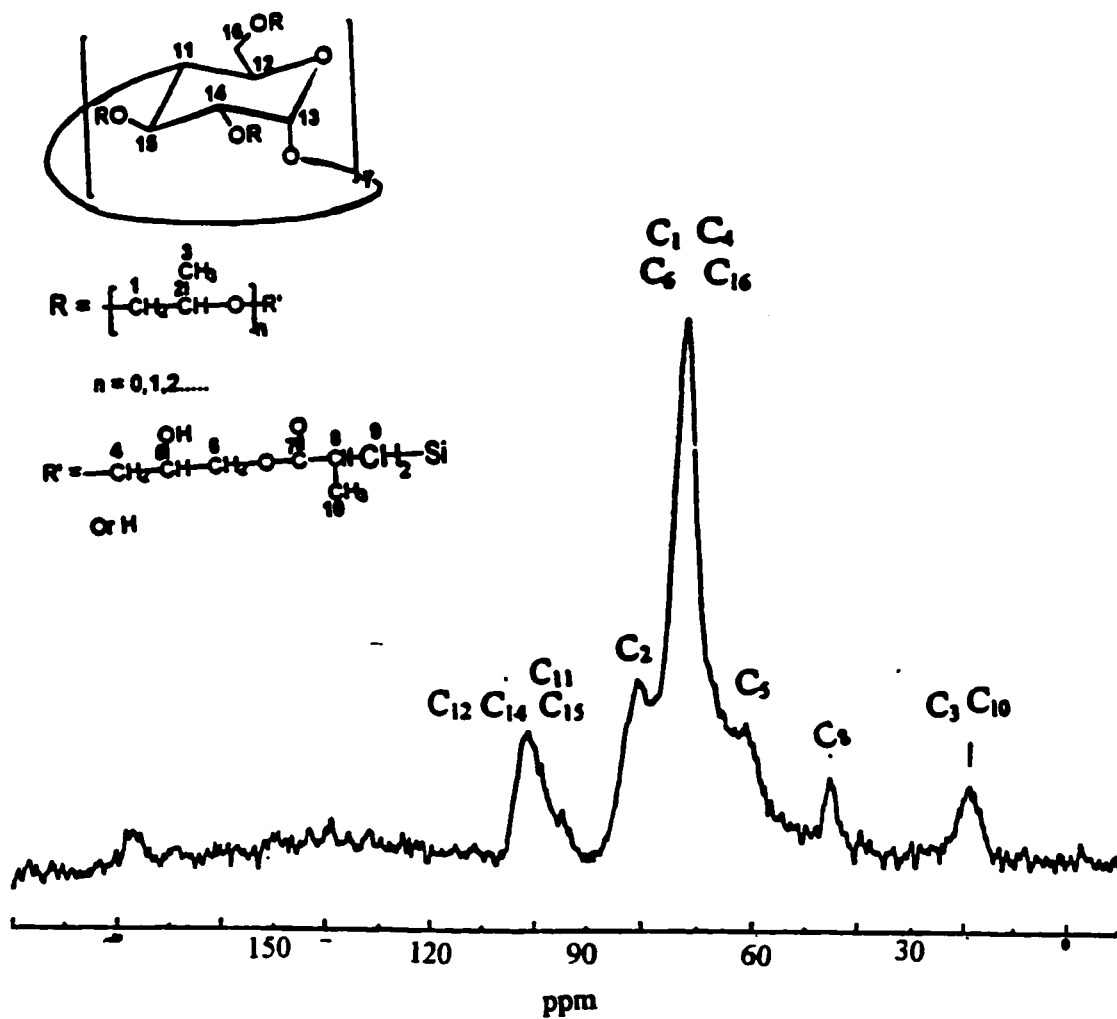


Figure 40b. ^{13}C CP-MAS NMR spectrum for the β -cyclodextrin bonded phase on Kromasil silica (removed from the column after 69 runs).

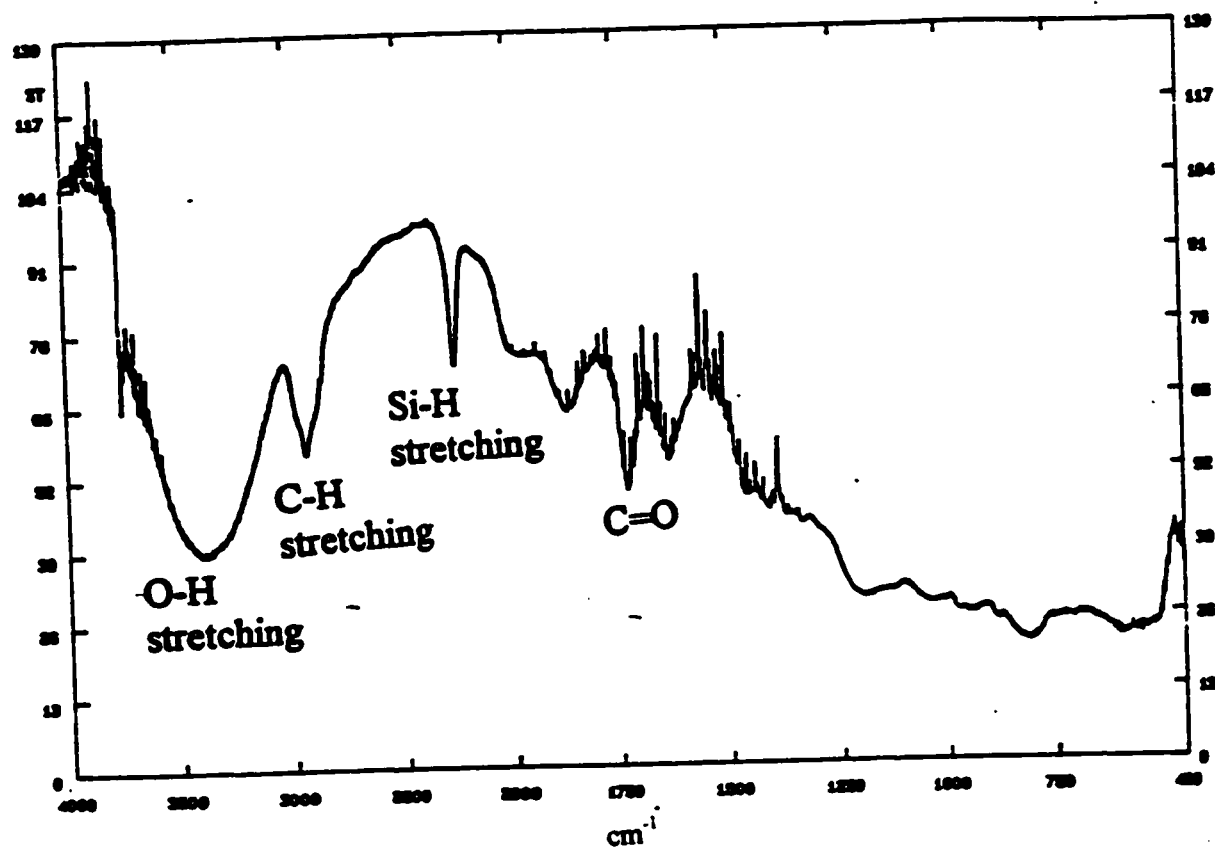


Figure 41. DRIFT spectrum for the β -cyclodextrin bonded phase on Kromasil silica (removed from the column after 69 runs).

the HPLC instrument, it was found that the set up of high back pressure was due to the partial clogging of the pump filter.

D. Chromatographic Studies

1. Structure and Chirality of Samples for chromatographic studies

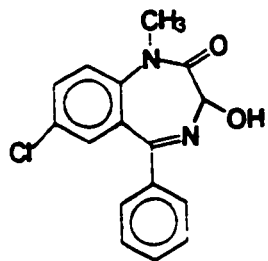
a. Benzodiazepines

The structures of the six benzodiazepines (clonazepam, chlorodiazepoxide, diazepam, nitrazepam, oxazepam and temazepam) are illustrated in Figure 42. chlorodiazepoxide, oxazepam and temazepam have an OH group at the only chiral center which is located at the 3 position of the benzediazepine ring. Meanwhile the chirality of the other three members of the groups arise from the non-planar benzodiazepine ring system. Figure 43 is an example showing the molecular structures of a pair of enantiomers of diazepam⁴². Because of the barrier to inversion of the seven membered ring, the two enantiomers do not interconvert to each other. The separation of the six benzodiazepines have been investigated on both the β -cyclodextrin chiral stationary phase and the (R)-(+)-acryloxy- β , β -dimethyl- γ -butyrolactone columns.

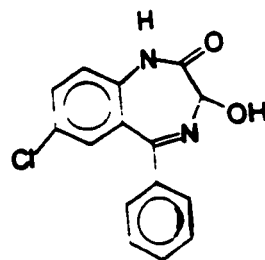
b. Dansyl amino acids.

Chiral separation of dansyl amino acids has been extensively studied on various native β -cyclodextrin or substituted β -cyclodextrin chiral stationary phases. Furthermore, the chiral recognition for their separation is well-established and explained. For the dansyl derivatives of amino acids, the introduction of the aromatic rings provides a good fit into

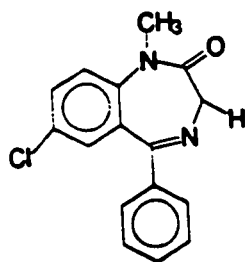
Temazepam



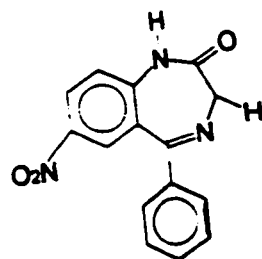
Oxazepam



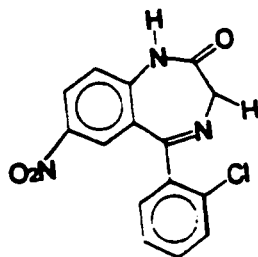
Diazepam



Nitrazepam



Clonazepam



Chlorodiazepoxide

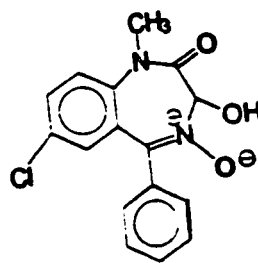


Figure 42. Structures of benzodiazepines.



Figure 43. Hyperchem molecular model of diazepam showing the non-planarity of the molecule.

the β -cyclodextrin cavity which is a necessity for the achievement of chiral separation. Also, this substitution adds a chromophore to the native amino acid so that analysis can be done by UV-visible detection. The chiral compounds of this format with the various side chains are shown in Figure 44. For the above reasons, this group of compounds was chosen for study on the β -cyclodextrin columns.

c. Drugs

In order to further explore the usefulness of the modified chiral stationary phase, four different drugs, DL-homatropine, terbutaline, tropicamide and clenbuterol, were studied in this project. The structures of the drugs are shown in Figure 45. They all consist of one chiral center as shown. With reference to the size of the molecules, they either consist of two aromatic rings or have bulky groups so that they can approximate the cavity requirement for separation by β -cyclodextrin. In addition, the molecules all possess of hydroxyl, amino groups and aromatic ring systems which can act as interactive sites for the multiple point interaction needed by a Pirkle type chiral stationary phases. Therefore, these four drugs were also used for the study of the (R)-(+)-acryloxy- β,β -dimethyl- γ -butyrolactone column.

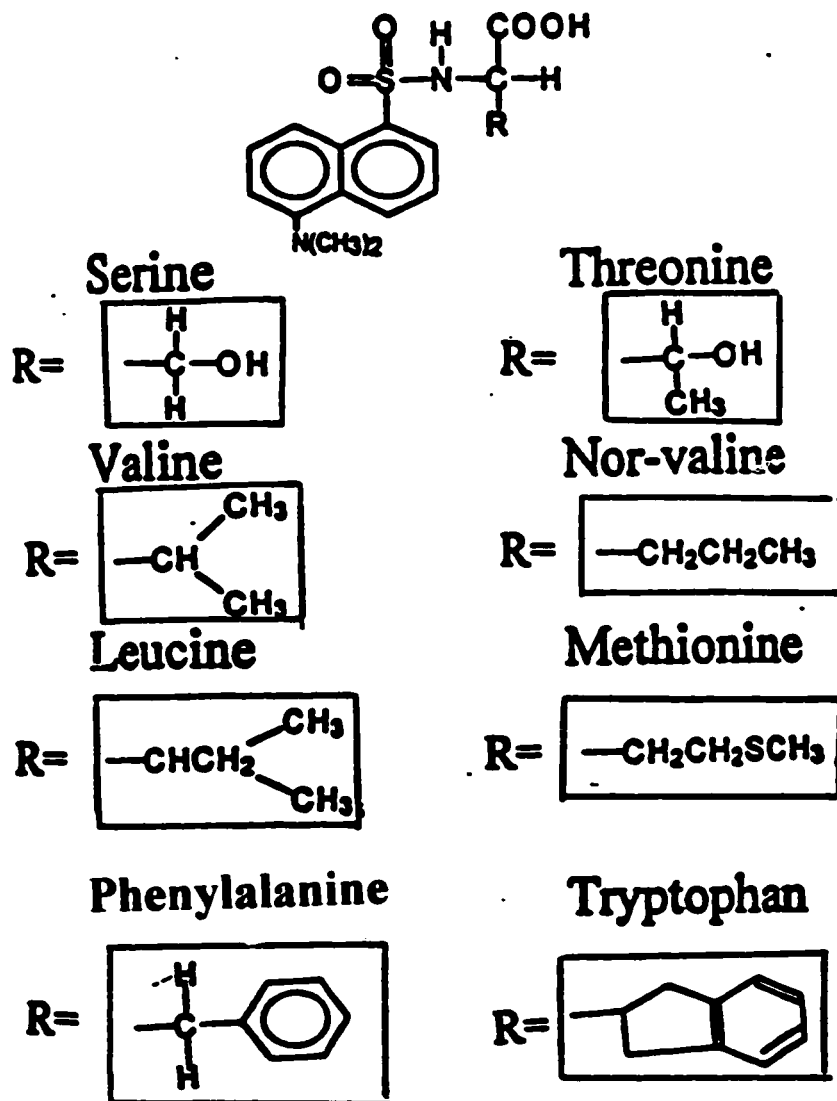
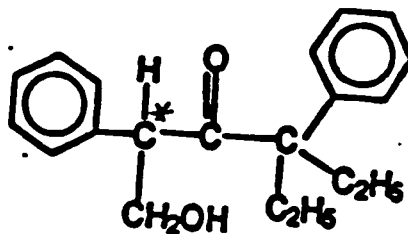


Figure 44. Structures of dansyl-amino acids.

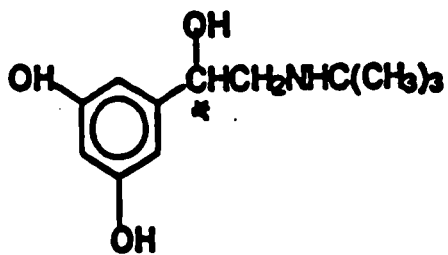
(A) Clenbuterol



(B) Tropicamide



(C) Terbutaline



(D) DL-Homatropine

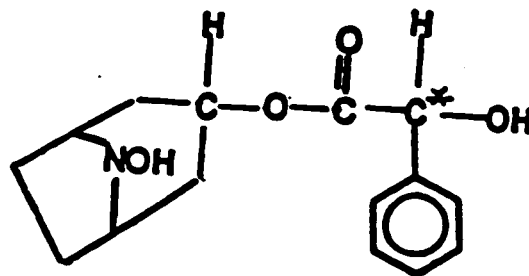


Figure 45. Structures of drugs.

2. Chromatographic conditions

Chromatographic measurements were made using the reversed phase mode with various methanol/water compositions at flow rates in the range of 0.5 mL/min to 0.6 mL/min. The dead time of the columns was determined by injection of potassium nitrate dissolved in methanol. A 10 μ L or 20 μ L sample volume was used in the analysis.

3. Chromatographic measurements

The capacity factor, k' , can be calculated from the retention time (t_r) of the solute and the dead time (t_o) as follows:-

$$k' = (t_r - t_o) / t_o$$

In the cases of chiral separation, k_1' and k_2' are defined as the capacity factors for the first and the second eluted optical isomers respectively. Furthermore, the extent to which the two optical isomers can be separated is expressed by separation factor (α) or resolution (R):-

$$\alpha = k_1' / k_2'$$

$$R = (t_{r1} - t_{r2}) / 0.5(w_1 + w_2)$$

where w_1 and w_2 are the width of the peaks and t_{r1} and t_{r2} are the retention times of the first and the second eluted optical isomer respectively.

In addition, the column efficiency can be estimated from the number of theoretical plates and it is given by $16(t_r / w)^2$

4. Interpretation of chromatographic data

a. Chiral separation of optical isomers of Benzodiazepines

i. β -cyclodextrin modified silica stationary phase

The chromatographic results obtained for the racemic benzodiazepines on three different columns of β -cyclodextrin bonded phases are reported in Tables 7, 8 and 9. For all six benzodiazepines studied on the Kromasil based β -cyclodextrin chiral columns, there was an increase in the capacity factor (k') with decreasing % methanol in the mobile phase. Similar results were obtained for the Vydac based β -cyclodextrin chiral column. Methanol functions as an organic modifier in the mobile phase for the separation. It is not surprising that it competes to a certain extent with the solute for the cavity of the cyclodextrin and forms inclusion complexes with cyclodextrin^{43,44}. Hence, the presence and the amount of methanol controls the retention of the solute. With a decrease in the % of methanol in the mobile phase, the solute interacts more extensively with the cavity and is retained longer on the stationary phase. This explains the trend of increasing retention times and hence capacity factors (k') with decreasing % methanol.

Based on the results obtained for all three columns shown above, chiral separations could only be achieved for oxazepam and temazepam. The typical chromatograms for these separations in various mobile phases are shown from Figure 46 to Figure 57. The chiral recognition mechanism for the separation of the benzediazepines by β -cyclodextrin is mainly the result of the formation of inclusion complexes of the solutes within the cyclodextrin cavity. The formation of the inclusion complexes involves the hydrophobic

Table 7: Variation of k' for benzodiazepines at different % methanol on β -cyclodextrin modified Kromasil silica chiral stationary phase (4.6 mm x 150 mm).

Sample	Flow rate (mL/min)	% Methanol	k'_1	k'_2
Temazepam	0.2	40%	0.67	0.67
	0.3	30%	1.23	1.62
	0.3	20%	3.31	4.17
	0.3	10%	4.35	5.53
Oxazepam	0.2	30%	1.91	4.04
	0.3	20%	2.30	4.22
	0.3	10%	4.74	10.55
Nitrazepam	0.3	30%	1.57	1.57
	0.3	20%	2.65	2.65
	0.3	10%	5.29	5.29
Clonazepam	0.3	30%	1.10	1.10
	0.3	20%	2.18	2.18
	0.3	10%	5.06	5.06
Diazepam	0.3	30%	1.50	1.50
	0.3	20%	3.17	3.17
	0.3	10%	3.80	3.80
Chlorodiazepam	0.25	30%	0.47	0.47
	0.2	20%	2.74	2.74
	0.2	10%	6.24	6.24

Table 8: Variation of k' for benzodiazepines at different % methanol on β -cyclodextrin modified Vydac silica chiral stationary phase (4.6 mm x 150 mm).

Sample	Flow rate (mL/min)	% Methanol	k'_1	k'_2
Temazepam	0.10	50%	1.25	1.25
	0.20	30%	1.63	1.84
	0.18	10%	3.25	3.99
Oxazepam	0.08	50%	1.30	1.58
	0.20	30%	1.57	2.72
	0.25	10%	5.16	9.79
Nitrazepam	0.20	50%	1.47	1.47
	0.09	40%	3.20	3.20
	0.12	30%	3.47	3.47
	0.27	10%	6.14	6.14
Clonazepam	0.20	50%	0.80	0.80
	0.20	30%	1.26	1.26
	0.18	10%	4.52	4.52
Diazepam	0.20	50%	1.12	1.12
	0.20	30%	1.40	1.40
	0.24	10%	6.80	6.80
Chlorodiazepam	0.20	50%	1.59	1.59
	0.20	30%	2.86	2.86
	0.27	10%	4.31	4.31

Table 9: Variation of k' for benzodiazepines at different % methanol on β -cyclodextrin modified Kromasil silica chiral stationary phase (4.6 mm x 50 mm short column).

Sample	Flow rate (mL/min)	% Methanol	k'_1	k'_2
Temazepam	0.20	50%	1.69	2.12
	0.15	30%	2.32	2.85
	0.10	12%	2.67	3.12
Oxazepam	0.15	40%	1.42	2.57
	0.15	30%	2.45	4.93
Nitrazepam	0.30	30%	0.26	0.26
	0.15	20%	0.39	0.39
	0.09	10%	0.40	0.40
Clonazepam	0.15	40%	1.27	1.27
	0.30	30%	1.35	1.35
Diazepam	0.15	40%	1.27	1.27
	0.30	30%	1.46	1.46
	0.15	25%	1.52	1.52
	0.09	15%	1.86	1.86
Chlorodiazepam	0.15	40%	4.39	4.39
	0.30	30%	8.77	8.77

Temazepam

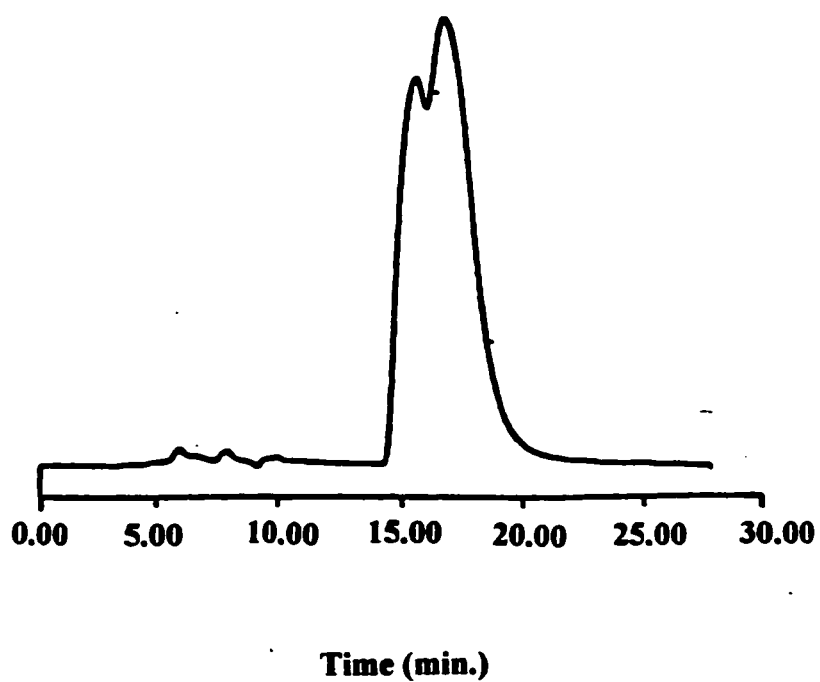


Figure 46. Reversed phase separation of the optical isomers of temazepam on a β -cyclodextrin modified Vydac silica column (4.6 mm x 150 mm); mobile phase: methanol:water (30:70); flow rate: 0.20 mL/min; temperature: 25°C
UV detection at 254 nm; sample injection: 20 μ L; column pressure :77 bars.

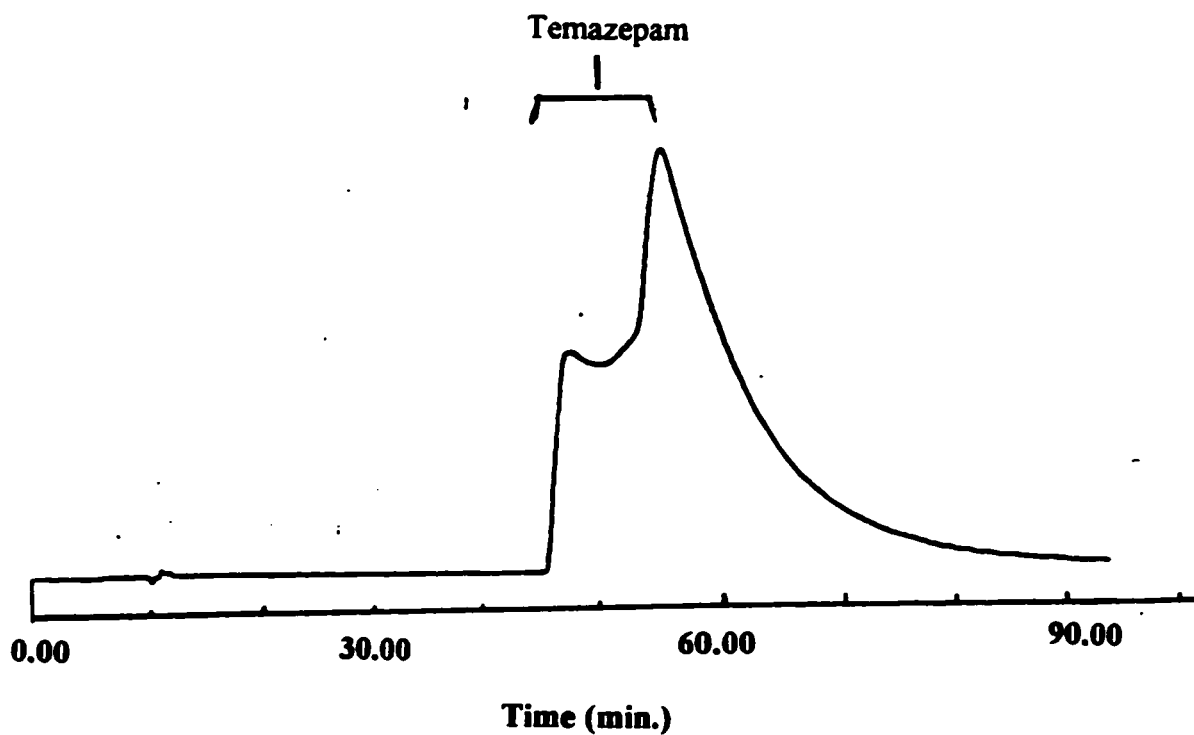


Figure 47. Reversed phase separation of the optical isomers of temazepam on a β -cyclodextrin modified Vydac silica column (4.6 mm x 150 mm); mobile phase: methanol:water (10:90); flow rate: 0.18 mL/min; temperature: 25°C; UV detection at 254 nm; sample injection: 20 μ L; column pressure: 50 bars.

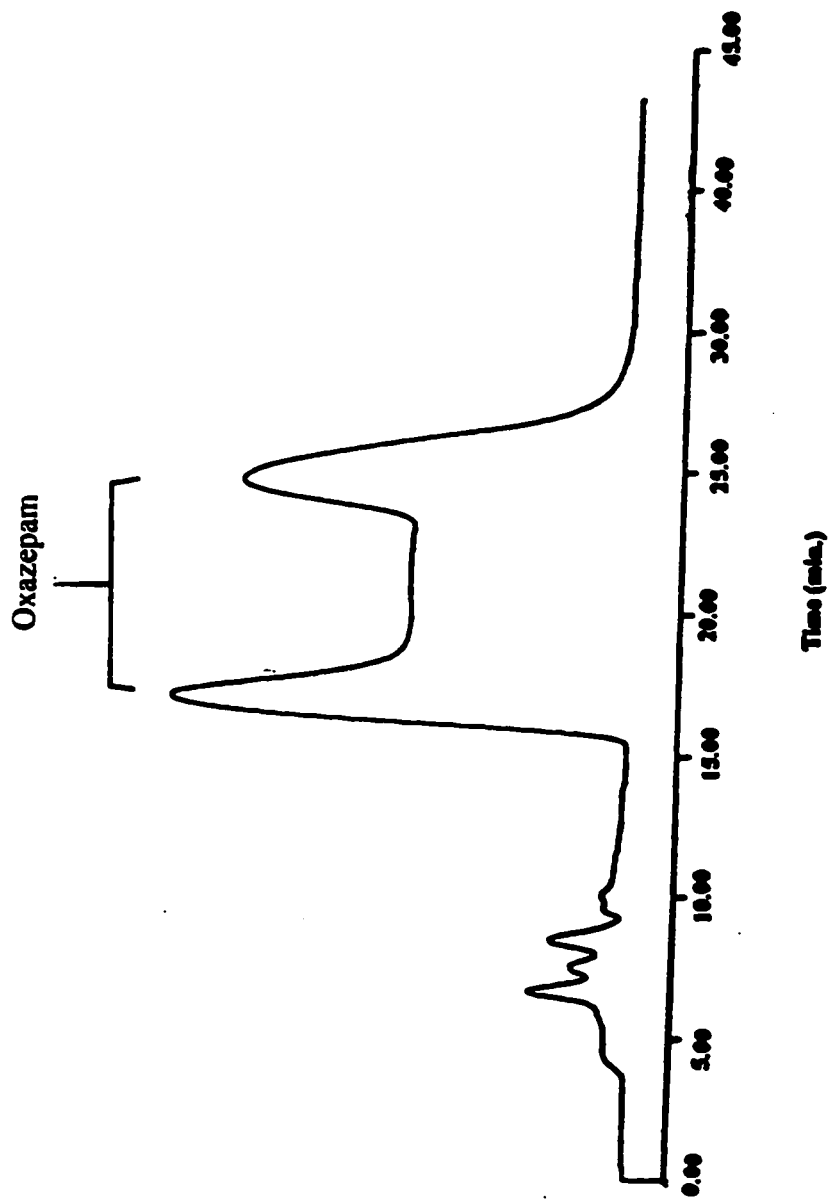


Figure 48. Reversed phase separation of the optical isomers of oxazepam on a β -cyclodextrin modified Vydac silica column (4.6 mm x 150 mm); mobile phase: methanol:water (30:70); flow rate: 0.20 mL/min; temperature: 25°C; UV detection at 254 nm; sample injection: 20 μ L; column pressure :77 bars.

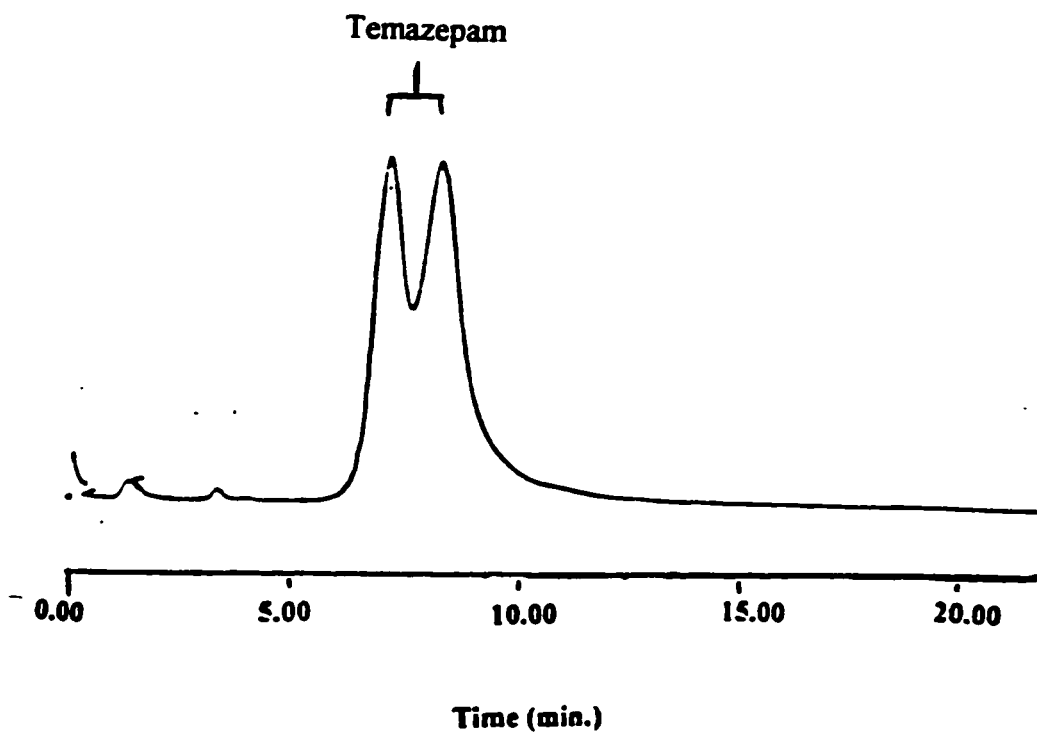


Figure 49. Reversed phase separation of the optical isomers of temazepam on a β -cyclodextrin modified Kromasil silica column (4.6 mm x 50 mm); mobile phase: methanol:water (50:50); flow rate: 0.20 mL/min; temperature: 25°C; UV detection at 254 nm; sample injection: 10 μ L; column pressure: 1140 psi.

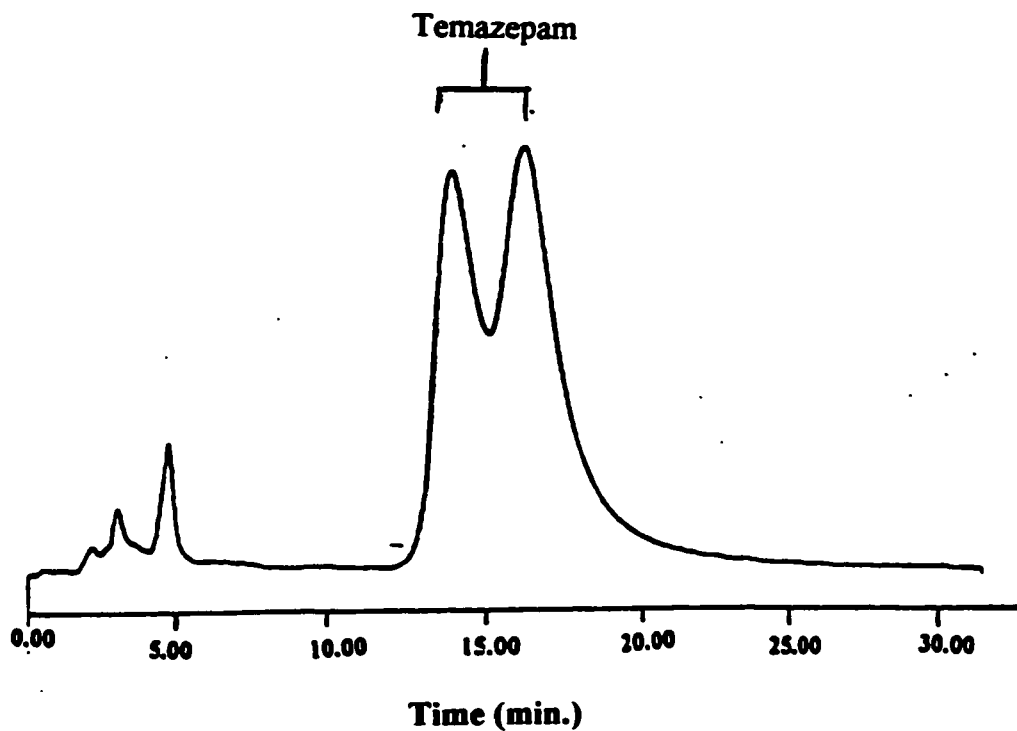


Figure 50. Reversed phase separation of the optical isomers of temazepam on a β -cyclodextrin modified Kromasil column (4.6 mm x 50 mm); mobile phase: methanol:water (30:70); flow rate: 0.15 mL/min; temperature: 25°C; UV detection at 254 nm; sample injection: 20 μ L; column pressure: 14 bars.

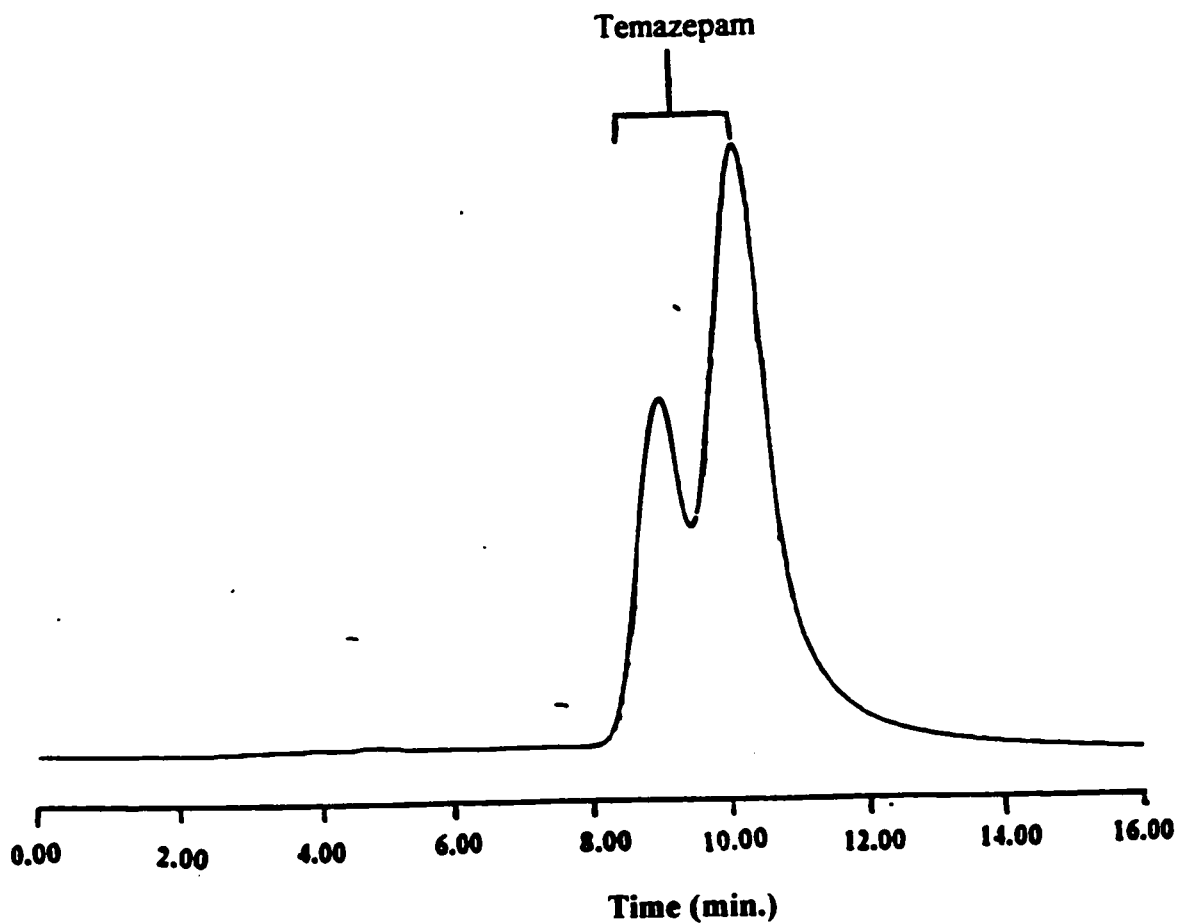


Figure S1. Reversed phase separation of the optical isomers of temazepam on a β -cyclodextrin modified Kromasil column (4.6 mm x 50 mm); mobile phase: methanol:water (12:88); flow rate: 0.10 mL/min; temperature: 25°C; UV detection at 254 nm; sample injection: 10 μ L; column pressure :783 psi.

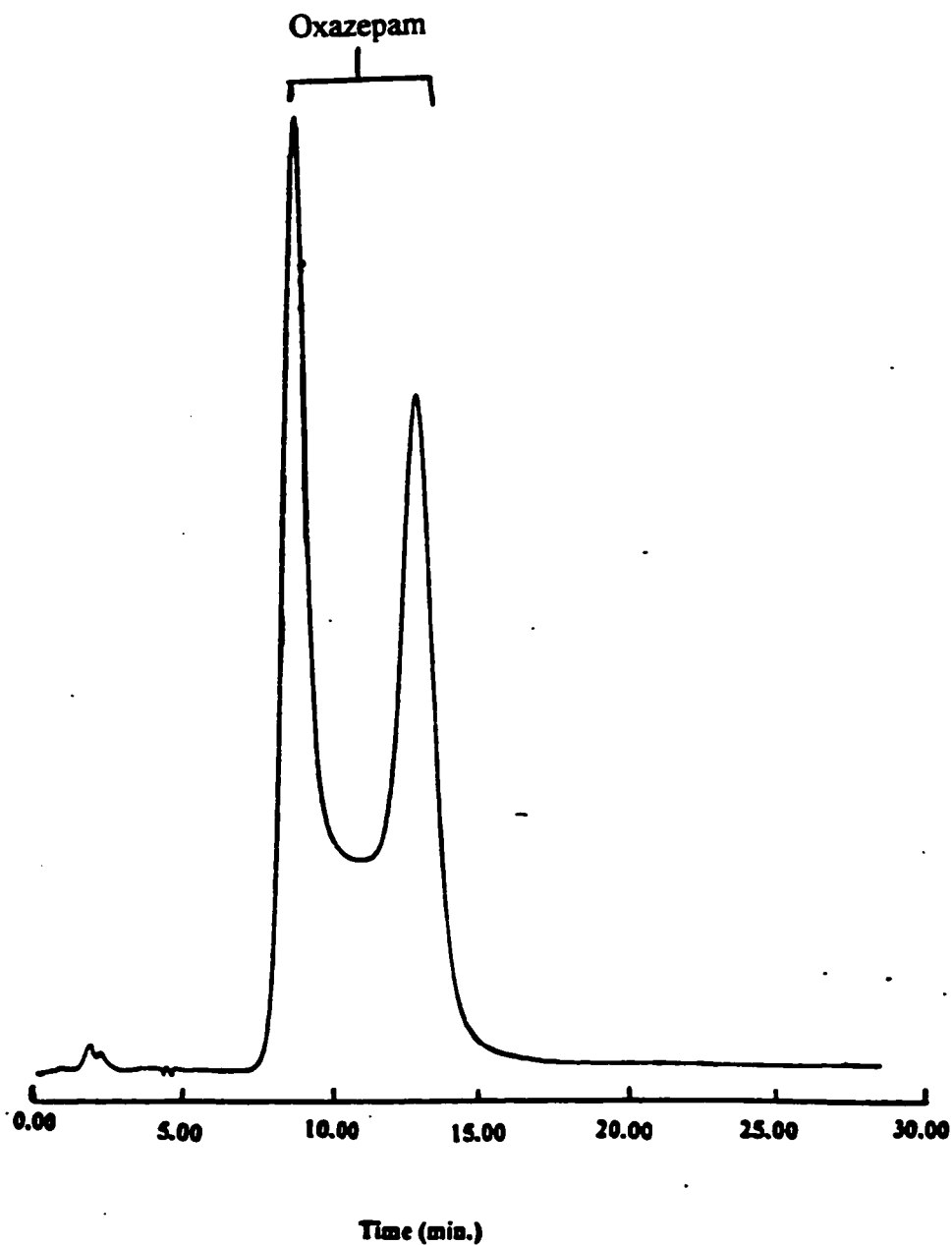


Figure 52. Reversed phase separation of the optical isomers of oxazepam on a β -cyclodextrin modified Kromasil column (4.6 mm x 50 mm); mobile phase: methanol:water (40:60); flow rate: 0.15mL/min; temperature: 25°C; UV detection at 254 nm; sample injection: 10 μ L; column pressure :755 psi.

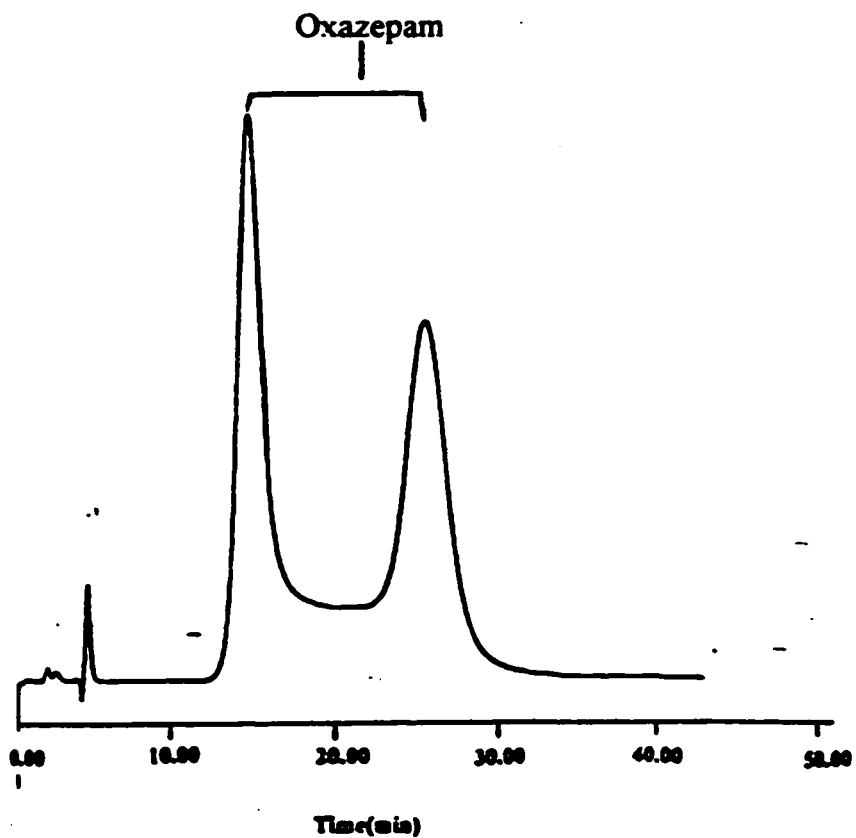


Figure 53. Reversed phase separation of the optical isomers of oxazepam on a β -cyclodextrin modified Kromasil column (4.6 mm x 50 mm); mobile phase: methanol:water (30:70); flow rate: 0.15mL/min; temperature: 25°C; UV detection at 254 nm; sample injection: 20 μ L; column pressure: 14 bars.

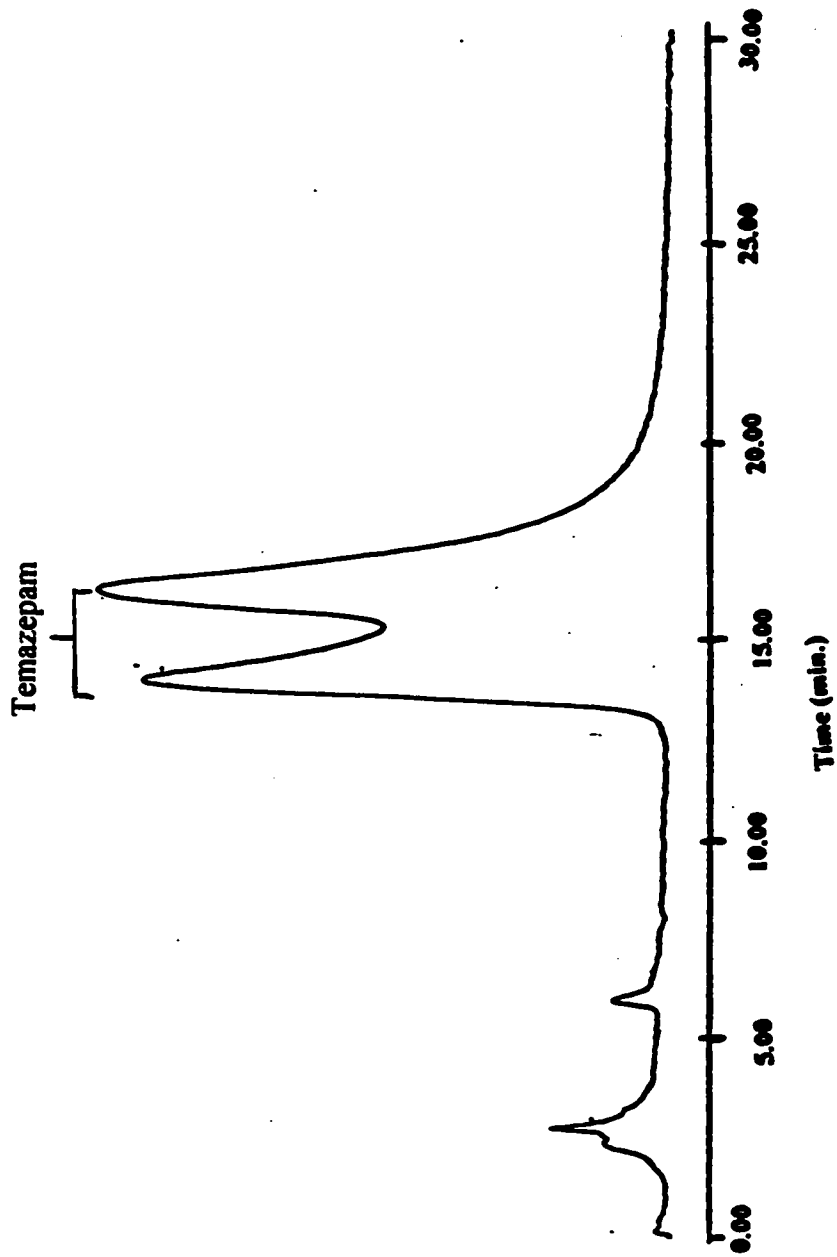


Figure 54. Reversed phase separation of the optical isomers of temazepam on a β -cyclodextrin modified Kromasil column (4.6 mm x 150 mm); mobile phase: methanol:water (30:70); flow rate: 0.30 mL/min; temperature: 25°C; UV detection at 254 nm; sample injection: 10 μ L; column pressure: 1425 psi.

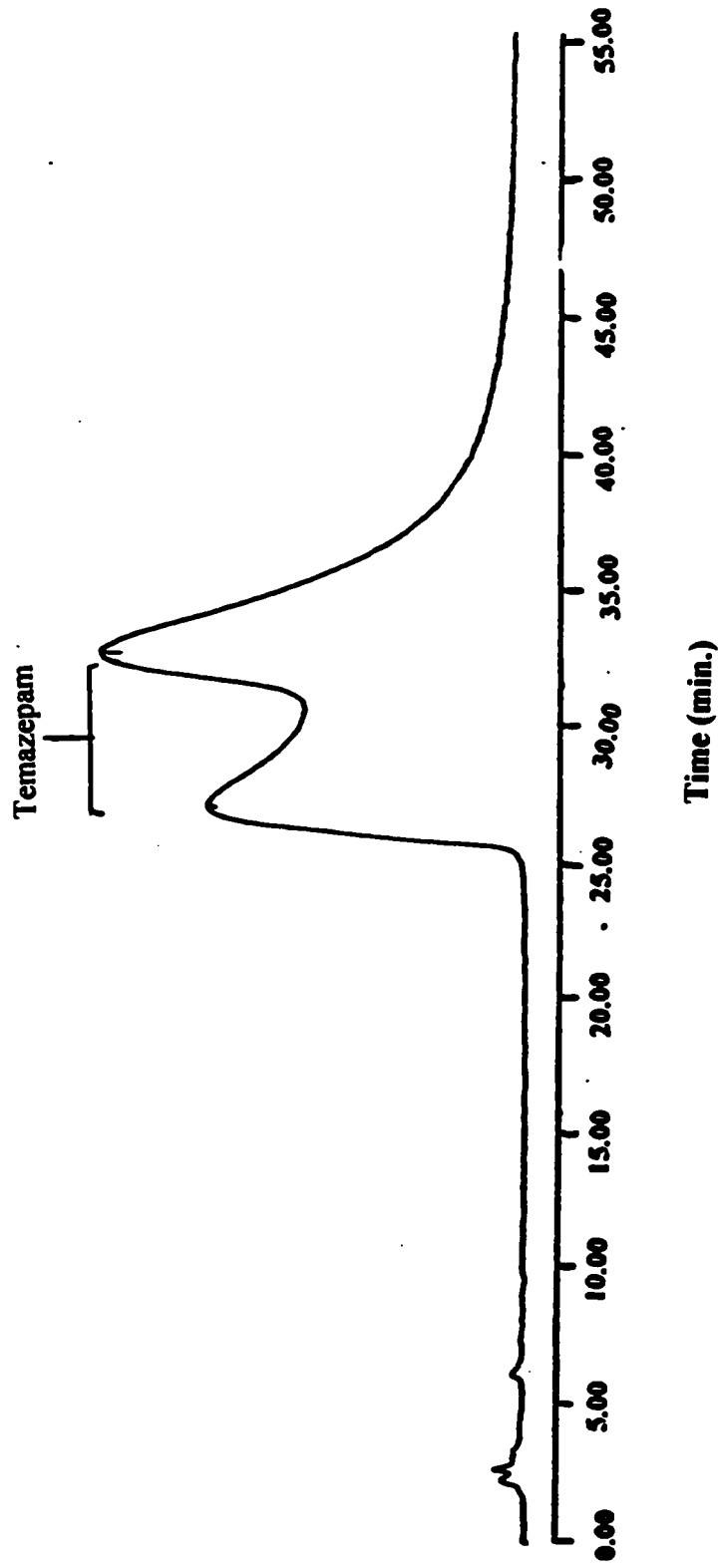


Figure 55. Reversed phase separation of optical isomers of temazepam on a β -cyclodextrin modified Kromasil column (4.6 mm x 150 mm); mobile phase: methanol:water (20:80); flow rate: 0.30 mL/min; temperature: 25°C; UV detection at 254 nm; sample injection: 10 μ L; column pressure: 1311 bars.

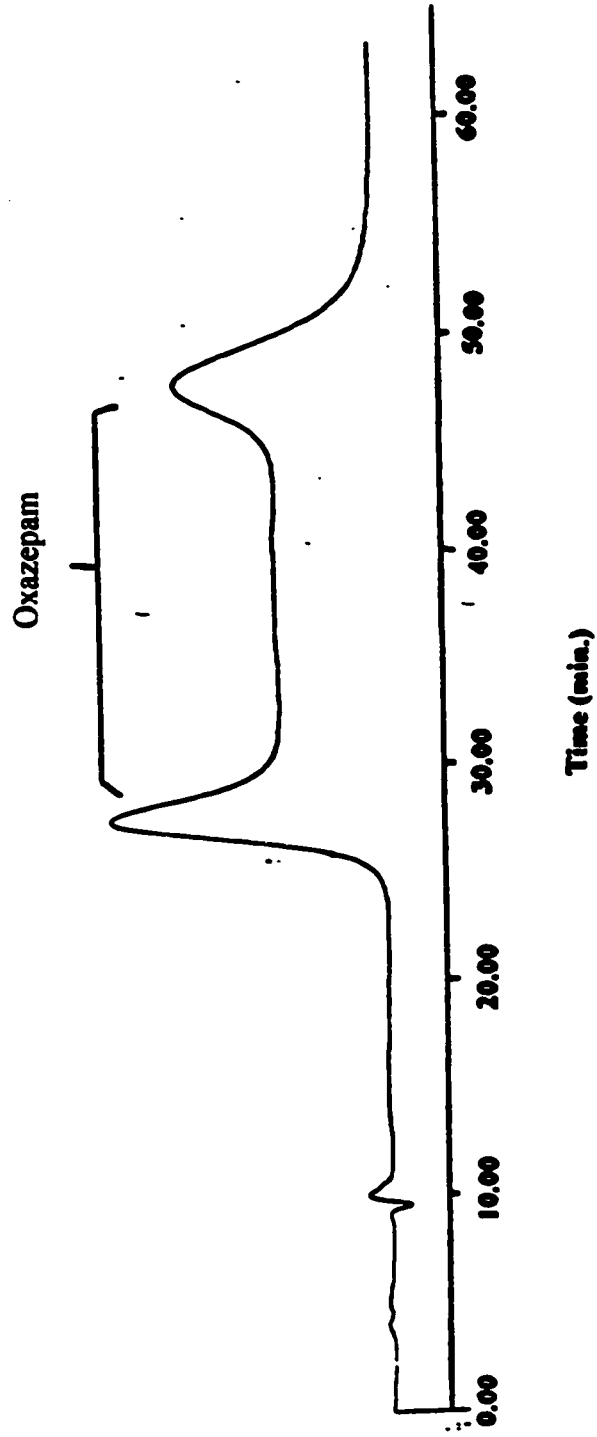


Figure 56. Reversed phase separation of the optical isomers of oxazepam on a β -cyclodextrin modified Kromasil column (4.6 mm x 150 mm); mobile phase: methanol:water (30:70); flow rate: 0.20 mL/min; temperature: 25°C; UV detection at 254 nm; sample injection: 20 μ L; column pressure: 67 bars.

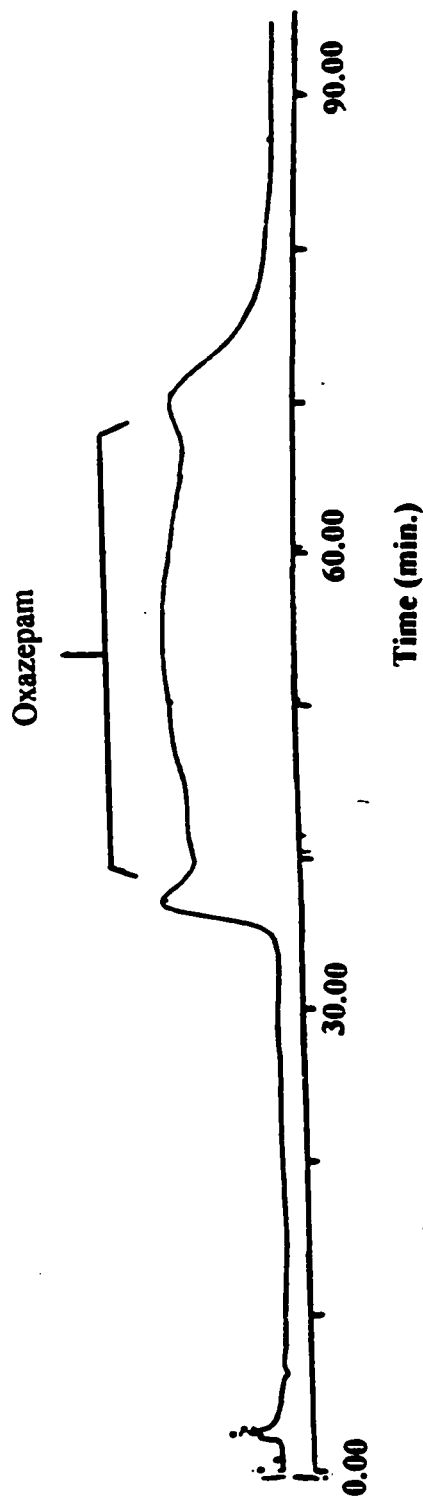


Figure S7. Reversed phase separation of the optical isomers of oxazepam on a β -cyclodextrin modified Kromasil column (4.6 mm x 150 mm); mobile phase: methanol:water (10:90); flow rate: 0.15 mL/min; temperature: 25°C; UV detection at 254 nm; sample injection: 10 μ L; column pressure: 1396 psi.

interaction of the inner cavity of the cyclodextrin with the hydrophobic moiety (aromatic rings) of the benzodiazepines molecules. The presence of the hydroxyl groups at the 3 position of the benzodiazepines is critical for the chiral separation of the enantiomers. Such hydroxyl groups are responsible for the hydrogen bonding which exists between the solute and either the oxygen ring or the carbonyl oxygen in the substituted cyclodextrin molecule. In addition, the existence of an acidic hydrogen on an amine group of the benzediazepine ring further introduces hydrogen bonding in the chiral recognition mechanism⁴⁴. Finally, the presence of the remaining polar or bulky non-polar groups may cause dipole stacking or steric repulsion respectively. With reference to the structural differences between the six members of benzediazepines, the absence of both the chiral center and the necessary hydroxyl group at the 3 position of the solute ring can account for the coelution of the optical isomers of diazepam, nitrazepam and clonazepam. Furthermore, the inability to separate chlorodiazepoxide isomers is probably due to the non-specific achiral interaction at the $C=N^+(H)-O$ of the benzodiazepines with the stationary phase. Alternatively, the -OH group at the 3 position of the chlorodiazepoxide can form intramolecular hydrogen bonding with the neighboring N-O group. Therefore, the -OH group will be less available for the chiral recognition interaction with the stationary phase.

Finally, according to the chromatographic data of oxazepam and temazepam as listed in Tables 10A and 10B below, it was found that both the separation factors and the resolution of oxazepam optical isomers are better than the other benzodiazepines regardless of the type of silica used as the solid support. The result is attributed to the fact

Table 10A: Comparison of separation factor and resolution of oxazepam and temazepam on β -cyclodextrin Komasil based chiral column, 4.6 mm x 150 mm.

Sample	%MEOH	Flow rate (mL/min)	k' ₁	k' ₂	α separation factor	R Resolution	Number of theoretical plates for 1 st peak, N ₁	Number of theoretical plates for 2 nd peak, N ₂
Temazepam	30%	0.30	1.22	1.59	1.30	0.84	442	516
	30%	0.20	1.54	1.99	1.29	0.64	202	247
	20%	0.30	3.31	4.17	1.26	0.59	105	217
Oxazepam	30%	0.20	1.91	4.04	2.11	2.34	256	246
	20%	0.30	2.30	4.22	1.84	1.11	121	51
	10%	0.30	4.74	10.55	2.23	1.83	197	122

Table 10B: Comparison of separation factor and resolution of oxazepam and temazepam on β -cyclodextrin Vydac based chiral column, 4.6 mm x 150 mm.

Sample	%MEOH	Flow rate (mL/min)	k' ₁	k' ₂	α separation factor	R Resolution	Number of theoretical plates for 1 st peak, N ₁	Number of theoretical plates for 2 nd peak, N ₂
Temazepam	30%	0.20	1.63	1.84	1.13	0.36	262	247
	10%	0.18	3.25	3.99	1.23	0.42	58	216
Oxazepam	30%	0.20	1.57	2.72	1.73	1.49	271	275
	10%	0.25	5.16	9.79	1.90	1.01	31	90

that the presence of the acidic hydrogen on the amine group in the benzodiazepine ring provides additional hydrogen bonding with the stationary phase. The presence of this proton donor is essential in the chiral recognition mechanism⁴⁴ and thus it enhances the enantioselectivity.

In general, it was determined that the resolution (R) for oxazepam and temazepam on both the β -cyclodextrin Kromasil chiral column (long) and β -cyclodextrin Vydac chiral column decreases with a significant drop in the % methanol (30% to 10%). In the case of the β -cyclodextrin Kromasil short chiral column, because the measurements were obtained on two different packing material, there wasn't any particular trend based on the % methanol for the resolution of the isomers. Even though the solute molecules have a stronger affinity and more extensive interaction with the stationary phase in a high % water (weak solvent) mobile phase composition, the significant increase in the retention time accompanied by the broadening of the peak causes an adverse effect on the resolution.

At a slower flow rate, more interaction should take place between the solutes and the stationary phase and thus a better separation should be achieved. However, the peak shapes will be broadened simultaneously. So an optimum flow rate is required for the best efficiency. Although analyses at a particular mobile composition have been done at different flow rates, the study was not extensive enough to lead to any conclusion concerning the effect of flow rate on the separation efficiency of the benzodiazepines.

Efficiency is another important parameter which determines the quality of the column. Overall, it was found that the number of theoretical plates varies in the range of

approximately from 30 to 500. It is a small value and it shows that mass transfer is slow in the reversed phase mode and thus the enantioselective resolution was low.

Finally, from the comparison of the general performance of Kromasil based and Vydac based chiral stationary phases in terms of separation factor, resolution and the number of theoretical plates, it was determined that the Kromasil based chiral stationary phase provides a better separation for the compounds tested.

ii. On (R)- (+)- acryloxy- β , β -dimethyl- γ -butyrolactone modified silica based chiral stationary phase.

There was no chiral separation for any of the six different benzodiazepines studied on the lactone-modified CSP. This indicated that there were not sufficient interactions to enantiomerically differentiate the optical isomers. For instance, the types of interaction existing between temazepam and the CSP are shown in Figure 58. They are identified as the non-polar bulky group steric repulsions and the interaction between the acidic π -aromatic ring (with Cl as an electron withdrawing group) with the basic sites on the lactone surface. Overall, the three point interactions in this case are not selective enough so that there is no resolution of the optical isomers.

In Table 11, the capacity factors (k') for the benzodiazepines are listed. The variations of k' with % methanol for the benzodiazepines are plotted in Figure 59. The capacity factor k' increases as the % of methanol decreases. This illustrates that the main interaction existing between the solutes and the CSP is hydrophobic in nature. A decrease in the amount of organic modifier (methanol) allows more extensive interaction between the solute and the stationary phase and thus more stable transient diastereoisomers should

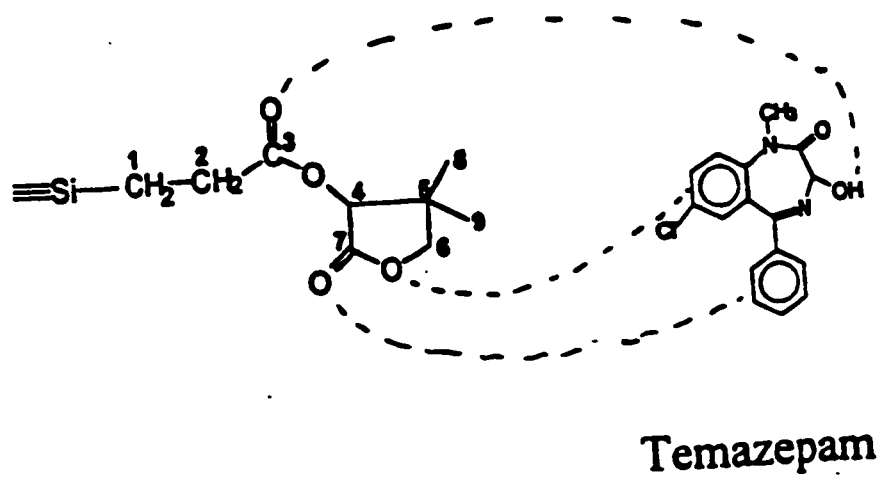


Figure 58. Diagram showing the interactions between (R)-(+)-acryloxy-β,β-dimethyl-γ-butyrolactone and temazepam.

Table 11: Variation of capacity factor (k') for benzodiazepines at different % methanol in the mobile phase. Flow rate for analysis is 0.5 mL/min

Sample	% methanol	k'
Temazepam	50%	0.90
	40%	1.54
	30%	3.97
	20%	6.26
Oxazepam	50%	0.68
	40%	1.12
	30%	2.51
	20%	4.91
Nitrazepam	50%	0.79
	40%	1.54
	30%	2.60
	20%	4.63
Clonazepam	50%	-0.17
	40%	0.08
	30%	0.16
	20%	5.50
Diazepam	50%	1.38
	40%	2.58
	30%	7.24
	20%	15.13
Chlorodiazepoxide	50%	2.31
	40%	5.43
	30%	18.85

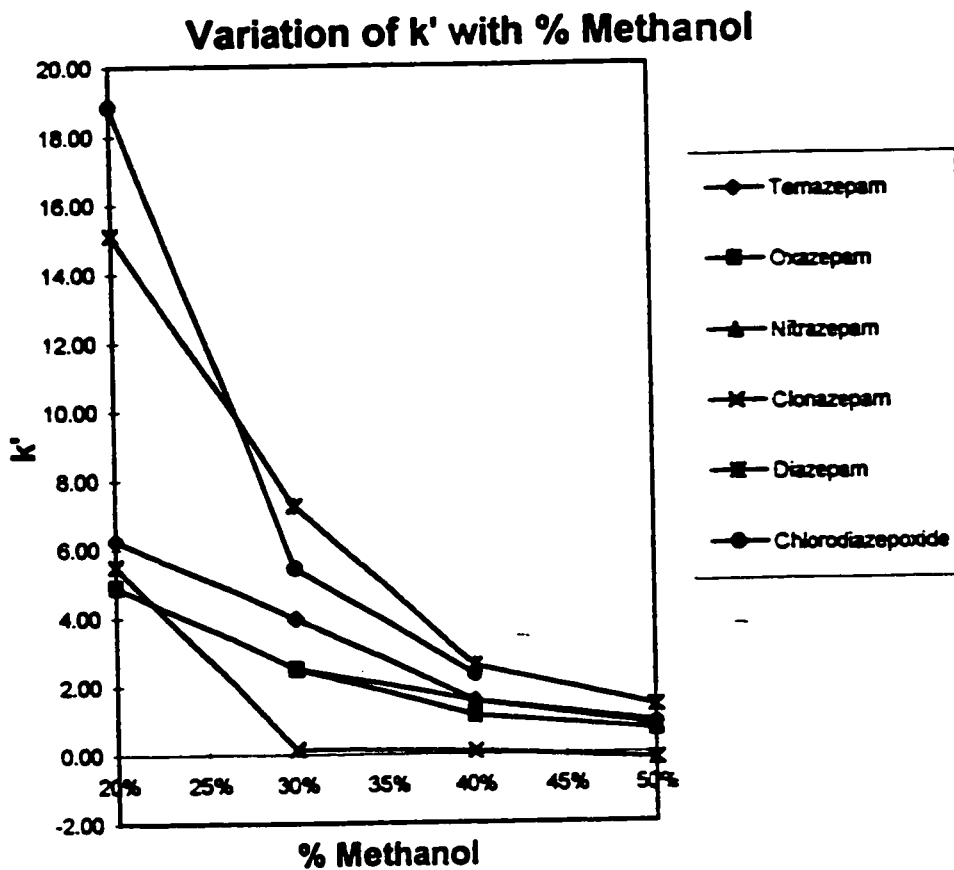


Figure 59. A plot of capacity factor (k') vs % methanol in the mobile phase for the chromatographic studies of benzodiazepines; Flow rate: 0.5 mL/min

form. This explains the greater retention on the stationary phase at high water content as well as the weak chiral interactions since no resolution of enantiomers is observed under these conditions.

b. Chiral separation of Dansyl-DL-amino acids

i. On β -cyclodextrin modified silica based chiral stationary phase

The cyclodextrin chiral stationary phase has been shown to be widely applicable for the separation of various derivatives of amino acids. The main factor that accounts for the enantioselectivity or retention of the solute is the formation of the inclusion complexes between the (dimethylamino)naphthyl moiety of the dansyl group on the solute into the cavity of the cyclodextrin stationary phase^{45,46}. This will make the substituents and the chiral carbon atom in the amino acid in close proximity to the hydroxyl groups or other active sites on the cyclodextrin rim. In this way, the carboxylic acid group/ carboxylate group and the amine group from the amino acid could form hydrogen bonds with the hydroxyl group of the cyclodextrin. In addition, it is possible for the sulfonyl oxygen to participate in hydrogen bond formation⁴⁵. Furthermore, the side chain on the chiral carbon atom of the amino acid can also affect the retention process. An increase in the hydrophobicity of the side chain will increase the tendency of being excluded from the relatively hydrophilic mobile phase^{46,47}. In the other words, the solute tends to be closer to the vicinity of the cyclodextrin which increases the extent of the penetration of the dansyl ring into the cavity. This results in longer retention and a greater capacity factor.

Table 12: Chromatographic data for dansyl-amino acids using β -cyclodextrin Kromasil chiral column, 4.6 mm x 150 mm.

Sample	% MEOH	Flow rate (mL/min)	k' ₁	k' ₂
Dansyl-DL-threonine	20%	0.20	-0.28	-0.28
	10%	0.20	-0.11	-0.11
Dansyl-DL-Tryptophan	30%	0.20	-0.16	-0.16
	20%	0.20	0.31	0.31
	10%	0.20	1.20	1.20
Dansyl-DL-Valine	30%	0.20	-0.36	-0.36
	20%	0.20	0.08	0.08
	10%	0.20	1.33	1.33
Dansyl-DL-Leucine	50%	0.30	0.34	0.40
	40%	0.30	0.34	0.45
	30%	0.30	0.57	0.97
	20%	0.30	0.64	1.16
	10%	0.20	1.92	2.75
Dansyl-DL-phenylalanine	30%	0.20	-0.02	-0.02
	20%	0.20	0.34	0.34
	10%	0.20	3.13	3.13
Dansyl-DL-methionine	30%	0.20	0.05	0.05
	20%	0.20	0.40	0.40
	10%	0.20	0.90	0.90
Dansyl-DL-Norvaline	30%	0.20	-0.30	-0.30
	20%	0.20	0.36	0.36
	10%	0.20	0.58	0.58
Dansyl-DL-Serine	30%	0.20	-0.32	-0.32
	20%	0.20	-0.12	-0.12
	10%	0.20	-0.06	-0.06

Table 13: Chromatographic data for dansyl-DL-amino acids using β -cyclodextrin Vydac chiral column, 4.6 mm x 150 mm.

Sample	% MEOH	Flow rate (mL/min)	k'₁	k'₂
Dansyl-DL-threonine	50%	0.15	0.25	0.25
	30%	0.12	1.05	1.05
Dansyl-DL-Tryptophan	50%	0.15	0.55	0.55
	30%	0.120	1.36	1.36
	10%	0.18	2.34	2.34
Dansyl-DL-Valine	50%	0.15	0.30	0.30
	30%	0.12	0.87	0.87
	10%	0.18	1.21	1.21
Dansyl-DL-Leucine	50%	0.15	1.16	1.16
	40%	0.10	1.33	1.52
	30%	0.12	1.45	1.90
	10%	0.09	3.34	3.86
Dansyl-DL-phenylalanine	50%	0.15	0.55	0.55
	30%	0.12	2.87	2.87
	10%	0.18	3.86	3.86
Dansyl-DL-methionine	50%	0.15	0.50	0.50
	30%	0.12	0.83	0.83
	10%	0.18	1.97	1.97
Dansyl-DL-Norvaline	50%	0.15	0.39	0.39
	30%	0.12	0.87	0.87
	10%	0.18	1.01	1.01
Dansyl-DL-Serine	50%	0.15	0.22	0.22
	30%	0.12	0.32	0.32
	10%	0.18	0.88	0.88

Table 14: Chromatographic data for dansyl-DL-amino acids by using β -cyclodextrin Kromasil chiral column, 4.6 mm x 50 mm (short).

Sample	% MEOH	Flow rate (mL/min)	k'₁	k'₂
Dansyl-DL-threonine	40%	0.15	0.20	0.20
	20%	0.15	1.11	1.11
Dansyl-DL-Tryptophan	40%	0.15	-0.07	-0.07
	20%	0.15	0.49	0.49
Dansyl-DL-Valine	40%	0.15	-0.26	-0.26
	20%	0.15	0.53	0.53
Dansyl-DL-Leucine	40%	0.15	0.15	0.15
	20%	0.12	0.23	0.23
	10%	0.06	0.62	0.62
Dansyl-DL-phenylalanine	40%	0.15	0.10	0.10
	20%	0.12	0.13	0.13
Dansyl-DL-methionine	40%	0.15	-0.05	-0.05
	20%	0.15	1.06	1.06
Dansyl-DL-Norvaline	40%	0.15	-0.21	-0.21
	20%	0.12	0.02	0.02
	15%	0.10	0.04	0.04
Dansyl-DL-Serine	40%	0.15	-0.11	-0.11
	20%	0.15	0.18	0.18

The results for the study of the chiral separation of eight dansyl-DL-amino acid on the three cyclodextrin modified silica surfaces are listed in Tables 12, 13 and 14. Basically, only dansyl-DL-leucine can be separated with low resolution on the β -cyclodextrin Kromasil chiral (long) column and the β -cyclodextrin Vydac chiral column. Examples of chromatograms for some amino acid analyses are shown from Figure 60 to Figure 63. The poor performance of the short β -cyclodextrin Kromasil chiral column for the separation of dansyl-amino acids is probably due to the fact that it can only provide a very small number of theoretical plates for interaction between the solute and the CSP. Such low column efficiency explains the coelution of the racemates of dansyl-DL-leucine.

The enantioselectivity and hence the possibility of separation of the dansyl-DL-amino acids is very much related to the structure of the substituted β -cyclodextrin. For the polymerizable substituted β -cyclodextrin used in this research, some of the hydroxyl groups at the C2, C3 or C6 carbons are derivatized and such modification changes the depth of the cyclodextrin cavity thus affecting the extent of penetration of the dansyl-ring into the cavity⁴⁶. As a result, the dansyl-DL-amino acids with large and bulky side chains such as phenylalanine and tryptophan cannot penetrate deep into the cavity and so the interaction is decreased and enantioselectivity is diminished. On the other hand, the dansyl-DL-amino acids with a hydrophilic side chain such as serine, threonine and methionine might not have sufficient interaction with the derivatized cyclodextrin in the formation of inclusion complexes and thus no chiral selectivities occurs. Finally, in the cases of valine

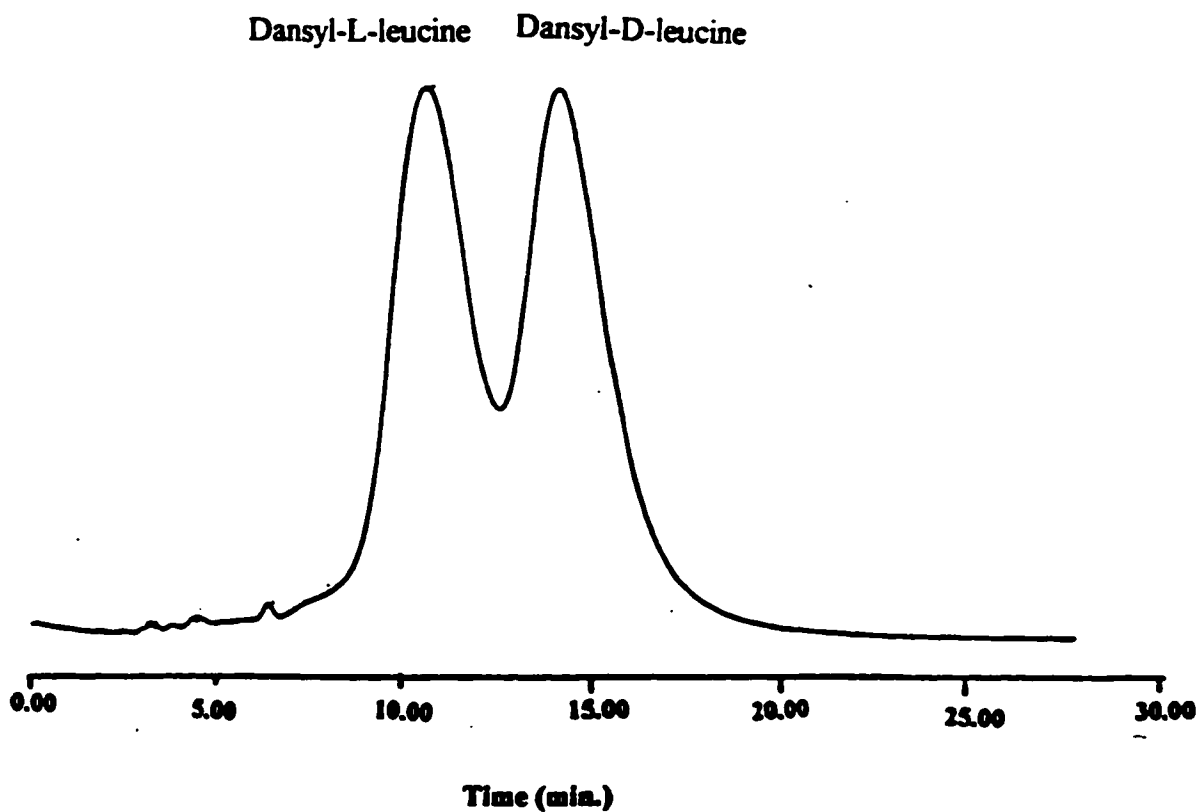


Figure 60. Reversed phase separation of the optical isomers of dansyl-DL-leucine on a β -cyclodextrin modified Kromasil column (4.6 mm x 150 mm); mobile phase: methanol/water (20:80); flow rate: 0.30 mL/min; temperature: 25°C; UV detection at 254 nm; sample injection: 10 μ L; column pressure: 1481 psi.

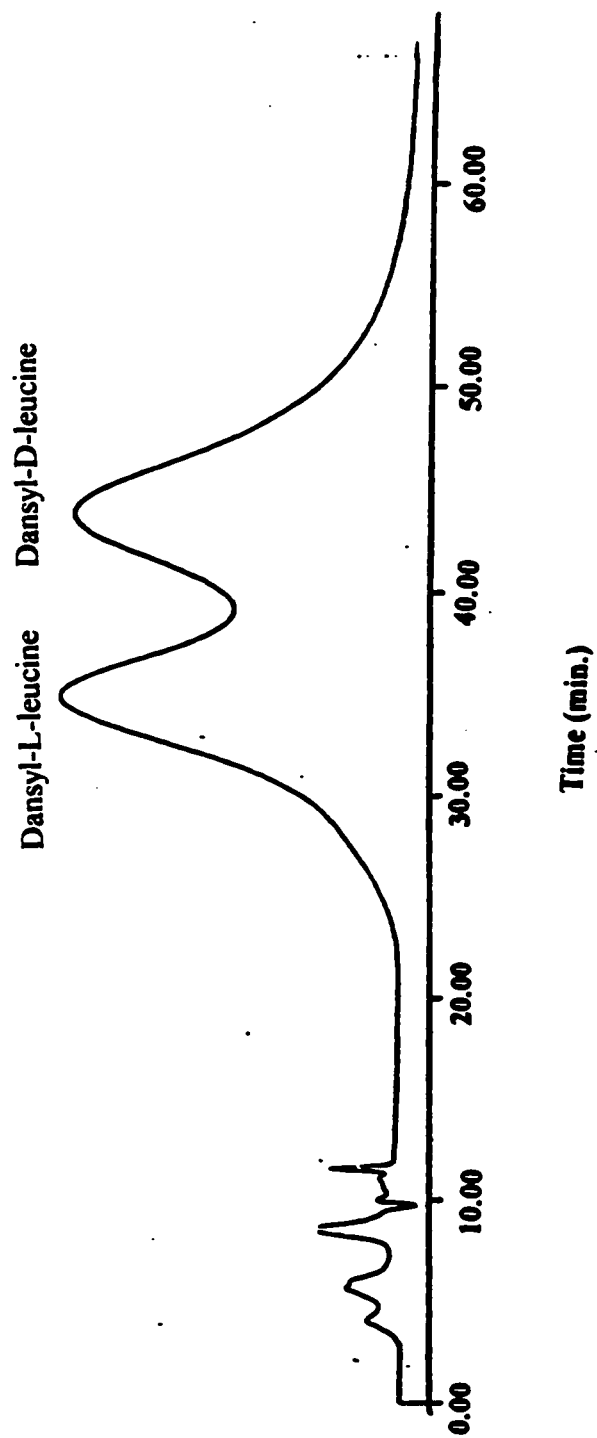


Figure 61. Reversed phase separation of the optical isomers of dansyl-DL-leucine on a β -cyclodextrin modified Kromasil column (4.6 mm x 150 mm); mobile phase: methanol/water (10:90); flow rate: 0.20 mL/min; temperature: 25°C; UV detection at 254 nm; sample injection: 10 μ L; column pressure: 59 bars.

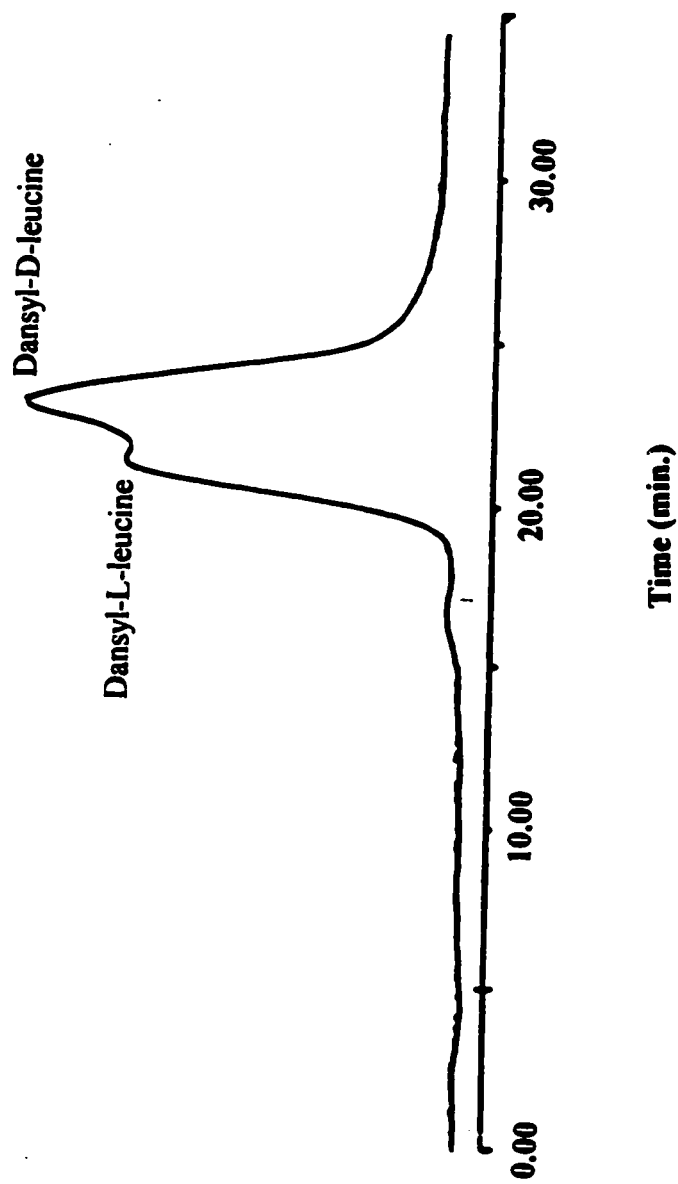


Figure 62. Reversed phase separation of optical isomers of dansyl-DL-leucine on a β -cyclodextrin modified Kromasil column (4.6 mm x 150 mm); mobile phase: methanol/water (40:60); flow rate: 0.10 mL/min; temperature: 25°C; UV detection at 254 nm; sample injection: 10 μ L; column pressure: 1510 psi.

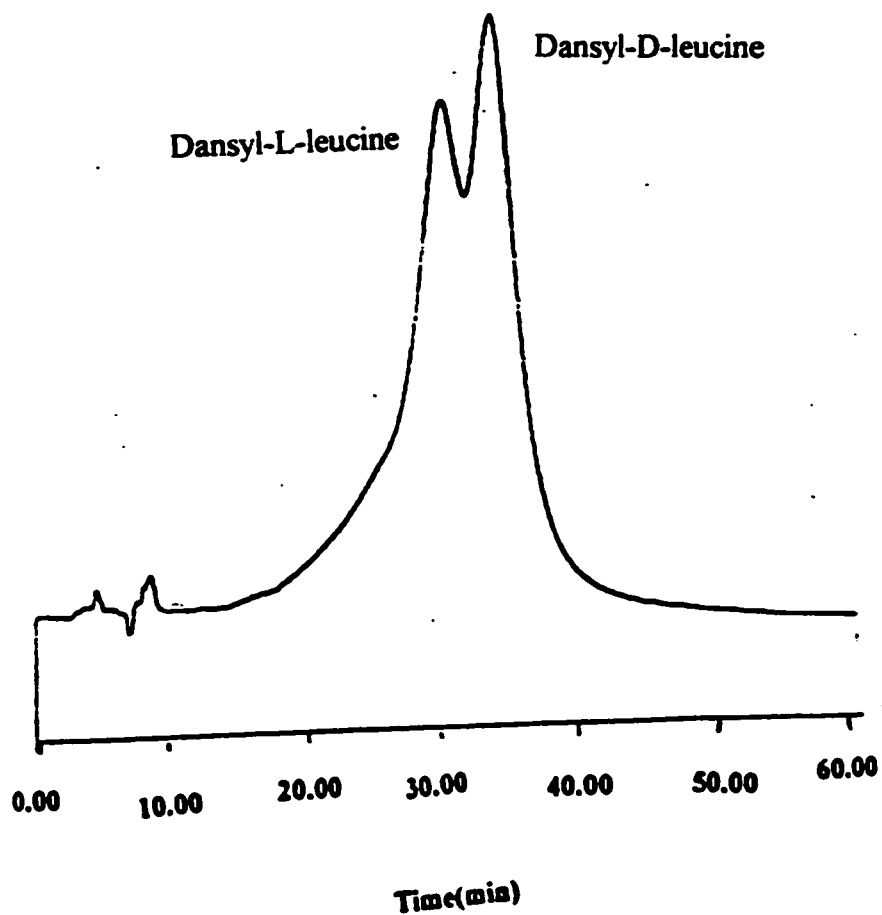


Figure 63. Reversed phase separation of optical isomers of dansyl-DL-leucine on a β -cyclodextrin modified Vydac column (4.6 mm x 150 mm); mobile phase: methanol/water (10:90); flow rate: 0.27 mL/min; temperature: 25°C; UV detection at 254 nm; sample injection: 20 μ L; column pressure: 73 bars.

or norvaline, the relatively smaller size of the side chains are not hydrophobic enough for interaction. As a consequence, dansyl-DL-leucine which has a side chain of appropriate size and hydrophobicity can form inclusion complexes of different stability so that they can be separated by the newly developed cyclodextrin CSP.

For all the dansyl-amino acid tested on the β -cyclodextrin chiral stationary, there was an increase in the capacity factor with the % of methanol in the mobile phase. Since the organic modifier can compete with the solute for the cavity of the cyclodextrin⁴⁴, an decrease in % of methanol will provide a better chance for the interaction between the stationary phase and the solute. Therefore, the retention of the solutes by the cyclodextrin cavity will be longer. Such a phenomenon is consistent with the chiral recognition suggested.

According to the results obtained on the long β -cyclodextrin Kromasil column and the β -cyclodextrin Vydac column, a general trend of increasing retention with the hydrophobicity of the side chain⁴ was observed. For instance, the presence of the hydroxyl group in the side chains of serine and threonine make the molecules more polar and so they have less extensive hydrophobic interaction with the inner cavity of the cyclodextrin. As a result, they are less retained on the columns and they exhibit relatively small capacity factors. However, this trend was not obvious on the short β -cyclodextrin column. This can be attributed to the fact that solutes did not interact sufficiently with the stationary phase as they passed through the short column. Hence, the effect of the structure of the side chain was not clearly shown. On the other hand, the results also

show that dansyl-amino acids with large bulky side chains such as phenylalanine, valine, tryptophan and leucine are usually accompanied by a larger capacity factor at different percentage of methanol in the mobile phase.

In Tables 15A and 15B, the resolution and the separation factor for the separation of dansyl-DL-leucine for the two cyclodextrin modified CSPs are tabulated. The resolution for all the separations is less than 1 even though the % of water in the mobile phase is as high as 90%. Furthermore, the average number of theoretical plates for the CD-Kromasil column and the CD-Vydac column for the separation of leucine is about 228 and 229 respectively. The results of the chiral separation of dansyl-DL-leucine obtained in this research is comparable to the analyses done by Fujumura et. al. (Table 15C)⁴⁶. Their work showed a resolution of 0.88 and a separation factor of 1.15 for the chiral separation of dansyl-DL-leucine by a native β -cyclodextrin chiral column in 20% methanol buffered at pH 6.5. Moreover, in conjunction with their work, it can be shown that enantioselectivity is greatly dependent on the types of substitution of the cyclodextrin side chain. For instance, optical isomers of dansyl-DL-leucine can be separated on the native β -cyclodextrin column and the laboratory prepared substituted- β -cyclodextrin column while there was no separation on both the phenylcarbamoylated or propylcarbamoylated β -cyclodextrin columns. On the other hand, dansyl-DL-phenylalanine was well-separated by the carbamoylated β -cyclodextrin columns despite the fact that no chiral separation of such a racemate was achieved in this research. As a consequence, it is worth developing

Table 15A: Optical resolution and separation factors of dansyl-DL-leucine on β -cyclodextrin Kromasil chiral column, 4.6 mm x 150 mm.

Sample	%MEOH	Flow rate	k' ₁	k' ₂	α_s separation factor	R _s Resolution	Number of theoretical plate for 1 st peak	Number of theoretical plate for 2 nd peak
Leucine	50%	0.30	0.34	0.40	1.19	0.24	310	371
	40%	0.30	0.34	0.45	1.35	0.56	300	382
	30%	0.30	0.57	0.97	1.68	0.65	113	119
	20%	0.30	0.64	1.16	1.83	0.81	77	145
	10%	0.20	1.92	2.75	1.43	0.62	106	122

Table 15B: Optical Resolution and separation factor of dansyl-DL-Leucine on β -cyclodextrin Vydac chiral column, 4.6 mm x 150 mm.

Sample	%MEOH	Flow rate	k' ₁	k' ₂	α_s separation factor	R _s Resolution	Number of theoretical plate for 1 st peak	Number of theoretical plate for 2 nd peak
Leucine	40%	0.10	1.33	1.52	1.15	0.17	26.	224
	30%	0.12	1.45	1.90	1.31	0.93	128	511
	10%	0.27	3.34	3.86	1.15	0.31	69	172

Table 15C: Separation of dansyl-DL-amino acids on various β -cyclodextrin stationary phases (Literature data done by Fujimura et al in 1990)

Sample	native β -cyclodextrin ^a				Phenylcarbamoylated β -cyclodextrin ^a			
	k ₁ '	k ₂ '	α	R	k ₁ '	k ₂ '	α	R
Dansyl-DL-Leucine	17.1	19.7	1.15	0.88	4.95	4.95	1.00	0
Dansyl-DL-phenylalanine	22.9	25.0	1.09	0.85	7.46	8.24	1.10	0.85
Sample	Propylcarbamoylated β -cyclodextrin ^a				β -cyclodextrin on Kromasil silica (laboratory) ^b			
	k ₁ '	k ₂ '	α	R	k ₁ '	k ₂ '	α	R
Dansyl-DL-Leucine	2.89	2.89	1.00	0	0.64	1.16	1.83	0.81
Dansyl-DL-phenylalanine	4.33	4.61	1.06	0.70	0.34	0.34	1.00	0

^a Column size : 4 mm i.d. x 20 cm; mobile phase: phosphate buffer ($\mu = 0.2$, pH = 6.5)/methanol (80:20), flow rate :0.7 mL/min

^b Column size: 4.6 mm i.d. x 15 cm; mobile phase: water/methanol (80:20); flow rate: 0.2 mL/min (laboratory prepared column)

different kinds of cyclodextrin stationary phases in order to widen its application to different classes of compounds.

ii. On (R)-(+)-acryloxy- β , β -dimethyl- γ -butyrolactone modified silica based chiral stationary phase

The chromatographic results for the analysis of dansyl-amino acids on the lactone-modified silica CSP are shown in Table 16. The variation of capacity factors (k') with % methanol is shown in Figure 64. There was no successful separation of the enantiomers of the amino acids. On the whole, the capacity factors for all the amino acids are very small indicating that the interactions between the solutes and the CSP are minimal.

Based on the eight different Dansyl-DL-amino acids investigated in this research, it is found that the retention of the amino acids on the new developed lactone-modified silica CSP depends on the hydrophobicity of the side chain. The more hydrophobic the side chain, the greater will be the interactions between the solutes and the CSP. For instance, the side chains of both threonine and serine consist of a hydroxyl group, which makes them more hydrophilic than the others, so the capacity factors of these two amino acids are particularly small. In the case of valine, the side chain is a branched isopropyl group which has low hydrophobicity, so the capacity factor is small. The bulky side chains in tryptophan, leucine and phenylalanine accounts for the relatively long retention time and thus the greater capacity factor.

Table 16: Chromatographic data of dansyl-DL-amino acids on Lactone-modified Kromasil chiral column, 4.6 mm x 150 mm at flow rate 0.5 mL/min.

Sample	% MEOH	k'₁
Dansyl-DL-threonine	40%	-0.31
	20%	0.01
	10%	0.17
Dansyl-DL-Tryptophan	40%	-0.12
	20%	0.74
	10%	1.02
Dansyl-DL-Valine	40%	-0.32
	20%	-0.51
	10%	0.63
Dansyl-DL-Leucine	40%	0.35
	20%	1.09
	10%	1.34
Dansyl-DL-Phenylalanine	40%	-0.05
	20%	1.02
	10%	1.06
Dansyl-DL-Methionine	40%	-0.23
	20%	0.96
	10%	1.02
Dansyl-DL-Norvaline	40%	-0.21
	20%	0.84
	10%	0.90
Dansyl-DL-Serine	40%	-0.20
	20%	-0.03
	10%	0.01

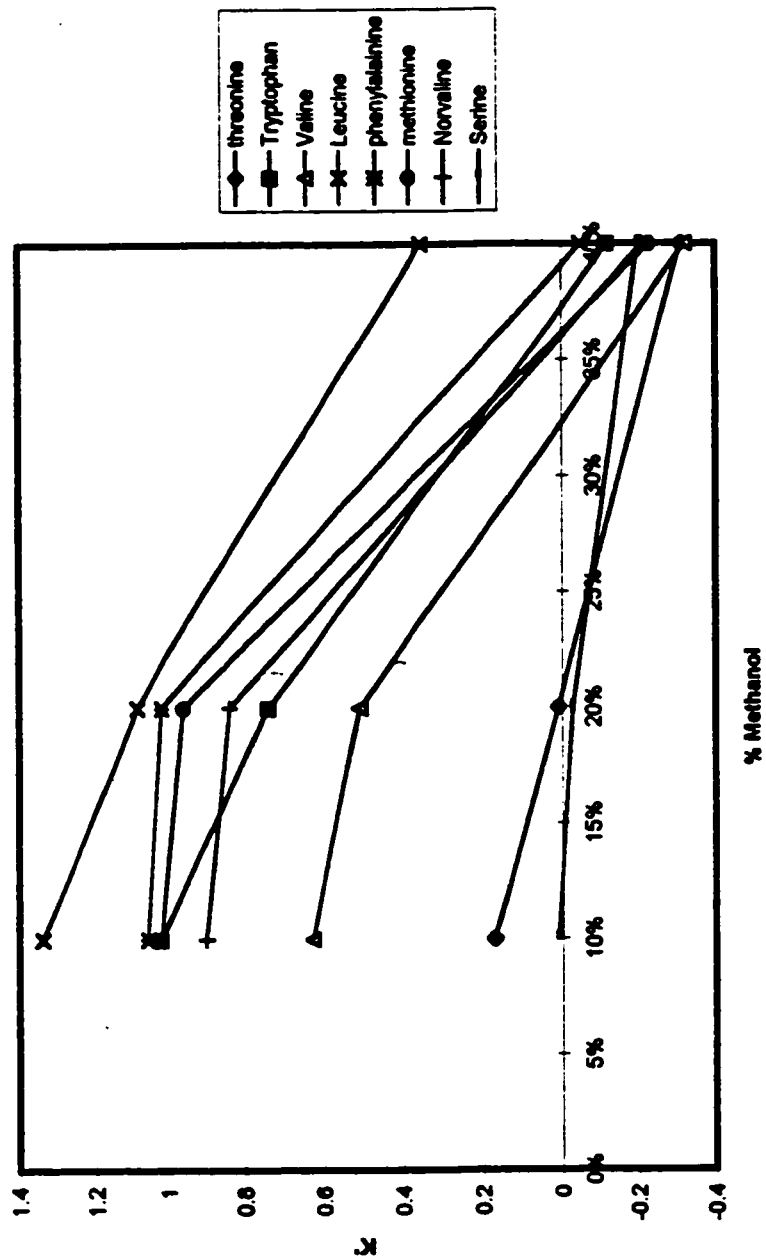


Figure 64. A plot of capacity factor (k') Vs % methanol in the mobile phase for the chromatographic studies of dansyl-DL-amino acids. Flow rate: 0.5 mL/min

c. Chiral separation of drugs

i. On β -cyclodextrin modified silica based chiral stationary phase

Based on the preliminary chromatographic analysis, there were no chiral separations of the drugs under investigation. With the exception of tropicamide, the other three drugs always showed a small capacity factor at all mobile phase compositions tested. This is attributed to the fact that only tropicamide has two aromatic rings which are bulky enough to fit into the cavity and form stable inclusion complexes with the CSP.

ii. On (R)-(+)-acryloxy- β , β -dimethyl- γ -butyrolactone modified silica based chiral stationary phase.

Similarly, no successful separation of the drugs was obtained on this column. In reversed phase HPLC, the interaction between the solute and the stationary phase is mainly hydrophobic in nature. The presence of the hydroxyl groups at the chiral centers and amine groups in the structure in clenbuterol, terbutaline and DL-homatropine increases the hydrophilicity of the molecules and thus lessens the interaction of the solutes with the CSP. This is a possible reason for the extraordinarily small capacity factors. In the case of tropicamide, the existence of two aromatic rings and two relatively bulky ethyl groups attached to the amine moiety accounts for the more extensive interaction between the solute and the lactone modified surface. Hence, even though a chiral separation has not occurred, the capacity factor suggests a reasonable degree of interaction. Also, the capacity factor increases with the % of water in the mobile phase which is a common phenomenon in reversed phase liquid chromatography.

5. Study of temperature effects on chiral separation

From the results obtained in the preliminary runs, the study of temperature effects on chiral separation were evaluated on the most promising separations - the separation of dansyl-DL-leucine, temazepam and oxazepam. Because of the presence of many different types of interactive sites on the cyclodextrin surface, the orientation of the neighboring glucose residues may affect the local environment for separation. It is anticipated that such microheterogeneity of the CSP can be “averaged” out at higher temperature⁴² and in conjunction with an expected faster mass transport at higher temperature, the peak shape and the selectivity are expected to be improved. The results for the study of temperature effects are reported in Table 17A, 17B and 17C. By increasing the temperature, the capacity factors were significantly decreased without any improvement in the chiral resolution. The changes in capacity factors are expected because the binding constant of the solute to the cyclodextrin is significantly affected by temperature. As temperature increases, the binding constant will be decreased so the solutes will be held less firmly by the cyclodextrin⁴. From our studies, it seems that the effect of decreasing the binding ability of the solute to the cyclodextrin predominates upon variation in temperature. Therefore, the difference in the stability of the two transient diastereomeric inclusion complexes formed is narrowed to an extent that enantioselectivity is greatly diminished. This accounts for the decrease in resolution for all the three tested samples.

Table 17A: Variation of k' of temazepam, oxazepam and dansyl-DL-leucine at different temperatures on β -cyclodextrin Vydac silica chiral column (4.6 mm x 150 mm).

Sample	25.0°C		40.0°C		50.0°C		60.0°C	
	k ₁	k ₂	k ₁	k ₂	k ₁	k ₂	k ₁	k ₂
Temazepam	0.65	0.78	0.57	0.57	0.36	0.36	0.25	0.25
Oxazepam	0.78	1.58	0.72	0.72	0.55	0.55	0.27	0.27
Dansyl-Dl-Leucine	0.59	0.84	0.21	0.21	0.02	0.02	-0.09	-0.09

Chromatographic condition: Flow rate: 0.2 mL/min; mobile phase: 30% MEOH 70% H₂O

Table 17B: Variation of k' of temazepam, oxazepam and dansyl-DL-leucine at different temperature on β -cyclodextrin Kromasil silica chiral column (4.6 mm x 150 mm).

Sample	25.0°C		40.0°C		50.0°C		60.0°C	
	k ₁	k ₂	k ₁	k ₂	k ₁	k ₂	k ₁	k ₂
Temazepam	1.54	1.99	1.22	1.22	0.87	0.87	0.77	0.77
Oxazepam	1.91	4.04	1.94	1.94	1.34	1.34	1.17	1.17
Dansyl-Dl-Leucine	1.11	1.11	0.49	0.49	-0.03	-0.03	-0.25	-0.25

Chromatographic condition: Flow rate: 0.2 mL/min; mobile phase: 30% MEOH 70% H₂O

Table 17C: Variation of k' of temazepam, oxazepam and dansyl-DL-leucine at different temperature on β -cyclodextrin Kromasil silica chiral column (4.6 mm x 50 mm).

Sample	25.0°C		40.0°C		50.0°C		60.0°C	
	k ₁	k ₂	k ₁	k ₂	k ₁	k ₂	k ₁	k ₂
Temazepam	2.32	2.85	1.37	1.37	1.00	1.00	0.80	0.80
Oxazepam	2.44	4.93	2.02	2.02	1.45	1.45	1.10	1.10
Dansyl-Dl-Leucine	0.95	0.95	0.80	0.80	0.04	0.04	0.03	0.03

Chromatographic condition: Flow rate: 0.15 mL/min; mobile phase: 30% MEOH 70% H₂O

From Figure 65 and figure 66, it can be observed that better peak shapes were obtained at higher temperature. This is probably due to an increase in mass transport of the solutes in and out of the cyclodextrin cavity so that the column efficiency is higher and the peak shapes are improved.

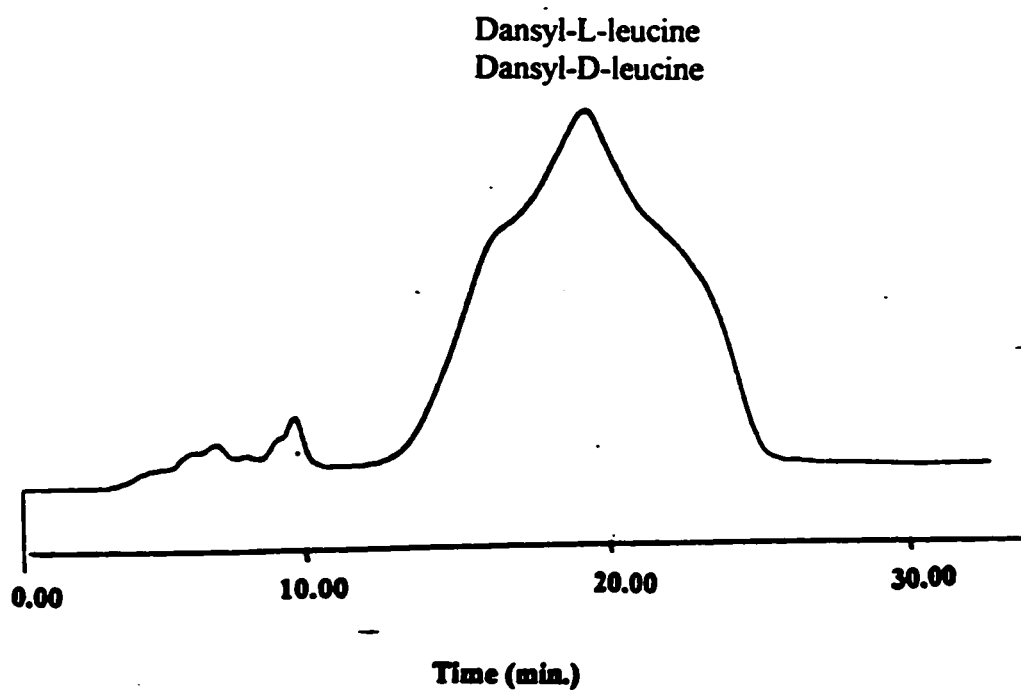


Figure 65. Reversed phase separation of the optical isomers of dansyl-DL-leucine on a β -cyclodextrin modified Kromasil column (4.6 mm x 150 mm); mobile phase: methanol/water (30:70); flow rate: 0.20 mL/min; temperature: 25°C; UV detection at 254 nm; sample injection: 20 μ L; column pressure: 68 bars.

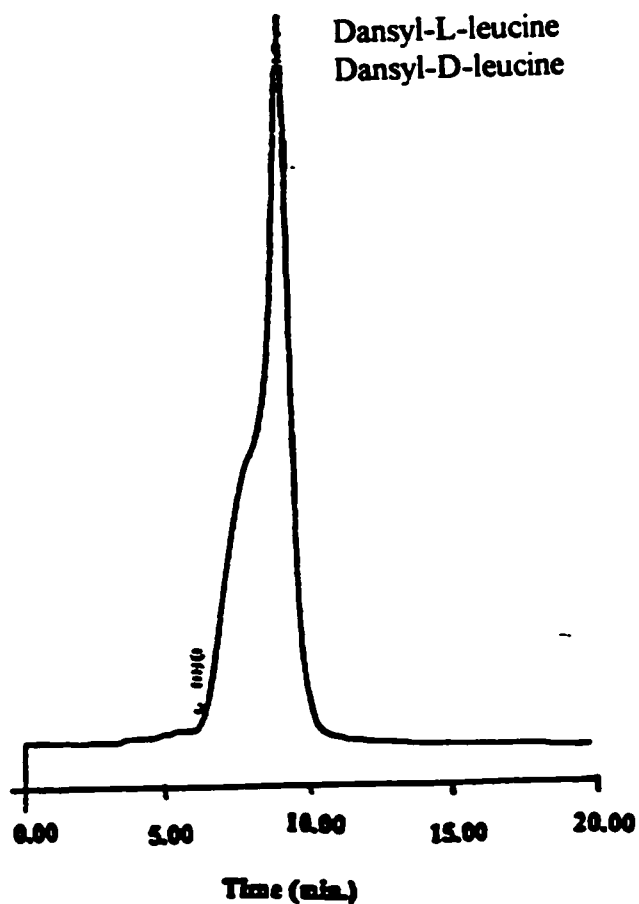


Figure 66. Reversed phase separation of the optical isomers of dansyl-DL-leucine on a β -cyclodextrin modified Kromasil column (4.6 mm x 150 mm); mobile phase: methanol/water (30:70); flow rate: 0.20 mL/min; temperature: 50°C; UV detection at 254 nm; sample injection: 20 μ L; column pressure: 41 bars.

Chapter IV

Conclusion

TES silanization followed by hydrosilation is a reliable synthetic pathway for attaching an organic moiety with a terminal olefinic group to a silica surface. This method can be extended to large molecules such as the substituted cyclodextrin used in this research. The extent of bonding is determined by both the availability of the silica hydride group on the silica surface and the concentration of the bonding material. To optimize the hydrosilation process for cyclodextrin, a non-polar solvent should be used. The success of bonding can be evaluated quantitatively by elemental analysis and qualitatively by infrared spectroscopy and nuclear magnetic resonance. Owing to the bulkiness of the β -cyclodextrin molecule, the surface coverage is only in the range of 0.36-0.64 $\mu\text{mol}/\text{m}^2$ whereas the surface coverage of (R)-(+)-acryloxy- β,β -dimethyl- γ -butyrolactone on Kromasil silica is 1.27 $\mu\text{mol}/\text{m}^2$. From the chromatographic studies using methanol/water mixture as the mobile phase, it was found that enantiomeric resolutions only occurred for oxazepam, temazepam and dansyl-DL-leucine. The enantiomeric separation of a benzodiazepine requires the presence of the hydroxyl group and an acidic hydrogen in the benzodiazepine ring whereas the enantioselectivity of dansyl-DL-amino acid is greatly enhanced by the bulkiness and the hydrophobicity of the side chain. Furthermore, enantiomeric resolution could not be improved by increasing temperature. Last but not

the least, β -cyclodextrin modified Kromasil silica showed better performance than the β -cyclodextrin modified Vydac silica chiral stationary phase.

Chapter V

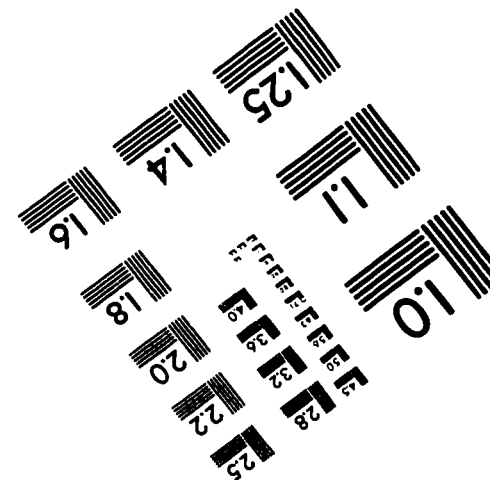
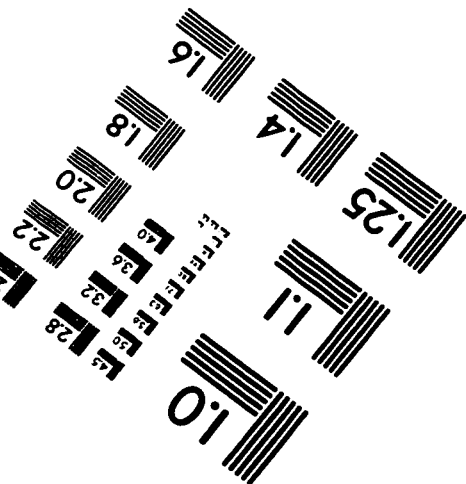
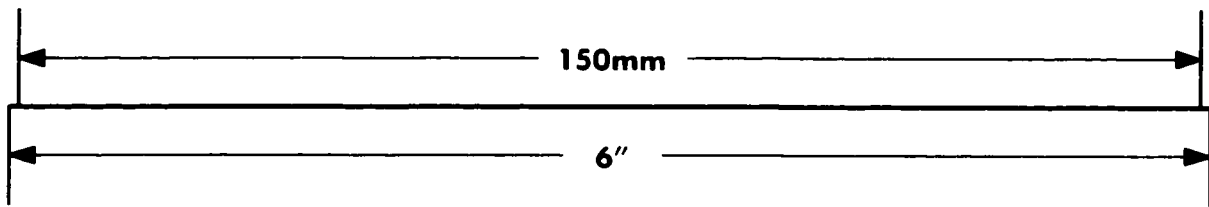
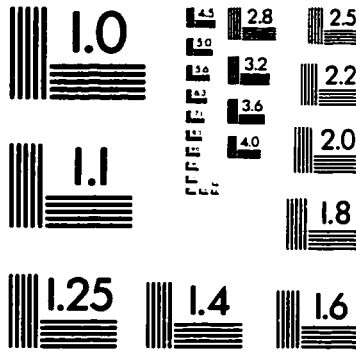
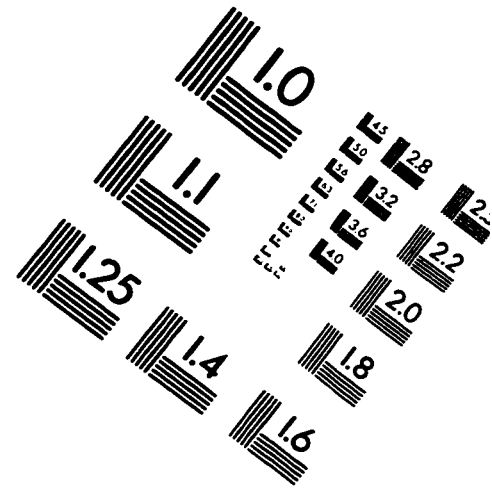
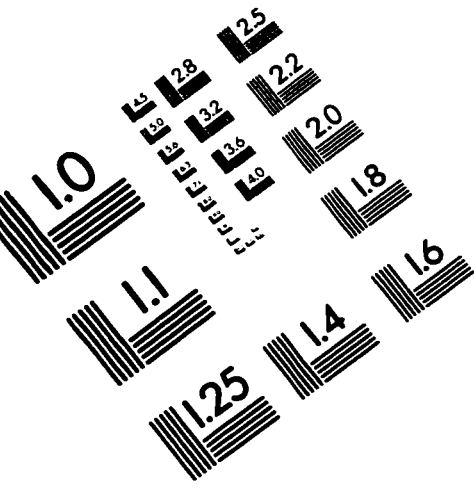
REFERENCES

1. Lough, W. J.; Chiral Liquid Chromatography, Blackie and Son Ltd., 1989, Chapter 1
2. Lin, B.; Zhu, X.; Koppenhodfer, B.; Epperlein, U.; *LC-GC* 1997, 15, 40-46.
3. Morris, Z.; Laura, J. C.; Chromatographic Chiral Separations, Marcel Dekker, Inc., 1988, p.2 - 4.
4. Ahuja, S.; Chiral Separations by Liquid Chromatography, American Chemical Society, Washington DC, 1991, Chapter 1
5. Lough, W. J.; Chiral Liquid Chromatography, Blackie and Son Ltd., 1989, Chapter 3
6. Soon M. H.; *Biomedical Chromatography* 1997, 11, 259-271.
7. Galen, W. E.; Instrumental methods of chemical analysis, 1985, Chapter 21.
8. Dagliesh, C. E.; *J. Chem. Soc.* 1952, 6, 3840.
9. Ahuja, S.; Chiral Separations by Liquid Chromatography, American Chemical Society, Washington DC, 1991, Chapter 3.
10. Davankov, V. A.; Kurganov, A. A.; *J. Chromatogr.* 1971, 60, 280-283.
11. Pirkle W. H.; Finn, J. M.; House, D. W.; *J. Chromatogr.* 1980, 192, 143-158
12. Oliveros, L.; Lopez, P.; Minguillon, C.; Franco, P.; *J. Liq. Chromatogr.* 1995, 18(8), 1521-1532.
13. Ahuja, S.; Chiral Separations by Liquid Chromatography, American Chemical Society, Washington DC, 1991, Chapter 4.
14. Lough, W. J.; Chiral Liquid Chromatography, Blackie and Son Ltd., 1989, Chapter 8.
15. Ward, T. J.; Armstrong, D. W.; *J. Liq. Chromatogr.* 1986, 9(2&3), 407-423.
16. Armstrong, D. W.; Ward, T. J.; Beesley, T. E.; *Science* 1986, 232. 1132-1135.

17. Maguire, J. H.; *J. Chromatogr.* **1987**, 387, 453-458.
18. Armstrong, D. W.; *J. Chromatogr.* **1984**, 7(S-2), 353-376.
19. Armstrong, D. W.; DeMond, W.; *J. Chromatogr. Sci.* **1984**, 22, 411-415.
20. Ciucanu, I.; *J. Chromatogr. A* **1996**, 727, 195-201.
21. Chang, C. A.; Wu, Q.; *J. Chromatogr.* **1986**, 354, 454-458.
22. Maier, N. M.; Uray, G.; *J. Chromatogr. A* **1996**, 740, 11-19.
23. Pirkle, W. H.; Koscho, M. E.; Wu, Z.; *J. Chromatogr. A* **1996**, 726, 91-97.
24. Pirkle, W. H.; Spence, P. L.; *J. Chromatogr. A* **1997**, 775, 81-90.
25. Majors, R. E.; *LC-GC* **1997**, May, S8-S19.
26. Dorsey, J. G.; Cooper, W. T.; *Anal. Chem.* **1994**, 66, 857A-867A.
27. Scott, R. P. W.; Silica Gel and Bonded Phases, Wiley and Son Ltd., **1993**, Chapter 7 and 8.
28. Pesek, J. J.; Matyska, M. T.; Sandoval, J. E.; Williamsen, E. J.; *J. Liq. Chromatogr. & Rel. Technol.*, **1996**, 19 (17&18), 2843-2865.
29. Wirth, M. J.; Fatnumbi, H. O.; *Anal. Chem.* **1993**, 65, 822-826.
30. Pesek, J. J.; Swedberg, S. A.; *J. Chromatogr.* **1986**, 361, 83-92.
31. Pesek, J. J.; Sandoval, J. E.; *J. Am. Chem. Soc.* **1991**, 63, 2634-2641.
32. Montes, M. C.; Amen, C. V.; Pesek, J. J.; Sandoval, J. E.; *J. Chromatogr. A* **1994**, 688, 31-45.
33. Pesek, J. J.; Matyska, M. T.; *J. Chromatogr. A* **1994**, 687, 33-44.
34. Pesek, J. J.; Chu, C. H., Jonsoon, E.; Auinen, M.; Sandoval, J. E.; *Anal. Chem.* **1993**, 65, 808-816.
35. Pesek, J. J.; Matyska, M. T.; *J. Liq. Chromatogr.* **1995**, 18, 2507-2526.

36. Pesek, J. J.; Matyska, M. T.; Williamsen, E. J.; Evanchic, M.; Konjuh, V. H. K.; Takhar, S.; Tranchina, R.; *J. Chromatogr. A* **1997**, 786, 219.
37. Kamath, S.; *Thesis*, San Jose State University, **December 1996**.
38. Berendsen, G. E.; Galen, L. D.; *J. Liq. Chromatogr.* **1978**, 1, 561.
39. Pesek, J. J.; Matyska, M. T.; Soczewinke, E.; Christensen, P.; *Chromatographia* **1994**, 39, 520-528.
40. Bayer, E.; Klaus, A.; Reiners, J.; Ninder, M.; *J. Chromatogr.* **1983**, 264, 197-213.
41. Pesek, J. J.; Sandoval, J. E.; Williamsen, E. J.; *Trends in Appl. Spectroscopy* **1993**, 1, 41-50.
42. Stalcup, A. M.; Wu, W.; Williams, K. L.; *Biomedical Chromatography* **1997**, 11, 325-330.
43. Li, S.; Purdy, W. C.; *J. Chromatogr.* **1992**, 625, 109-120.
44. Bressolle, F.; Audran, M.; Pham, T. N.; Vallon, J. J.; *J. Chromatogr. B* **1996**, 687, 303-336.
45. Hinze, W. L.; Riehl, T. E.; *J. Amer. Chem. Soc.* **1985**, 57, 237-242.
46. Fujimura, K.; Suzuki, S.; Hayashi, K.; Masuda, S.; *Anal. Chem.* **1990**, 62, 2198-2205.
47. Felix, G.; Cachau, C.; Thienpont, A.; Soulard, M. H.; *Chromatographia* **1996**, 42, 583-590.

IMAGE EVALUATION TEST TARGET (QA-3)



APPLIED IMAGE, Inc
 1653 East Main Street
 Rochester, NY 14609 USA
 Phone: 716/482-0300
 Fax: 716/288-5989

© 1993, Applied Image, Inc., All Rights Reserved